Dipodal Ferrocene Derivatives for Nano-structured Redox-Functionalised Surfaces

by

DAG ROTHER

DISSERTATION

submitted in fulfilment of the requirements
for the degree of

DOCTOR OF SCIENCE
(Dr. rer. nat.)

in

CHEMISTRY

in the

DEPARTMENT OF SCIENCE

at the

UNIVERSITY OF KASSEL

MAY 2008

SUPERVISOR: PROF. U. SIEMELING
CO-SUPERVISOR: PROF. N. J. LONG

Declaration

The work described in this thesis was carried out in the Institute of Chemistry, University of Kassel (Germany), between August 2005 and May 2008 in the research group of Prof. Siemeling and in the Department of Chemistry, Imperial College London, between December 2005 and June 2006 under supervision of Prof. Long. The entire body of work is my own unless stated to the contrary and has not been submitted previously for a degree at this or any other university.

Erklärung

Hiermit versichere ich, dass ich die vorliegende Dissertation selbständig und ohne unerlaubte Hilfe angefertigt und andere als die in der Dissertation angegebenen Hilfsmittel nicht benutzt habe. Alle Stellen, die wörtlich oder sinngemäß aus veröffentlichten oder unveröffentlichten Schriften entnommen sind, habe ich als solche kenntlich gemacht. Kein Teil dieser Arbeit ist in einem anderen Promotions- oder Habilitationsverfahren verwendet worden.

Kassel, den 27. Mai 2008

List of Publications:

Different aspects of the work in this thesis have been published previously:

U. Siemeling, D. Rother, C. Bruhn, H. Fink, T. Weidner, F. Träger, A. Rothenberger, D. Fenske, A. Priebe, J. Maurer, R. Winter, *J. Am. Chem. Soc.* **2005**, *127*, 1102.

T. Weidner, B. Krohn, M. Trojtza, C. Bruhn, D. Rother, U. Siemeling, F. Träger, *Proc. SPIE Int. Soc. Opt. Eng.* **2006**, *6106*, 61061S/1.

U. Siemeling, D. Rother, C. Bruhn, *Chem. Commun.* **2007**, 4227.

T. Weidner, N. Ballav, M. Zharnikov, A. Priebe, N. J. Long, J. Maurer, R. Winter, A. Rothenberger, D. Fenske, D. Rother, C. Bruhn, H. Fink, U. Siemeling, *Chem. Eur. J.* **2008**, *14*, 4346.

Summary

Self-assembled monolayers (SAMs) on solid surfaces are of great current interest in science and nanotechnology. This thesis describes the preparation of several symmetrically 1,1′-substituted ferrocene derivatives that contain anchoring groups suitable for chemisorption on gold and may give rise to SAMs with electrochemically switchable properties.

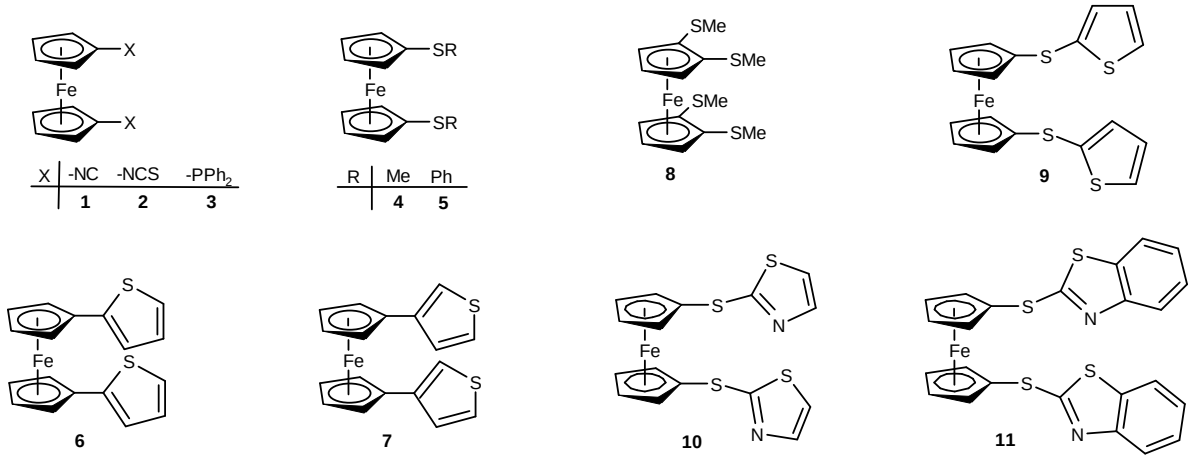

Figure I: Ferrocene-based ligands investigated in this study. The derivatives **1** – **7** possess two anchoring units, ligands **8** – **11** display four potential attachment possibilities.

The binding groups are isocyano (**1**) (-NC), isothiocyanato (**2**) (-NCS), phosphanyl (**3**) (-PPh_2), thioether (**4**, **5** and **8**–**11**) (-SR) and thienyl (**6** and **7**). In the context of SAM fabrication, isothiocyanates and phosphanes are adsorbate systems which, surprisingly, have remained essentially unexplored.

SAMs on gold have been fabricated with the adsorbates **1** – **8** from solution and investigated primarily by X-ray photoelectron spectroscopy and near-edge X-ray absorption fine structure spectroscopy. The results of these analytical investigations are presented and discussed in matters of the film quality and possible binding modes. The quality of self-assembled monolayers fabricated from 1,1′-diisocyanoferrocene (**1**) and 1,1′-diisothiocyanatoferrocene (**2**) turned out to be superior to that of films based on the other adsorbate species investigated. Films of **1**, **2** and **3** afforded well-defined SAMs of good quality. Films **1** and **2** exhibit a high degree of chemical homogeneity, high packing density and orientational order. Film

3 also shows a high degree of chemical homogeneity and orientational order, but this film is characterised by a lower packing density due to the "flat" adsorption geometry of the bulky PPh_2 headgroups. All other films of this study (**4** – **8**) exhibit chemical inhomogeneity and low orientational order of the film constituents and therefore failed to give rise to well-defined SAMs.

SAM formation can be viewed to rely to a large extent on surface coordination chemistry, which is naturally related to molecular coordination chemistry. Since all SAMs described in this thesis were prepared on gold (111) surfaces, the ferrocene-based ligands of this study have been investigated in their ability for complexation towards gold(I). The sulfur-based ferrocene ligands [$fc(SR)_2$] failed to give stable gold(I) complexes, but their reaction with AuCl provides clear evidence that complexation with these thioethers takes place, followed by a redox-chemical decomposition to elemental gold. In contrast, 1,1'-diisocyanoferrocene (**1**) proved to be an excellent ligand for the complexation of gold(I). Several complexes were prepared and characterised utilising a series of gold(I) acetylides.

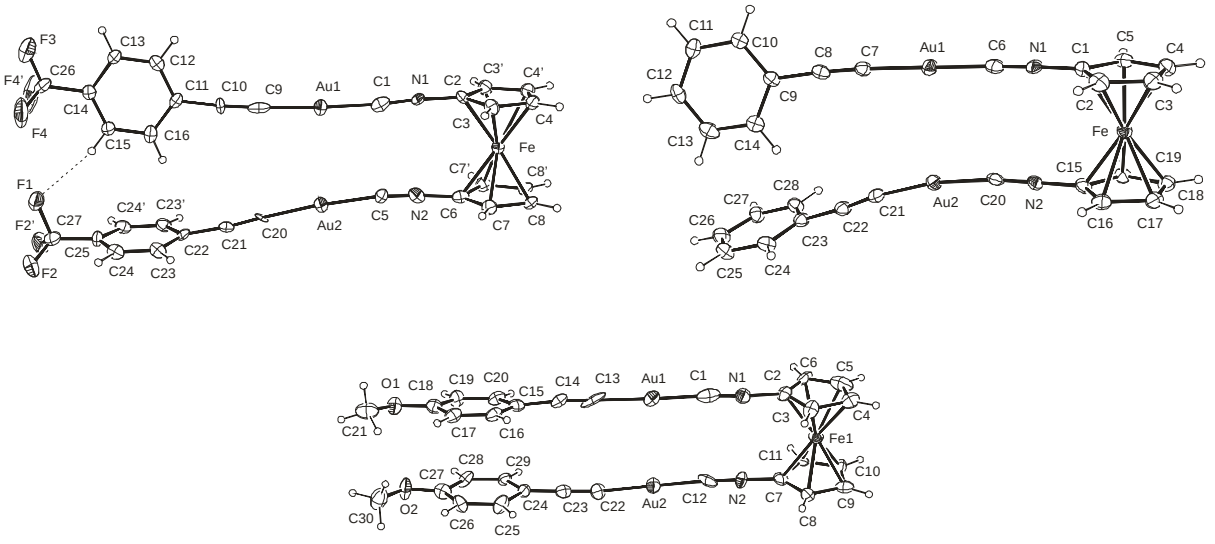

Figure II: Molecular structure of the complexes [{Au(C≡C-*p*-$C_6H_4CF_3$)}$_2$(μ-**1**)] (**13a**), [{Au(C≡C-*p*-C_6H_5)}$_2$(μ-**1**)] (**13b**) and [{Au(C≡C-*p*-C_6H_4OMe)}$_2$(μ-**1**)] (**13c**) in the crystal.

These complexes show interesting structural motifs in the solid state, since intramolecular aurophilic interactions lead to a parallel orientation of the isocyano moieties, combined with an antiparallel alignment of neighbouring units.

The reaction of **1** with the gold(I) acetylide $[Au(C{\equiv}C{-}Fc)]_n$ turned out to be very unusual, since the two chemically equivalent isocyano groups undergo a different reaction.

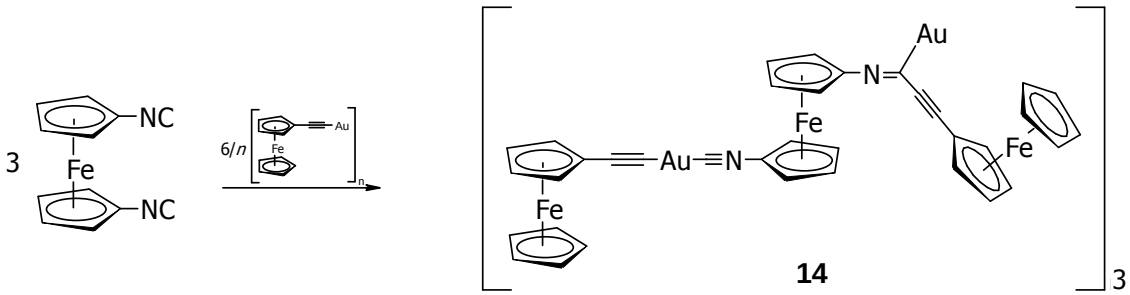

Figure III: Reaction of **1** with $[Au(C{\equiv}C{-}Fc)]_n$.

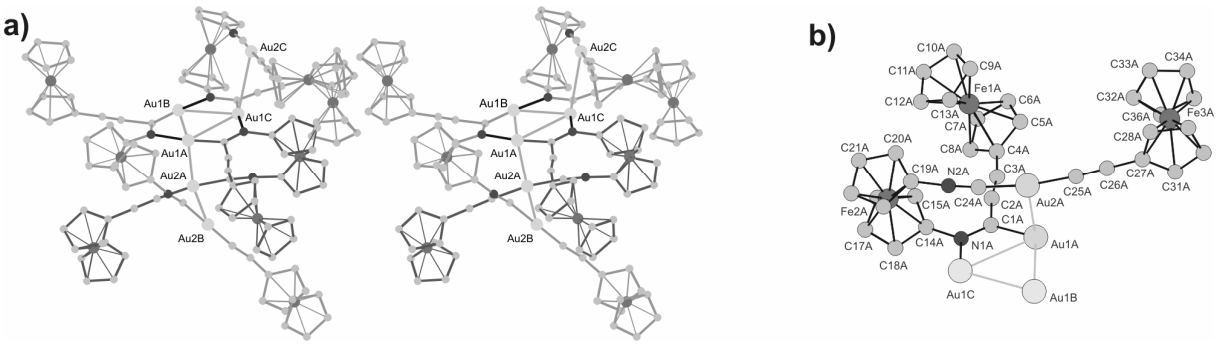

Figure IV: Molecular structure of the complex $[(Fc\text{-}C{\equiv}C\text{-}Au\text{-}C{\equiv}N\text{-}C_5H_4)Fe\{C_5H_4\text{-}N{=}C(Au)\text{-}C{\equiv}C\text{-}Fc\}]_3$, which is composed of three subunits **14**, in the crystal.

One group shows an ordinary coordination and the other one undergoes an extraordinary 1,1-insertion into the Au-C bond. This type of 'schizoid' reactivity is unprecedented and gives scope for further studies of this novel variant of induced reactivity asymmetry.

Reaction of $[Au(C{\equiv}C{-}Fc)]_n$ with dppf yielded the expected complex $[(Au\text{-}C{\equiv}C\text{-}Fc)_2(\mu\text{-}dppf)]$ and structural data confirm an ordinary coordination mode. The coordination behaviour towards silver(I) was also investigated to fathom the coordination

chemistry of **1** and the structure of the complex $[Ag_2(\mu\text{-}\mathbf{1})_2](NO_3)_2 \cdot H_2O$ was determined by X-ray diffraction analysis.

Reactions on monolayers are an attractive synthetic approach for tailoring surface properties. As a sideline of the research of this thesis several ferrocene derivatives have been tested for their suitability for potential surface reactions. Copper(I) mediated 1,3-dipolar cycloadditions of azidoferrocene derivatives with terminal alkynes appeared very promising in this context, but failed to a certain extent in terms of 'click' chemistry, since the formation of the triazoles depended on the strict exclusion of oxygen and moisture and yields were only moderate. Staudinger reactions between dppf and azidoferrocene derivatives were also tested. Only the monosubstituted species, FcN_3, gave rise to a well defined product, while 1,1'-diazidoferrocene probably leads to the formation of polymeric material. The nucleophilic additions of secondary amines to 1,1'-diisothiocyanatoferrocene (**2**) led to the respective thiourea derivatives in quantitative yields. **2** is therefore best suited for reactions on monolayers with terminal amino groups.

Zusammenfassung

Die gezielte Oberflächenmodifizierung mittels dünner Filme ist von großer Bedeutung in gegenwärtiger Grundlagenforschung und Nanotechnologie. Die vorliegende Arbeit beschäftigt sich mit der Synthese und Untersuchung symmetrisch 1,1'-disubstituierter Ferrocenderivate, die sich für die Fabrikation von monomolekularen Filmen durch Selbstassemblierung (engl. self-assembled monolayer; SAM) eignen. Da die Oxidation von Ferrocen bekanntermaßen reversibel ist (Ferrocen ist im positiv geladenen wie auch im neutralen Zustand stabil), ist zu erwarten, dass monomolekulare Filme aus solchen Adsorbaten elektrochemisch schaltbare Eigenschaften aufweisen. Solche (im Sinne eines definierten Antwortverhaltens auf äußere Reize) „intelligenten" Oberflächen sind ihrerseits interessant im Hinblick auf mögliche Anwendungen zur hochdichten Daten- oder Ladungsspeicherung. Im äußersten Fall könnte hier ein einzelnes Oberflächenmolekül als elektronischer Baustein dienen.

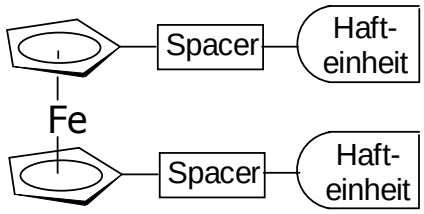

Abbildung I: Allgemeine Architektur der Zielverbindungen.

Funktionalisierung der redoxaktiven Ferroceneinheiten an 1- und 1'-Position mit chemischen Gruppen, die an Gold (111)-Oberflächen chemisorbieren können, führt zu potentiell mehrzähnigen Oberflächenliganden, was die Anbindung an das Substrat verbessern und zu besonders stabilen Monolagen führen sollte. Abbildung II zeigt die verschiedenen Ferrocenderivate, die im Rahmen dieser Arbeit synthetisiert und untersucht wurden.

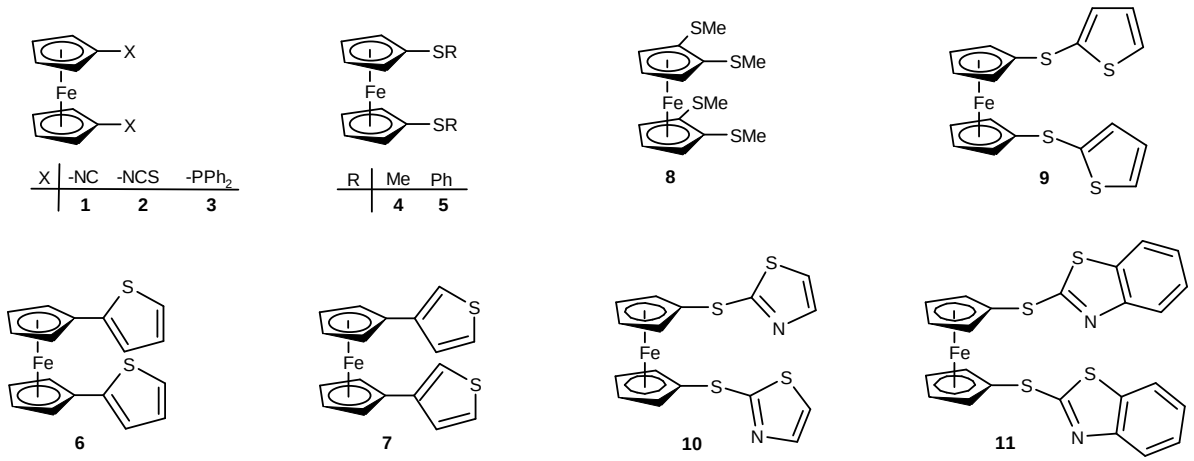

Abbildung II: Auf Ferrocen basierende Liganden, die im Rahmen dieser Arbeit synthetisiert und untersucht wurden. Derivate **1** – **7** besitzen potentiell zwei Hafteinheiten, während sich die Liganden **8** – **11** durch vier Anknüpfungsmöglichkeiten auszeichnen.

Von Verbindungen **1** – **8** wurden Monolagen präpariert und hauptsächlich mittels XPS und NEXAFS untersucht. Bei den Hafteinheiten handelt es sich um Isocyano- (**1**) (-NC), Isothiocyanato- (**2**) (-NCS), Phosphanyl- (**3**) (-PPh_2), Thioether- (**4**, **5** und **8**) (-SR) und Thienylgruppen (**6** und **7**). Überraschenderweise sind Isothiocyanate und Phosphane dabei praktisch unerforschte Systeme im Gebiet der SAM-Herstellung.

Die Ergebnisse der oberflächenanalytischen Untersuchungen werden im Hinblick auf die Filmqualität der SAMs wie auch die mögliche Anbindungsweise der Adsorbate dargestellt und diskutiert. Hierbei erwiesen sich die aus den Adsorbaten **1** (1,1'-Diisocyanoferrocen) und **2** (1,1'-Diisothiocyanatoferrocen) hergestellten Monolagen allen anderen untersuchten Filmen als qualitativ überlegen. Die Filme der Liganden **1**, **2** und **3** zeichnen sich durch ein hohes Maß an Einheitlichkeit und eine hohe Güte aus. **1** und **2** weisen dabei ein hohes Maß an chemischer Homogenität, hohe Packungsdichte und Ordnung in Bezug auf die molekulare Orientierung auf. Auch Film **3** zeigt eine wohlgeordnete Orientierung der Moleküle und ein hohes Maß an chemischer Homogenität, allerdings ist dieser Film durch eine geringere Bedeckungsdichte gekennzeichnet, was sich auf eine „flache" Adsorptionsgeometrie der räumlich anspruchsvollen PPh_2 Gruppen zurückführen lässt. Alle anderen Filme dieser Studie (**4** – **8**) sind chemisch inhomogen und besitzen nur geringe Orientierungsordnung; daher sind sie für eine Fabrikation wohl definierter SAMs nicht geeignet.

Die Bildung von Monolagen beruht zu einem großen Teil auf Oberflächen-koordinationschemie, die natürlich mit der molekularen Koordinationschemie in Beziehung steht. Im Gegensatz zur molekularen Koordinationschemie ist die Oberflächenkoordination allerdings nur schwierig zu untersuchen. Das Ausloten des Koordinationsverhaltens der untersuchten Adsorbatmoleküle ist somit eine logische Erweiterung der Forschung, da der Einblick in die molekularen Bindungs-verhältnisse einen Brückenschlag zur Oberflächenchemie liefern kann. Da sämtliche SAMs in dieser Arbeit auf Gold (111)-Oberflächen präpariert wurden, sind die Ferrocen-basierten Liganden dieser Studie vor allem in Hinblick auf ihr Koordinationsverhalten gegenüber Gold(I) untersucht worden. Dabei stellte sich heraus, dass die Thioether unter den Ferrocenderivaten keine stabilen Komplexe mit Gold(I) bilden. Durch die Umsetzung mit AuCl konnte jedoch eindeutig gezeigt werden, dass eine Komplexierung von Gold(I) mit diesen S-Donor-Liganden stattfindet, an die sich eine redoxchemische Zersetzung zu elementarem Gold anschließt. Im Gegensatz dazu erwies sich 1,1′-Diisocyanoferrocen (**1**) als äußerst fruchtbarer Ligand in der Gold(I)-Chemie. Verschiedene Komplexe wurden mit einer Serie von Gold(I)-Acetyliden hergestellt und charakterisiert.

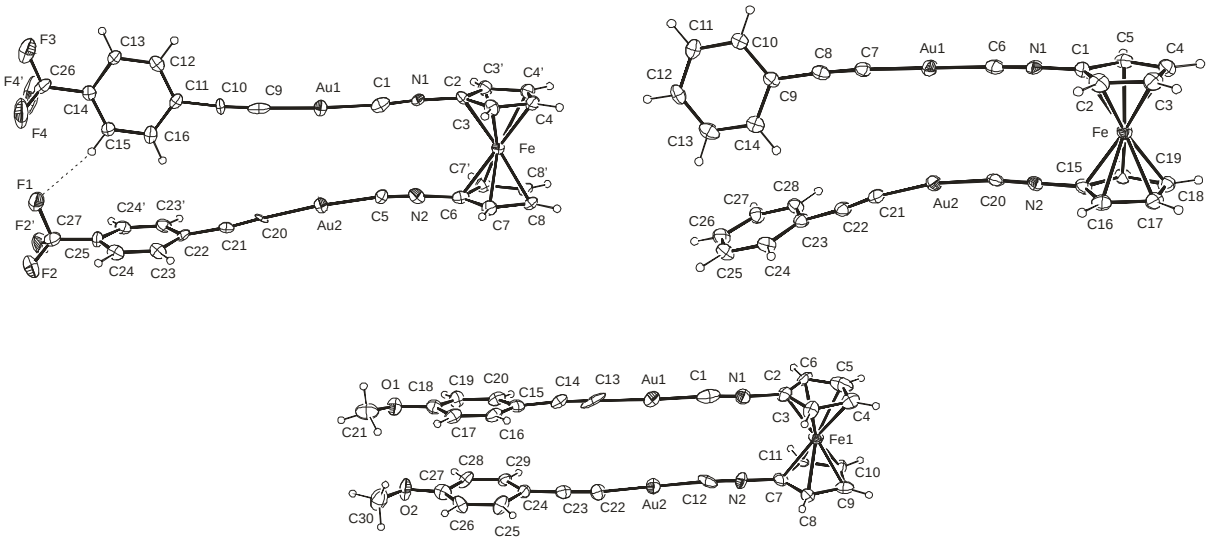

Abbildung III: Molekülstrukturen der Komplexe [{Au(C≡C-*p*-$C_6H_4CF_3$)}$_2$(μ-**1**)] (**13a**), [{Au(C≡C-*p*-C_6H_5)}$_2$(μ-**1**)] (**13b**) und [{Au(C≡C-*p*-C_6H_4OMe)}$_2$(μ-**1**)] (**13c**) im Kristall.

Diese Komplexe weisen im Festkörper interessante Strukturmotive auf, da intramolekulare aurophile Wechselwirkungen zu einer parallelen Anordnung der Isocyanoeinheiten führen, kombiniert mit einer antiparallelen Orientierung der benachbarten Einheiten.

Die Umsetzung von **1** mit dem Gold(I) Acetylid $[Au(C{\equiv}C–Fc)]_n$ erwies sich als ausgesprochen ungewöhnlich, da die beiden chemisch äquivalenten Isocyanogruppen jeweils unterschiedliche Reaktionen eingehen.

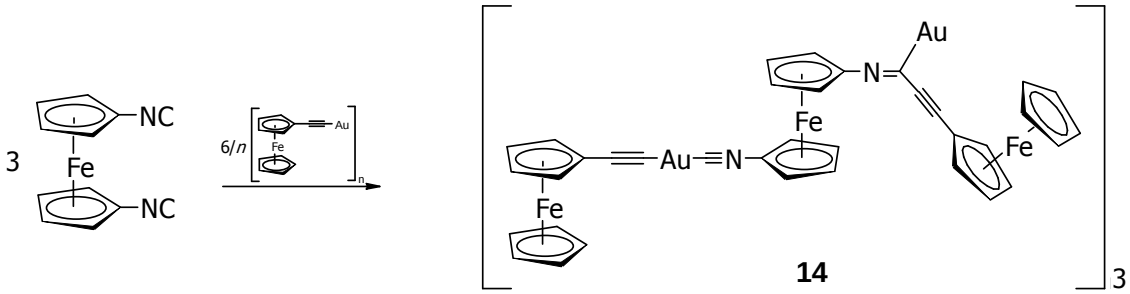

Abbildung IV: Umsetzung von **1** mit $[Au(C{\equiv}C–Fc)]_n$.

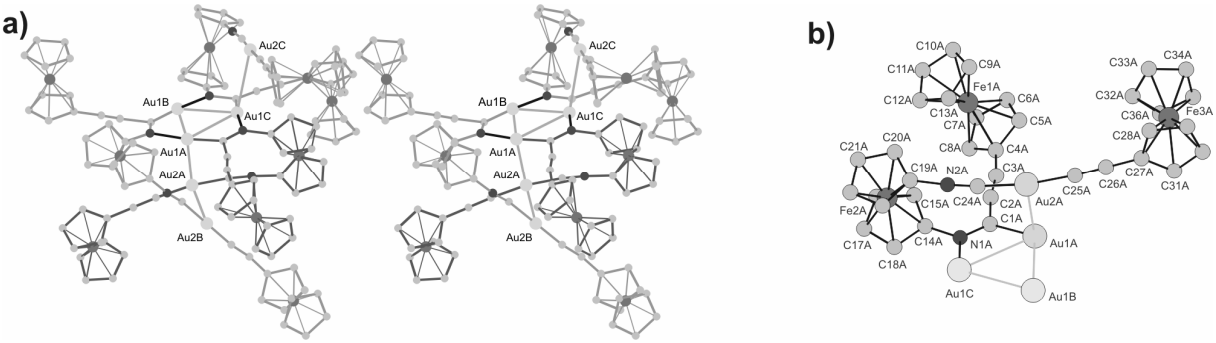

Abbildung V: Molekülstruktur des aus drei Untereinheiten **14** zusammengesetzten Komplexes $[(Fc\text{-}C{\equiv}C\text{-}Au\text{-}C{\equiv}N\text{-}C_5H_4)Fe\{C_5H_4\text{-}N{=}C(Au)\text{-}C{\equiv}C\text{-}Fc\}]_3$ im Kristall.

Eine der Isocyanogruppen zeigt eine gewöhnliche Koordination, während die andere eine außergewöhnliche 1,1-Insertion in die Au-C Bindung eingeht. Diese Art „schizoider“ Reaktivität ist bislang beispiellos, und weitergehende Untersuchungen dieser neuartigen Variante induzierter Reaktivitätsasymmetrie bieten einen interessanten Rahmen für zukünftige Forschung.

Die Umsetzung von $[Au(C{\equiv}C{-}Fc)]_n$ mit dppf lieferte den erwarteten Komplex $[(Au\text{-}C{\equiv}C\text{-}Fc)_2(\mu\text{-}dppf)]$, und die erhaltenen Strukturdaten bestätigen eine gewöhnliche Koordination. Um die Komplexchemie von **1** abzurunden, wurde dessen Koordinationsverhalten auch gegenüber Silber(I) untersucht, und die Struktur des Komplexes $[Ag_2(\mu\text{-}\mathbf{1})_2](NO_3)_2{\cdot}H_2O$ konnte mittels einer Röntgenstrukturanalyse bestimmt werden.

Die Modifizierung bereits bestehender Monolagen durch darauf folgende Reaktionen ist ein attraktiver Ansatz, um Oberflächen nach Maß zu funktionalisieren. Im Rahmen dieser Arbeit wurden einige Ferrocenderivate auf ihre Eignung für mögliche Oberflächenreaktionen untersucht. Hierbei erschien die kupferkatalysierte 1,3-dipolare Cycloaddition von Azidoferrocenderivaten mit terminalen Alkinen ein viel versprechender Ansatz. Die Umsetzung gelang, scheiterte jedoch in einem engeren Sinne als „Click"-Chemie, da die Triazolbildung hier nur unter striktem Ausschluss von Sauerstoff und Feuchtigkeit und mit nur mäßigen Ausbeuten möglich war. Erprobt wurden in diesem Zusammenhang auch Staudinger-Reaktionen zwischen den Azidoferrocenderivaten und dppf. Die Umsetzung mit dem monosubstituierten Azidoferrocen, FcN_3, lieferte das erwartete Produkt glatt, während die Reaktion von dppf mit 1,1'-Diazidoferrocen zu einem aller Wahrscheinlichkeit nach polymeren Material führte. Die nukleophile Addition sekundärer Amine an 1,1'-Diisothiocyanatoferrocen (**2**) hingegen verlief quantitativ, und die entsprechenden Thioharnstoffderivate konnten so ohne weitere Aufreinigung in analysenreiner Form isoliert werden. Daher stellt **2** ein bestens geeignetes System für eine anschließende Funktionalisierung von Monolagen mit terminalen Aminogruppen dar.

Acknowledgements

I would like to express my sincerest gratitude to all who have encouraged, supported and advised me during the work presented in this thesis. In particular I would like to thank the following people and institutions.

My academic teacher, Prof. U. Siemeling, for giving me the opportunity to work in his group, his scientific guidance and for providing the interesting topic of this thesis.

I have had the good fortune to work under the supervision of Prof. Nick Long at Imperial College London and I would like to thank sincerely for the generousness and the support during this time and for the invaluable opportunity to experience a different (academic) culture from the best.

Dr. Ballav, Dr. Zharnikov and especially Dr. Weidner from the research group 'Applied Physical Chemistry' at the University of Heidelberg for their important contribution to this thesis by dealing with the surface analysis.

Dr. Bruhn and Astrid Pilz for collecting and solving the X-ray crystal structures.

Dr. Maurer for recording excellent NMR spectra.

Dr. Fürmeier for mass spectrometry.

Jörg Ho for excellent elemental analyses.

My colleagues from the MOC in Kassel, Christian, Frauke, Jens, Mario and Tanja, and the great people from the Long group, Ian, Kathryn, Kin, Mel, Phil and Steve for all the help and for creating stimulating and pleasant environments.

The Otto-Braun-Fonds is thanked for a doctoral fellowship and the DAAD for a research grant.

Finally I would like to thank my family, Claudia, Liv and Elvin and Gordana, Gerd and Eja for all their love and endless support throughout.

Abbreviations

Å	Ångstrom (10^{-10} m)
btc	1,2,4,5-benzenetetracarboxylate
BE	binding energy
Bu	butyl
cp	cyclopentadienyl / C_5H_5
CV	cyclic voltammetry (cyclic voltammogram respectively)
d	doublet
DMS	dimethylsulfide
DiPA	diisopropylamine
dppf	1,1′-bis(diphenylphosphino)ferrocene
EA	elemental analysis
eV	electron volt
fc	ferrocene-1,1′-diyl group, [Fe(η^5-C_5H_4)$_2$]
Fc	ferrocenyl group, [Fe(η^5-C_5H_4)(η^5-C_5H_5)]
fwhm	full width at half maximum
hmt	hexamethylenetetramine
Hz	hertz, [s^{-1}]
i-Pr	isopropyl
IR	infrared spectroscopy
IRRAS	infrared reflection absorption spectroscopy
J	coupling constant

m	multiplet
NEXAFS	near edge X-ray absorption fine structure
NMR	nuclear magnetic resonance
OTf	trifluoromethylsulfonate, $CF_3SO_3^-$, triflate
p	para-position on benzene ring
Ph	phenyl
ppm	parts per million
s	singlet
SHG	second harmonic generation
SPR	surface plasmon resonance
surfactant	surface active agent
t	triplet
TDM	transition dipole moment
THF	tetrahydrofuran
THT	tetrahydrothiophene
TMEDA	N,N,N′,N′-tetramethylethylenediamine
VE	valence electron
XP	X-ray photoelectron
XPS	X-ray photoelectron spectroscopy
δ	chemical shift (NMR)
ν	frequency

Contents

Chapter 1
Introduction

1.1 General Introduction – Motivation and Outline

Nanotechnology is one of the most fascinating and progressing branches of applied science in the recent past. It is a highly multidisciplinary field of research whose unifying theme is the control of matter on the atomic and molecular scale. The term 'nano' is normally used for objects with at least one dimension less than 100 nm. These dimensions are already reached in current microelectronics by downscaling of 'classical' fabrication techniques like lithography. However, there are fundamental physical limits linked to an ongoing miniaturisation by this *top-down* approach.[1] The opposite strategy, namely a *bottom-up* approach, is the preparation of very small, functional structures by self-assembly of single functional units. In this case the ultimate limit for such a unit, e.g. a device or switch, is a single molecule.

Molecular self-assembly has been defined by Whitesides as "the spontaneous association of molecules under equilibrium conditions into stable, structurally well-defined aggregates joined by noncovalent bonds".[2] ('Structurally well-defined' means that self-assembled structures are 100% 'crystalline' organised within the domains in the object.)[3]

Since the surface-to-volume ratio increases with decreasing scale (cube-square law) and interactions between assembling molecules take place at the interface, in some sense, nanostructures are 'all surface'.[4] Thus, the control of surface properties is crucial for nanofabrication and the key step for a *bottom-up* approach may be considered in functionalisation of highly ordered surfaces.

A very attractive way to obtain highly ordered surfaces with tailored properties is the fabrication of self-assembled monolayers (SAMs) on solid surfaces.[4,5,6,7,8]

SAMs are monomolecular films, formed spontaneously by the adsorption of surfactants on suitable substrates and are themselves nanostructures. Due to the ease

of their preparation and the possibility to add an enormous variety of organic or organometallic functions at the surface of metals, semiconductors and metal oxides, SAMs play a decisive role for the development of nanotechnology.

SAMs can be used to stabilise and functionalise preformed nanometer-scale structures as well as macroscopic structures and thus provide an extraordinarily broad field of potential applications, ranging from protective coatings (e.g. corrosion inhibition),[4,6] microelectronics (or *nano*electronics)[3,9,10] mentioned above to modified electrodes,[11] biosensors,[12,13] chemical sensors[14,15,16] and catalysis[17] up to molecular machines.[18,19]

The possibility to incorporate functional groups with switchable properties into a SAM offers a convenient method to fashion 'smart surfaces', i.e. surfaces which change their interfacial properties in a defined manner in response to an external stimulus.[20] Stimuli responsive surfaces are well known in surface engineering and find application for example in 'smart windows', where the light transmittance is altered by impressing voltage to the interface. SAMs in which the physical, chemical and biological properties are reversibly tuneable are an intriguing field for many applications[21] and already realised for light-induced,[22,23] pH-driven[24] or electrochemical switching.[25,26]

In the field of SAM fabrication two adsorbate/substrate combinations became most common and intensively investigated,[27] viz. alkylsilanes on oxide surfaces[28] and sulfur-containing molecules on gold.[29] Since gold is the noblest metal and chemically highly inert (it does not react with atmospheric oxygen), Au(111) films became the standard substrate for SAM preparation. Sulfur-containing molecules, especially thiols, have a high affinity for gold and displace other organic material from this surface. Hence the SAM preparation is conveniently possible under ambient conditions and sulfur-based adsorbates on gold can be considered as the prototypical[4] or archetypal[7] system and are by far the most extensively studied class of SAMs.

The aim of the research described in this thesis is the preparation and investigation of SAMs with electrochemically switchable properties based on a single molecular component. The electroactive functional units employed are based on ferrocene.[30,31,32] The oxidation of ferrocene is reversible. Ferrocene is almost as stable in its positively charged form (+) as in the neutral form (0). A surface regularly decorated with ferrocene moieties therefore could be applicable for high density charge and/or data storage.[33]

Since a highly ordered array of the molecules on the surface is crucial for an optimised system and the process of self-assembly depends on miscellaneous molecular parameters, an investigation of the impact of variations of the molecular structure of the adsorbates is necessary. For the reasons mentioned above the substrates of choice are gold (111) surfaces. Therefore, the research will place emphasis on sulfur-containing ferrocene ligands.

Nevertheless, sulfur chemistry on gold surfaces is related to serious concerns with regard to the long-term stability[11,34,35] and an increase of the attractive forces between the adsorbates and the substrate is desirable. This may be achieved by different chemistry, i.e. surface-active groups which form more robust bonds and/or by chelating ligands using multiple attachment points to the substrate.[34,36,37,38]

These demands lead to the following general architecture for the target molecules:

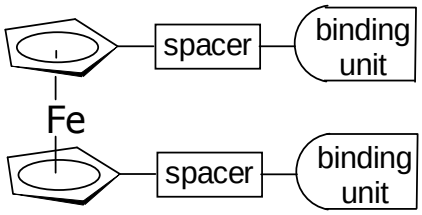

Figure 1-1: Design of the target compounds.

The ferrocene-nucleus serves as a terminal redox-active unit. Functionalisations at the 1- and 1'- position with groups suitable for attachment to gold lead to symmetrically disubstituted ferrocene derivatives. The binding units can be separated by variable spacers from the cyclopentadienyl rings. Within the scope of

the research described in this thesis I have focused on the systematic variation and investigation of the contribution of the binding units towards SAM morphology and stability. Therefore the synthesis of different spacer groups was less important in this context.

The present thesis deals with surface coordination chemistry of ferrocene-based ligands, which is difficult to study. An investigation of the molecular coordination chemistry of these ligands is a meaningful extension of this research. Since all SAMs described in this thesis were prepared on gold, insight into structural properties of relevant gold(I) complexes of the ligands may provide a bridge between surface chemistry and molecular coordination chemistry.[39] Therefore the focus of efforts in this direction is put on the coordination chemistry towards gold(I) compounds.

Although all SAMs in this study are based on a single molecular component, intentionally leading to a densely packed array of the functional units, this is not desirable in every case. A 'diluted' functionalisation of SAMs can be advantageous for different applications and one attractive synthetic approach to realise such structures is the modification of a SAM after formation by a subsequent chemical reaction with terminal functional groups on the SAM.[40,41,42] Therefore, the capability of some ferrocene derivatives for potential surface reactions will be explored as well.

1.2 Self-Assembled Monolayers

Self-assembled monolayers are highly ordered molecular assemblies, which form spontaneously by the absorption of surfactants with a specific affinity of their binding units to a substrate.[4,5] The handling of gold substrates is particularly simple, since the clean substrate can be used under standard conditions, including oxygen and moisture. The process of SAM preparation from solution is shown in figure 1-2.

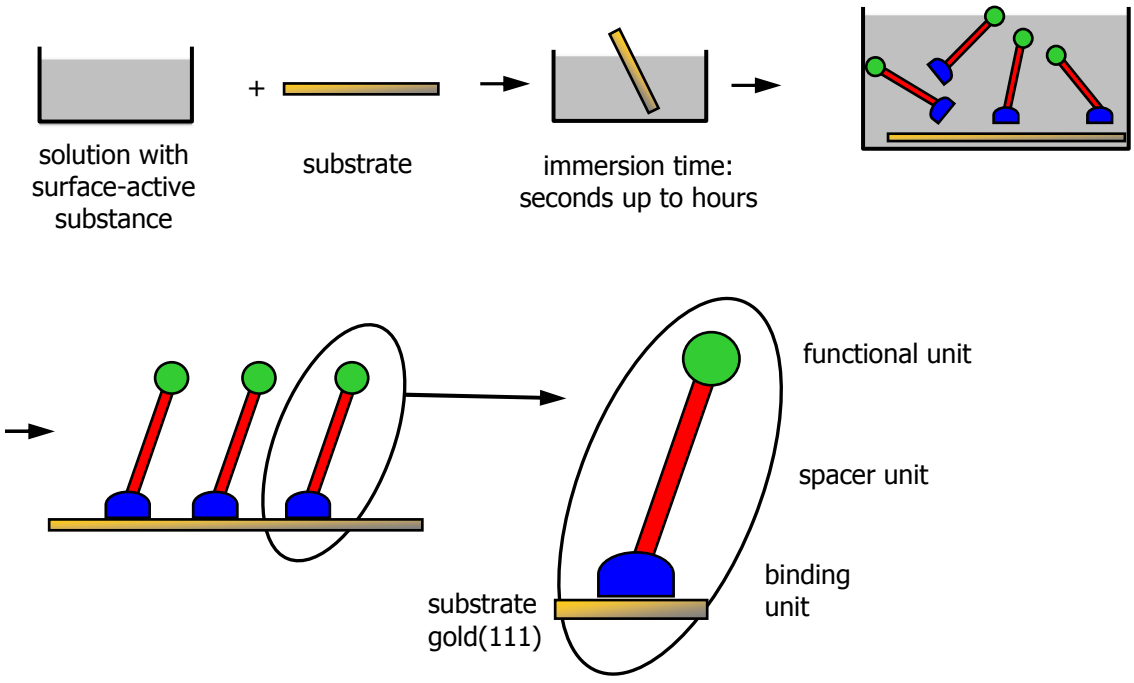

Figure 1-2: SAM-Preparation.

SAMs can be conveniently prepared by immersing the substrate into a dilute (~ 1 – 10 µM) adsorbate solution. Strong interactions between the binding units of the surfactants and the surface quickly lead (milliseconds to minutes) to a dense coverage (usually 80 – 90 % of the maximum coverage). Lateral interactions between the adsorbates cause a subsequent reorganisation on the surface, resulting in a maximisation of packing density and order. (The maximum coverage of alkanethiols on planar gold is ~2 x 10^{14} molecules/cm².)[40] This latter process largely depends on the immersion time and usually takes several hours (~12 – 18 h at room temperature

for *n*-alkane thiols in ethanolic solution).[4] The self-assembly process is also largely dependent on the solvent[43] and the right choice is crucial for the quality of a SAM. Highly ordered SAMs are usually obtained from ethanol. Since ethanol has a low vapour pressure, low toxicity and is available in high purity it is the most common solvent for SAM fabrication on gold. Dichloromethane also usually gives rise to well defined SAMs and can be a good alternative for adsorbates which are insoluble in ethanol.

1.2.1 SAM Characterisation

SAM preparation may be simple, but the opposite is true for the characterisation of a monomolecular film. To obtain detailed data about the quantitative chemical composition of the monolayer, the type of binding, the orientation and the degree of order of the absorbates on the surface it is necessary to combine quite an arsenal of complementary analysis techniques.[7,40]

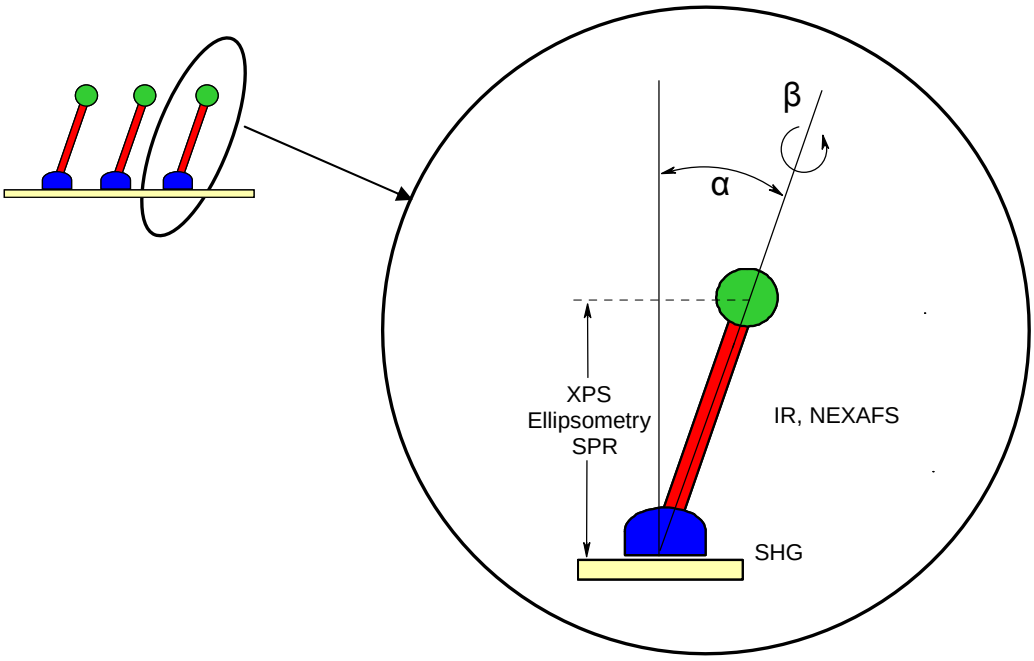

Figure 1-3: Schematic side view of a molecule chemisorbed on a substrate and surface analytical methods suitable for extracting pertinent information indicated in the figure.

Figure 1-3 shows the most common surface analysis techniques for SAM characterisation.

The chemisorption process and kinetics can be studied in real time by second harmonic generation spectroscopy (SHG).[44,45] Film thickness can be investigated by ellipsometry, surface plasmon resonance spectroscopy (SPR) and X-ray photoelectron spectroscopy (XPS).[46] XPS is probably the most important tool in the field of SAM characterisation since it is a quantitative analysis technique that measures the elemental surface composition as well as the chemical and electronic state of the elements at the surface. A complementary technique to XPS is near edge X-ray absorption fine structure spectroscopy (NEXAFS)[47,48] which is highly sensitive to bond angles and therefore suitable to investigate the orientation of the molecules on the surface and their near-range order. Infrared spectroscopy (IR)[49] is also a powerful tool for SAM characterisation since it is possible to obtain data about the chemical composition as well as the orientation of the molecules with respect to the surface normal. Microscopy-based techniques (STM, AFM) provide a direct image of the structure and are irreplaceable in terms of local information of the SAM morphology.

1.3 Ferrocene

Ferrocene was first prepared in 1951 by two different groups, simultaneously and unintentionally in both cases. Kealy and Pauson tried to synthesise fulvalene by the oxidative coupling of cyclopentadienyl magnesium bromide with ferric chloride.[50] The group around Miller prepared ferrocene by high temperature reaction of freshly distilled cyclopentadiene with iron.[51] The elucidation of its structure in 1952, again by two groups simultaneously and independently, led to the award of the Nobel prize for Chemistry in 1973 to Wilkinson[52] and Fischer[53] - and to an explosion of interest in complexes of transition metals with hydrocarbons. Historically this may be considered as the starting shot for the flourish of organometallic chemistry.

Ferrocene is the prototypical metallocene: two cyclopentadienyl rings bind on opposite sides of a central metal atom leading to the sandwich compound fashion of the complex. Since its discovery ferrocene has witnessed a remarkable career and applications of ferrocene-based compounds are ranging from material science and catalysis to bioorganometallic chemistry.

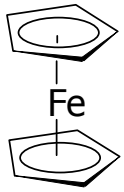

Figure 1-4: Structure of Ferrocene.

1.3.1 Physical Properties and Chemical Behaviour of Ferrocene

Ferrocene is an air-stable orange solid and sublimes easily in vacuum or upon heating at atmospheric pressure. It is soluble in most organic solvents but is insoluble in water. The electronic structure can be considered formally by the binding of two aromatic cyclopentadienyl anions and an iron(II) cation leading to an uncharged 18-valence-electron complex. The resulting noble gas electron configuration of krypton makes ferrocene particularly stable. On the other hand the iron(II) centre is readily oxidised to iron(III) at low potential (~0.5 V vs. SCE). The ferrocenium cation is

particularly stable and the ferrocene/ferrocenium redox couple therefore reversible, hence ferrocene is often used as an internal standard in electrochemical experiments. In its chemical properties ferrocene undergoes many reactions characteristic for electron-rich aromatic compounds. Ferrocene is susceptible to electrophilic substitution. Due to the high electron density of the cyclopentadienyl rings it reacts 3 x 10^6 times faster than benzene.[54] Reactions with strongly oxidising electrophiles lead to oxidation of ferrocene to ferrocenium, which is inert to electrophilic attacks. Therefore, direct nitration or halogenation of ferrocene is impossible. Alternatively, derivatisation of ferrocene is often possible via metallation reactions.

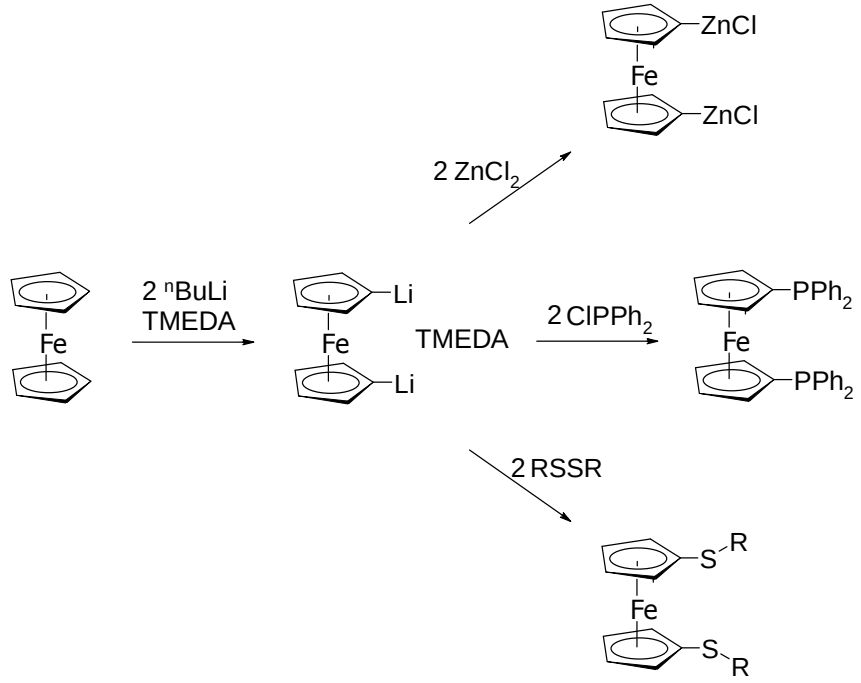

Figure 1-5: Synthetic Routes to 1,1'-symmetrical Ferrocene Derivatives relevant to this thesis.

Symmetrical 1,1'-substituition is usually carried out by lithiation of ferrocene with two equivalents of butyllithium in the presence of N,N,N',N'-tetramethylethylene-diamine (TMEDA) in hexane[55] and subsequent reaction with an electrophile. Figure 1-5 shows the derivatisation of ferrocene with a series of electrophiles used within the scope of this thesis.

1.4 Chemistry of Gold

Since all surfactants in this thesis are tailored for adsorption to gold (111) surfaces the investigation of their coordination behaviour towards gold(I) is a logical extension of the surface-chemical research.

The electronic configuration of gold is $1s^2\ 2s^2\ 2p^6\ 3d^{10}\ 4s^2\ 4d^{10}\ 4f^{14}\ 5s^2\ 5d^{10}\ 6s^1$. The chemistry of gold is dominated by the oxidation states (I) and (III), having the electron configuration [Xe] $4f^{14}\ 5d^{10}\ 6s^0$ and [Xe] $4f^{14}\ 5d^8\ 6s^0$, respectively.

Compounds of Au^I assume the coordination number two with a linear coordination geometry and a 14 VE configuration in most cases. Au^I complexes with a coordination number of three (16 VE, trigonal planar) or four (18 VE, tetrahedral) are also known but less common,[56] since the participation of the energetically high lying $6p_y$ and $6p_z$ orbitals causes high promotion energies. The general form of gold(I) complexes is LAuX (L= neutral ligand; X = anionic ligand) and gold(I) exhibits a strong preference for large and soft (easily polarisable) donor ligands L.[57] The most stable gold(I) complexes are formed with P- or S-donor ligands and isocyanides and stability increases with rising polarisability (softness) of the ligand (PR_3 > RNC > SR_2).

1.4.1 Relativistic Effects

Nowhere in the periodic table are relativistic effects more pronounced than in gold chemistry.[58,59,60] These effects can be attributed qualitatively to the high speed of electrons if they move near the heavy nucleus under the influence of a pronounced point charge. The velocity of the 1*s* electrons of gold is 58% of the speed of light,[58] thus relativistic mass increase for these electrons becomes significant, also with consequences for the orbital radii of these electrons. To keep the equilibrium between the Coulomb force and the centripetal force for the increased mass, the Bohr radii of the inner electrons shrink. This reduction of the radii causes an energetic stabilisation and radial contraction of the *s*- and to a smaller extent also the *p*-orbitals. (The radial shrinkage for the 1*s* orbital is 19% compared to the nonrelativistic estimated Bohr

radius.)[56] On the other hand there is an enhanced screening of the nuclear attraction for the 'outer' electrons, resulting in an energetic destabilisation and expansion on the *d*- and *f*-orbitals. Since the *s*- and *p*-orbitals are pushed down in energy and the *d*- and *f*-orbitals up, the 6*s* and 5*d* states are brought much together in energy. This effect explains qualitatively the unique chemical behaviour of gold. Due to the energetically stabilised low lying 6*s* state, gold exhibits the highest oxidation potential and the highest electron affinity of all metals. On the other hand the separation between the 6*s* and 5*d* orbitals is rather small and a hybridisation therefore requires only very little promotion energy.

1.4.2 Aurophilicity

From a classical point of view gold(I) cations posses closed shells [$5d^{10}$] and no attractive forces are expected between two ions of the same charge, but electrostatic repulsion. However, there is a lot of crystallographic evidence for Au–Au distances in sterically unhindered gold(I) complexes typically at 2.8 – 3.3 Å, well below the sum of the estimated van der Waals radii (~ 3.6 Å).[60] The energy of this unexpected bonding is in the region of 29 – 46 kJ mol^{-1}, comparable with hydrogen bonds,[59] and similarly determines in part the molecular configuration and crystal lattices of gold compounds. Schmidbaur introduced the term "aurophilicity" or "aurophilic attraction" for this bonding between atoms with a seemingly closed-shell configuration.[61] Aurophilicity can be rationalised by the hybridisation of 5*d* and 6*s* orbitals, giving rise to interactions between two donor ligands and gold along the molecular z-axis. The aurophilic attraction occurs parallel or perpendicular to the molecular axis and is a result of overlaps between the 'broken up' $5d^{10}$ shells.

1.5 References

[1] M. Schulz, *Nature* **1999**, *399*, 729.

[2] G. M. Whitesides, J. P. Mathias, C. T. Seto, *Science* **1991**, *254*, 1312.

[3] A. P. H. J. Schenning, E. W. Meijer, *Chem. Commun*. **2005**, 3245.

[4] J. C. Love, L. A. Estroff, J. K. Kriebel, R. G. Nuzzo, G. M. Whitesides, *Chem. Rev.* **2005**, *105*, 1103.

[5] A. Ulman, *Chem. Rev.* **1996**, *96*, 1533.

[6] F. Schreiber, *J. Phys.: Condens. Matter* **2004**, *16*, R881.

[7] F. Schreiber, *Prog. Surf. Sci.* **2000**, *65*, 151.

[8] E. Gomar-Nadal, J. Puigmartí-Luis, D. B. Amabilino, *Chem. Soc. Rev.* **2008**, *37*, 490.

[9] J. M. Tour, *Acc. Chem. Res.* **2000**, *33*, 791.

[10] G. Bottari, D. Olea, C. Gómez-Navarro, F. Zamora, J. Gómez-Herrero, T. Torres *Angew. Chem.* **2008**, *120*, 2056.

[11] J. J. Gooding, F. Mearns, W. Yang, J. Liu, *Electroanalysis* **2003**, *15*, 81.

[12] N. K. Chaki, K. Vijayamohanan, *Biosens. Bioelectron.* **2002**, *17*, 1.

[13] Th. Wink, S. J. van Zuilen, A. Bult, W. P. van Bennekom, *Analyst* **1997**, *122*, 43R.

[14] E. U. T. van Velzen, J. F. J. Engbersen, D. N. Reinhoudt, *J. Am. Chem. Soc.* **1994**, *116*, 3597.

[15] S. Flink, F. C; J. M. van Veggel, D. N. Reinhoudt, *Sensors Update* **2001**, *8*, 3.

[16] J. Rickert, T. Weiss, W. Göpel, *Sensors & Actuators* **1996**, *B 31*, 45.

[17] E. J. Calvo, M. S. Rothacher, C. Bonazzola, I. R. Wheeldon, R. C. Salvarezza, M. E. Vela, G. Benitez, *Langmuir* **2005**, *21*, 7907.

[18] S. Saha, E. Johansson, A. H. Flood, H.-R. Tseng, J. I. Zink, J. F. Stoddart, *Chem. Eur. J.* **2005**, *11*, 6846.

[19] H.-R. Tseng, D. Wu, N. X. Fang, X. Zhang, J. F. Stoddart, *Chem.Phys.Chem.* **2004**, *5*, 111.

[20] Y. Liu, L. Mu, B. Liu, J. Kong, *Chem. Eur. J.* **2005**, *11*, 2622.

[21] L. Mu, Y. Liu, S. Cai, J. Kong *Chem. Eur. J.* **2007**, *13*, 5113.

[22] K. Ichimura, S.-K. Oh, M. Nakagawa *Science* **2000**, *288*, 1624.

[23] N. Delorme, J.-F. Bardeau, A. Bulou, F. Poncin-Epaillard *Langmuir* **2005**, *21*, 12278.

[24] F. Auer, D. W. Schubert, M. Stamm, Arnebrant, A. Swietlow, M. Zizlsperger, B. Sellergren, *Chem. Eur. J.* **1999**, *5*, 1150.

[25] J. Lahann, S. Mitragotri, T.-N. Tran, H. Kaido, J. Sundaram, I. S. Choi, S. Hoffer, G. A. Somorjai, R. Langer, *Science* **2003**, *299*, 371.

[26] I. S. Choi, Y. S. Chi, *Angew. Chem. Int. Ed.* **2006**, *45*, 4894.

[27] S. Onclin, B. J. Ravoo, D. N. Reinhoudt, *Angew. Chem. Int. Ed.* **2005**, *44*, 6282.

[28] J. Sagiv, *J. Am. Chem Soc.* **1980**, *102*, 92.

[29] R. G. Nuzzo, D. L. Allara, *J. Am. Chem. Soc.* **1983**, *105*, 4481.

[30] N. J. Long, *Metallocenes: An Introduction to Sandwich Complexes*, Blackwell Science, Oxford, UK, **1998**.

[31] P. Stepnicka (Ed.), *Ferrocenes: Ligands, Materials and Biomolecules*, Wiley, Chichester, **2008**.

[32] A. Togni, T. Hayashi, (Ed.), *Ferrocenes*, VCH, Weinheim, **1995**.

[33] K. M. Roth, J. S. Lindsey, D. F. Bocian, W. G. Kuhr, *Langmuir* **2002**, *18*, 4030.

[34] C.-J. Zhong, M. D. Porter, *J. Am. Chem. Soc.* **1994**, *116*, 11616.

[35] Y.-S. Shon, T. R. Lee, *J. Phys. Chem. B* **2000**, *104*, 8192.

[36] H. Liu, S. Liu, L. Echegoyen, *Chem. Commun.* **1999**, 1493.

[37] J.-S. Park, A. N. Vo, D. Barriet, Y.-S. Shon, T. R. Lee, *Langmuir* **2005**, *21*, 2902.

[38] N. Garg, T. R. Lee, *Langmuir* **1998**, *14*, 3815.

[39] U. Siemeling, D. Rother, C. Bruhn, H. Fink, T. Weidner, F. Träger, A. Rothenberger, D. Fenske, A. Priebe, J. Maurer, R. Winter, *J. Am. Chem. Soc.* **2005**, *127*, 1102.

[40] T. P. Sullivan, W. T. S. Huck, *Eur. J. Org. Chem*. **2003**, 17.

[41] J. P. Collman, N. K. Devaraj, C. E. D. Chidsey, *Langmuir* **2004**, *20*, 1051.

[42] J. K. Lee, Y. S. Chi, I. S. Choi, *Langmuir* **2004**, *20*, 3844.

[43] D. Käfer, G. Witte, P. Cyganik, A. Terfort, C. Wöll, *J. Am. Chem. Soc.* **2006**, *128*, 1723.

[44] N. J. Long, *Angew. Chem. Int. Ed. Engl.* **1995**, *34*, 21.

[45] Y. R. Shen, *Annu. Rev. Phys. Chem.* **1989**, *40*, 327.

[46] J. F. Watt, J. Wolstenholme, *An Introduction to Surface Analysis by XPS and AES*, Wiley, Chichester, UK, **2003**.

[47] J. Haase, *Chem. Unserer Zeit* **1992**, *26*, 219.

[48] J. Stöhr, *NEXAFS Spectroscopy*, Springer, New York, **1992**.

[49] A. N. Parikh, D. L. Allara, *J. Chem. Phys.* **1992**, *96*, 927.

[50] T. J. Kealey, P. L. Pausen, *Nature* **1951**, *168*, 1039.

[51] S. A . Miller, J. A. Tebboth, J. F. Tremaine, *J. Chem. Soc.*, **1952**, 632.

[52] G. Wilkinson, M. Rosenblum, M. C. Whiting, R. B. Woodward, *J. Am. Chem. Soc.* **1952**, *74*, 2125.

[53] E. O. Fischer, W. Pfab, *Z. Naturforschung B*, **1952**, *7*, 377.

[54] C. Elschenbroich, A. Salzer, *Organometallics,* 2nd Ed., VCH, Weinheim, **1992**.

[55] M. D. Rausch, D. J. Ciapenelli, *J. Organometal. Chem.* **1967**, *10*, 127.

[56] M. C. Gimeno, A. Laguna, *Chem. Rev.* **1997**, *97*, 551.

[57] H. Schmidbaur, *Chem. Soc. Rev.*, **1995**, *24*, 391.

[58] T. M. Klapötke in: S. Patai, Z. Rappoport (Eds.), *The chemistry of organic derivatives of gold and silver*, Wiley, Chichester, UK, **1999**, 401-430.

[59] P. Pyykkö, *Angew. Chem. Int. Ed.* **2004**, *43*, 4412.

[60] H. Schmidbaur. S. Cronje, B. Djordjevic, O. Schuster, *Chem. Phys.* **2005**, *311*, 151.

[61] H. Schmidbaur, *Gold Bull*. **1990**, *23*, 11.

Chapter 2
Ferrocene-Based SAMs

The preparation of several symmetrically 1,1'-substituted ferrocene derivatives that contain anchoring groups suitable for chemisorption on gold is described.
The results of analytical investigations of SAMs formed from several of the ferrocene ligands are presented and discussed in matters of the film quality and possible binding modes.

2.1 Introduction

Self-assembled monolayers (SAMs) on solid surfaces are of great current interest in science and technology.[1,2,3,4,5] SAMs formed by the aggregation of organosulfur compounds on gold have received most attention, ever since it was first reported that SAMs on gold can be prepared conveniently by chemisorption of di-*n*-alkyl disulfides or related cyclic derivatives from dilute solutions.[6] Adsorbate molecules carrying terminal functional units can lead to functional SAMs.[2,3] Depending on the nature of the functional units, such SAMs can be utilised for diverse applications. For example, redox-active adsorbate species based on tetrathiafulvalene,[7] ferrocene and porphyrin[8] have been widely used for electrode modification and related purposes.[9]
Owing to a surface chelate effect, oligodentate adsorbate molecules can bind particularly strongly to a substrate. Even with relatively weakly binding anchor units such as, for example, thioethers[10] stable and densely packed SAMs on gold have been achieved this way.
The preparation of several new sulfur-containing 1,1'-disubstituted ferrocene derivatives will be presented together with the results of a detailed investigation concerning the behaviour of these and related dipodal adsorbate molecules on gold. The ferrocene derivatives investigated in this study are collected in Figure 2-1.

Synthetic work and crystal structures will be dealt with first, followed by a surface science section focusing on film fabrication and characterisation.

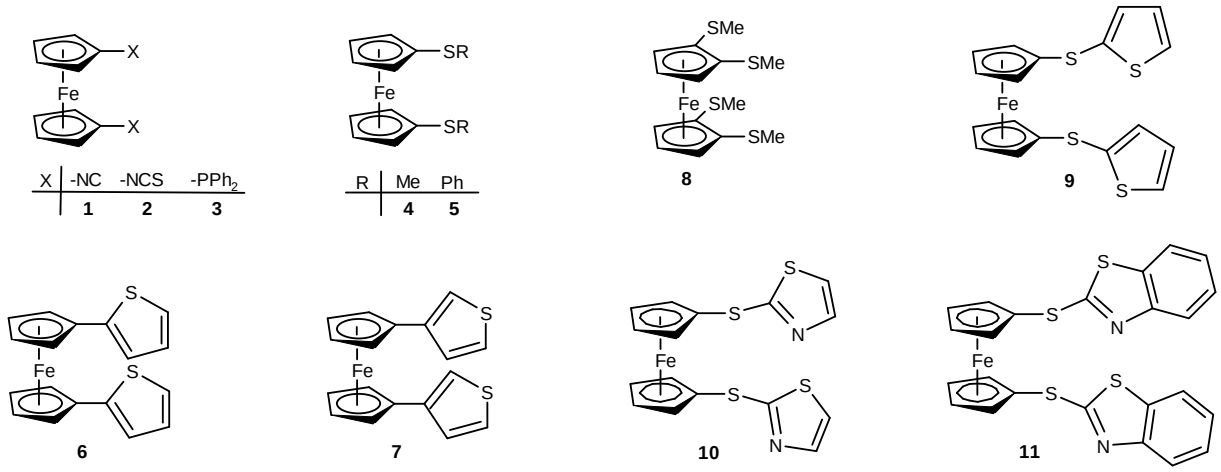

Figure 2-1: Ferrocene-based ligands investigated in this study. The derivatives **1** – **7** posses two anchoring units, ligands **8** – **11** display four potential attachment possibilities.

2.2 Synthesis and Characterisation of Compounds

The preparation of compounds **2**, **7** and **9** – **11** has not been described before.

2.2.1 Synthesis and Characterisation of 1,1'-Diisothiocyanatoferrocene (2)

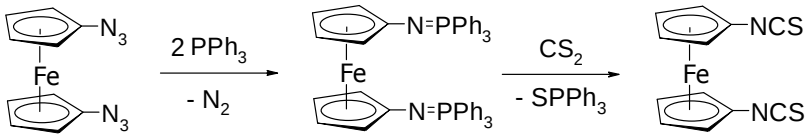

Figure 2-2: Synthesis of 1,1'-Diisothiocyanatoferrocene.

1,1'-Diisothiocyanatoferrocene (**2**) was obtained in good yield (82%) from the aza-Wittig reaction of $[Fe\{C_5H_4(N{=}PPh_3)\}_2]$[11] with CS_2.[12] $[Fe\{C_5H_4(N{=}PPh_3)\}_2]$ was prepared by the Staudinger reaction between 1,1'-diazidoferrocene[13] and triphenylphosphane. The subsequent reaction was carried out in a thick-walled 'Rotaflo' ampoule at 90°C for 3h with an extensive excess of carbon disulfide, which served as solvent as well. Work-up was done by removing volatile components under vacuum and purification of the crude product by column chromatography on silica gel with *n*-hexane.

The ^{1}H NMR spectrum of **2** in $CDCl_3$ shows two singlets at 4.20 and 4.51 ppm. In the ^{13}C NMR spectrum three signals were found at 67.1, 68.0, 87.0 ppm in the region typical for cyclopentadienyl C atoms, the fourth signal at 133.8 ppm corresponds to the isothiocyanato carbon atom. The ESI mass spectrum of **2** shows the molecular ion with peaks at 299.95, 300.95 and 301.94 amu in a ratio of 100 : 18 : 9, in nice accordance with the calculated pattern.

Due to the very broad and dominant ν(NCS) stretching mode at 2088 cm^{-1}, the IR spectrum is quite significant for **2**.

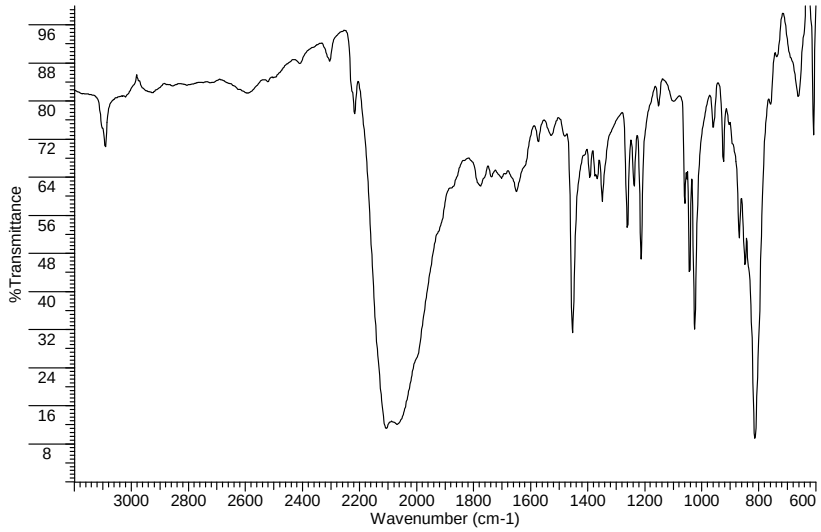

Figure 2-3: IR-Spectrum of **2**.

The electrochemical behaviour of **2** has been investigated by cyclic voltammetry.

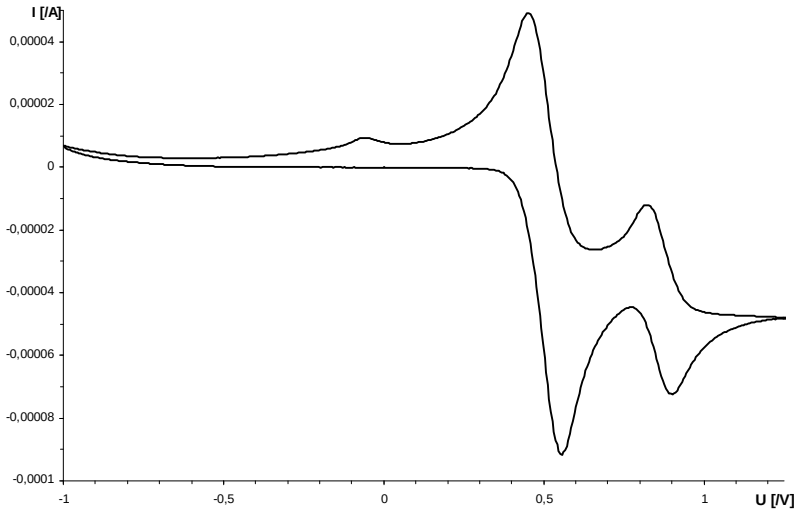

Figure 2-4: Cyclic voltammogram of **2**. The chosen conditions were: 0.0001 M solution of **2** in CH_2Cl_2 with 0.1 M $[N^nBu_4][PF_6]$ as supporting electrolyte at a scan rate of 50 mV/s at room temperature with Ag/AgCl reference electrode and Pt working and auxiliary electrodes and ferrocene as internal standard.

1,1'-Diisothiocyanatoferocene exhibits a quasi-reversible oxidation at $E_{½}$ = +0.86 V with a ΔE_P value of 78 mV. The redox potential is anodically shifted by ~0.36 V with respect to ferrocene (at +0.50 V). This reflects the expected electron-withdrawing effect of the NCS groups.

2.2.2 Synthesis and Characterisation of 1,1'-Di(3-thienyl)ferrocene (7)

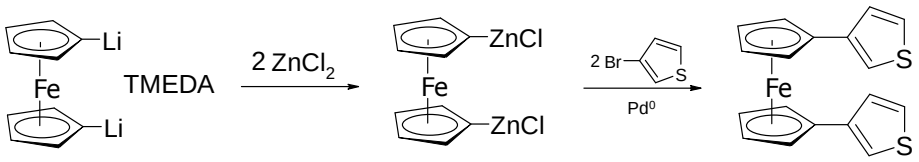

Figure 2-5: Synthesis of 1,1'-Di(3-thienyl)ferrocene.

7 was prepared by Negishi coupling of $[Fe\{C_5H_4(ZnCl)\}_2]$ with 3-bromothiophene in the presence of $[Pd(PPh_3)_4]$ in analogy to the 2-thienyl analogue.[14] $[Fe\{C_5H_4(ZnCl)\}_2]$ was generated by the drop wise addition of a THF solution of $ZnCl_2$ to a suspension of 1,1'-dilithioferrocene-TMEDA adduct in hexane. The overall yield could be enhanced notably by the use of air-tight glassware (a thick-walled 'Rotaflo' ampoule or a Young-flask) instead of standard Schlenk equipment, increase of the reaction temperature up to 60 °C and an extended reaction time (4 d).

The workup was done by hydrolysis with 1 M HCl and subsequent extraction with Et_2O and CH_2Cl_2. The combined organic layers were dried with Na_2SO_4 and after filtration the volatile components were removed in vacuo. The crude product was purified by column chromatography on silica gel with *n*-hexane/CH_2Cl_2 (20 : 1) as eluent. The first two bands contained ferrocene and the mono-substitution product (3-thienyl)ferrocene, while the third band afforded the product as an orange, microcrystalline solid in good yield (68%).

1,1'-Di(3-thienyl)ferrocene shows two singlets in the ^1H NMR spectrum ($CDCl_3$) in the region typical for cyclopentadienyl rings at 4.21 and 4.39 ppm and three signals at 6.90, 6.95 and 7.18 ppm, typical for aromatic protons. The ^{13}C NMR spectrum

shows signals at 68.1, 69.9, 118.0, belonging to the cyclopentadienyl carbon atoms, and at 125.2, 126.3 and 138.6 ppm, caused by the thiophene units.

2.2.3 Synthesis of the Di(thioether) Derivatives 9, 10 and 11

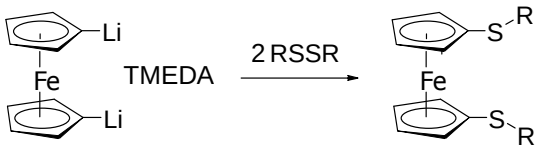

Figure 2-5: Synthesis of Ferrocene-based Sulfide Derivatives.

The di(thioether) derivatives [Fe{C_5H_4(SR)}$_2$] (**9**: R = thien-2-yl, **10**: R = thiazol-2-yl, **11**: R = benzothiazol-2-yl) were obtained from the reaction of 1,1'-dilithioferrocene[15] with the respective disulfide RSSR in analogy to the synthesis of [Fe{C_5H_4(SPh)}$_2$].[16]

2.2.3.1 Synthesis and Characterisation of 1,1'-Di(thien-2-ylthio)ferrocene (9)

Two equivalents of di(2-thienyl)disulfide in toluene were added drop wise to a suspension of the TMEDA adduct of 1,1'-dilithioferrocene (one equivalent) in *n*-hexane and stirred overnight. The workup was done under ambient conditions. Water was added to the reaction mixture and stirring continued for 10 min. The organic layer was separated, washed with water and dried with $MgSO_4$. Volatile components were removed in vacuo after filtration leading to the crude product as a yellow sticky material. Analytically pure material could be obtained by column chromatography on silica gel, using *n*-hexane/CH_2Cl_2 (10 : 1) as eluent. After removing the solvent with a rotary evaporator the product was obtained as a yellow, microcrystalline solid with 68 % yield.

The ^{1}H NMR spectrum confirmed the identity of the product and shows two singlets at 4.27 and 4.42 ppm ($CDCl_3$), typical for symmetrically disubstituted ferrocene, and a multiplet at 6.89 and two doublets at 7.04 (J = 2.4 Hz) and 7.23 (J = 5.4) ppm corresponding to the thienyl protons. The ^{13}C NMR spectrum shows signals at 66.9,

74.2, 127.2 and 128.4 ppm, the former two attributed to the tertiary cyclopentadienyl carbon atoms, the latter two belonging to the tertiary thienyl carbon atoms.
Crystals suitable for an X-ray diffraction analysis were obtained by slow evaporation of a concentrated CH_2Cl_2 solution of **9** in the fume hood. Unfortunately the quality of the crystal structure determination was severely affected by disorder.

X-ray crystallographic data of **9**:

Empirical formula	$C_{18}H_{14}FeS_4$
Formula weight	414.38
Temperature [K]	153(3)
Crystal system	orthorhombic
Space group	*F d d* 2
a [Å]	21.883(11)
b [Å]	19.335(18)
c [Å]	8.303(4)
α, *β*, *γ* [°]	90, 90, 90
V [Å^3]	3513(4)
Z	8
ρ_{calcd} [g cm^{-3}]	1.567
μ [mm^{-1}]	1.328
F(000)	1696
Crystal size [mm]	0.60 × 0.31 × 0.13
θ range [°]	2.81 – 25.00
Reflections collected	5554
Independent reflections	1492
R_{int}	0.1060
Reflections with $I>2\sigma(I)$	1424
Data/restraints/parameters	1492/1/100
GOF on F^2	1.079
$R1$ ($I>2\sigma(I)$)/w$R2$	0.0589/0.1583
largest diff. peak/hole [e·Å^{-3}]	1.476/–0.761

2.2.3.2 Synthesis and Characterisation of 1,1'-Di(thiazol-2-ylthio)ferrocene (10)

A solution of di(2-thiazolyl)disulfide in toluene was added dropwise to a stirred suspension of 1,1'-dilithioferrocene TMEDA adduct in *n*-hexane. After reaction over night water was added and stirring continued for 10 min. The organic layer was separated, washed with water and dried over $MgSO_4$. Volatile components were removed in vacuo. The brownish-yellow crude product was dissolved in a minimal amount of CH_2Cl_2 and purified by chromatography on neutral alumina, activity grade II, with *n*-hexane/CH_2Cl_2 (3 : 1) as eluent, affording the product as a yellow, microcrystalline solid in moderate yield (38 %). **10** is slightly sensitive to oxidation by

air in solution. Workup therefore should be performed rapidly and the isolated product stored under nitrogen.

The ^{1}H NMR spectrum ($CDCl_3$) shows two singlets in the region typical for cyclopentadienyl protons at 4.45 and 4.61 ppm and two doublets at 7.10 (J = 2.9 Hz) and 7.58 (J = 2.8 Hz) ppm, belonging to the thiazolyl protons. All expected signals were also found in the ^{13}C NMR spectrum, namely at 69.8, 72.6, 76.3 (cyclopentadienyl) and 119.0, 143.1, 169.2 ppm (thiazolyl).

Single crystals of **10** were obtained by evaporation of a concentrated solution of **10** in CH_2Cl_2. **10** exhibits perfectly staggered cyclopentadienyl rings, which is due to its crystallographically imposed centrosymmetric molecular structure.

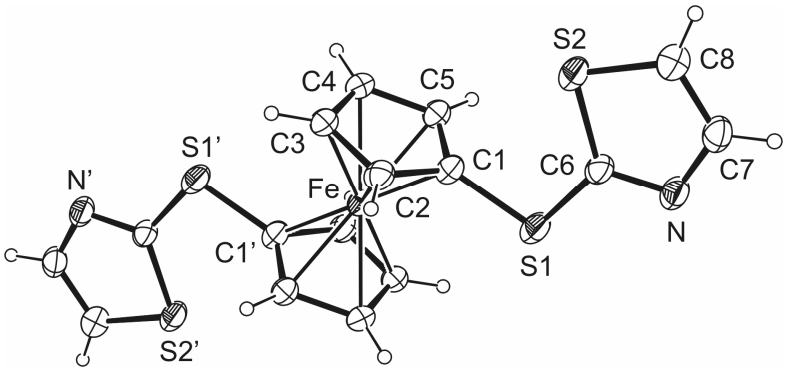

Figure 2-6: Molecular structure of **10** in the crystal. Selected bond lengths [Å] and angles [°]: C1–S1 1.772(5), C6–S1 1.755(6), C6–S2 1.736(5), C6–N 1.323(6), C7–N 1.378(8), C7–C8 1.382(8), C8–S2 1.731(6); C1–S1–C6 101.7(3), C6–S2–C8 89.4(3), C6–N–C7 110.2(4).

Bond parameters are unexceptional and compare well with those of related species such as, for example, $(RSCH_2CH_2)_2$,[17] $(RSCH_2)_2$-*p*-C_6H_4[18] as well as RSSR (R = thiazol-2-yl), whose crystal structure was also determined as a sideline of this research.

X-ray crystallographic data:

Compound	RSSR (R = thiazol-2-yl)	**10**
Empirical formula	$C_6H_4N_2S_4$	$C_{16}H_{12}FeN_2S_4$
Formula weight	232.35	416.37
Temperature [K]	133(2)	133(2)
Crystal system	monoclinic	triclinic
Space group	*P* $2_1/c$	*P* –1
a [Å]	5.5034(9)	6.8474(12)
b [Å]	19.354(3)	8.0194(16)
c [Å]	8.5337(14)	8.3936(16)
α, *β*, *γ* [°]	90, 96.07(1), 90	110.72(1), 94.77(2), 97.97(2)
V [Å^3]	903.9(3)	422.58(14)
Z	4	1
ρ_{calcd} [g cm^{-3}]	1.707	1.636
μ [mm^{-1}]	0.991	1.384
F(000)	472	212
Crystal size [mm]	0.6 × 0.09 × 0.07	0.48 × 0.20 × 0.02
θ range [°]	2.10 – 25.00	2.62 – 25.00
Reflections collected	5753	2760
Independent reflections	1595	1402
R_{int}	0.1399	0.0901
Reflections with $I>2\sigma(I)$	1174	1017
Data/restraints/parameters	1595/0/109	1402/0/106
GOF on F^2	0.927	0.934
$R1$ ($I>2\sigma(I)$)/w$R2$	0.0515/0.1272	0.0590/0.1484
largest diff. peak/hole [e·Å^{-3}]	0.405/–0.494	0.573/–0.860

2.2.3.3

Synthesis and Characterisation of 1,1'-Di(benzothiazol-2-ylthio)ferrocene (11)

11 was prepared by the drop wise addition of two equivalents of di(2-benzothiazolyl)disulfide in toluene to a stirred suspension of the TMEDA adduct of 1,1'-dilithioferrocene in *n*-hexane. After reaction overnight water was added and stirring continued for 10 min. The dark yellow precipitate was isolated by filtration and dried in vacuo. Its purity turned out to be already > 95 % by NMR spectroscopic analysis. The yield was 92 %. An analytical sample was obtained by column chromatography on silica gel with *n*-hexane/CH_2Cl_2 (3 : 1) as eluent.

^{1}H NMR spectroscopy confirmed the identity of the product. The spectrum shows two singlets at 4.59 and 4.70 ppm (in $CDCl_3$), typical for cyclopentadienyl protons, as well as signals at 7.23, 7.37, 7.63 and 7.82 ppm, which is in the region of aromatic protons, corresponding to the benzothiazolyl rings. In the ^{13}C NMR spectrum signals were found at 73.0, 78.0, 82.8 ppm (cyclopentadienyl) and at 120.8, 121.8, 124.1, 126.1 ppm (benzothiazolyl).

11 crystallised readily by evaporation of the solvent and the result of an X-ray diffraction analysis is shown in figure 2-7.

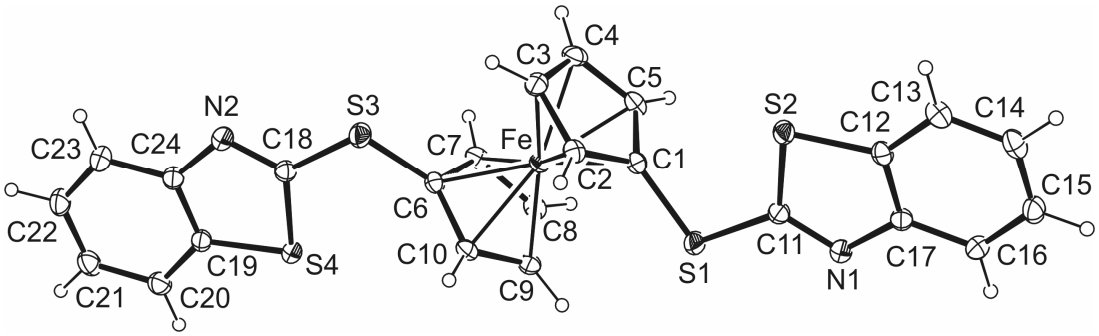

Figure 2-7: Molecular structure of **11** in the crystal. Selected bond lengths [Å] and angles [°]: C1–S1 1.759(2), C6–S3 1.759(2), C11–S1 1.759(2), C11–N1 1.289(2), C11–S2 1.758(2), C12–S2 1.744(2), C12–C17 1.406(2), C17–N1 1.398(2), C18–S3 1.757(2), C18–N2 1.289(2), C18–S4 1.7552(17), C19–C24 1.399(2), C19–S4 1.744(2), C24–N2 1.398(2); C1–S1–C11 102.61(8), C11–S2–C12 88.29(8), C11–N1–C17 110.1(1), C6–S3–C18 101.88(8), C18–S4–C19 88.18(8), C18–N2–C24 109.8(2).

The cyclopentadienyl rings of **11** are arranged in an essentially eclipsed orientation, as is usually the case for 1,1′-disubstituted ferrocene derivatives. Again, bond parameters are unexceptional and compare well with those of related species such as, for example, RSMe,[19] $(RS)_2CH_2$ and $(RSCH_2CH_2OCH_2)_2$ (R = benzothiazol-2-yl).[20]

X-ray crystallographic data:

Empirical formula	$C_{24}H_{16}FeN_2S_4$
Formula weight	516.48
Temperature [K]	153(2)
Crystal system	monoclinic
Space group	$P\ 2_1/c$
a [Å]	6.9969(4)
b [Å]	10.3383(8)
c [Å]	30.2641(18)
α, β, γ [°]	90, 103.394(5), 90
V [Å^3]	2129.6(2)
Z	4
ρ_{calcd} [g cm^{-3}]	1.611
μ [mm^{-1}]	1.116
F(000)	1056
Crystal size [mm]	$0.55 \times 0.26 \times 0.13$
θ range [°]	2.09 – 25.0
Reflections collected	13454
Independent reflections	3751
R_{int}	0.0301
Reflections with $I>2\sigma(I)$	3249
Data/restraints/parameters	3751/0/281
GOF on F^2	1.061
$R1$ ($I>2\sigma(I)$)/$wR2$	0.0215/0.0529
largest diff. peak/hole [e·Å^{-3}]	0.210/–0.217

Intermolecular S···S distances close to the sum of the estimated van der Waals radii of 3.7 Å[21] are present in the crystal structures of RSSR (R = thiazol-2-yl), **10** and **11**, as is typical for such sulfur-rich compounds. The origin of these S···S contacts is commonly attributed to weakly attractive interactions between the `soft´ sulfur atoms.

2.3 Film Preparation and Characterisation

The investigation of the SAMs presented in this thesis was done in cooperation with Dr. Ballay, Dr. Weidner and Dr. Zharnikov from the research group 'Applied Physical Chemistry' at the University of Heidelberg (Germany).

Most of the adsorbate species collected in figure 2-1 (namely **1** – **8**) have been used for the fabrication of molecular films on gold, which were prepared at room temperature by immersion of the substrate in a dilute (typically ~10 μM) solution of the respective adsorbate species for several hours. Acetonitrile and especially ethanol proved to be the preferred solvents. For example, according to near-edge X-ray absorption fine structure data **1** did not form well oriented SAMs from DMF, whereas from ethanol no such problems occurred. These observations are in line with results of a recent systematic investigation concerning the solvent influence on SAM quality by Witte and coworkers.[22]

SAM fabrication with isocyanides[23] and thioethers[24] on gold is well known.[2] SAM formation of thiophene and its oligomers on gold, which was first reported in 1996 for pristine thiophene in contradiction to theoretical predictions,[25] is of great current interest, since the corresponding films are potentially useful for electronic devices due to high electronic conductivity.[26] However, SAM formation of thiophene derivatives continues to be a matter of current debate, since conflicting reports concerning the mechanism of chemisorption, growth morphology as well as the structure, integrity and stability of the resulting SAMs exist in the recent

literature.[27,28,29,30,31] Isothiocyanates have not yet been investigated in detail in this context. Perusal of the literature afforded only one report addressing this issue, utilising, however, gold nanoparticles and not solid gold substrates.[32,33] On the basis of surface-enhanced Raman scattering (SERS) data, the author comes to the conclusion that aromatic isothiocyanides have vertical stances on gold, binding through the sulfur atom. A similar lack of knowledge can be noted for SAMs on gold based on phosphanes, although phosphane-protected gold nanoparticles are ubiquitous. Again only a single relevant report exists in the literature. Persson and coworkers have investigated the chemisorption of tertiary phosphanes on several coinage and platinum metals and found multilayer formation from solution. After removal of physisorbed PR_3 by ultrasonic treatment, the analysis of the remaining thin film by infrared reflection absorption spectroscopy (IRRAS) suggested binding of the adsorbate molecules to the metal surface by the phosphorus atom, similar to metal coordination in molecular chemistry.[34]

The identity, composition, integrity, and structure of all target films were investigated by two complementary experimental techniques, viz. X-ray photoelectron spectroscopy (XPS) and near-edge X-ray absorption fine structure (NEXAFS) spectroscopy. Due to the heterogeneity of the target systems just a representative selection of spectra and respective numerical parameters in tabular form are presented. As the first step the available experimental data are presented and general statements are made on their interpretation and respective implications. Most of these implications refer to all the systems of this study. Further the specific results for every particular system are considered.

XPS gives quantitative information about the composition, chemical identity, and effective thickness of the target films. For the sake of brevity, a film fabricated from adsorbate species ***n*** will be termed `film ***n***´ (***n*** = **1** – **8**) in the following. The relevant adsorbate molecules **1** – **8** consist mostly of carbon and hydrogen and also contain iron as well as sulfur, phosphorus and nitrogen, depending on the individual molecular composition. The observation of the characteristic photoemission peaks

assigned to the latter atoms is a fingerprint for the presence of the respective adsorbate species in the derived films, whereas the respective binding energies provide information on the chemical integrity and bonding configuration of the film constituents. The total intensities of the S 2*p*, N 1*s*, and Fe 2*p* signals in the various films investigated are summarised in figure 2-8.

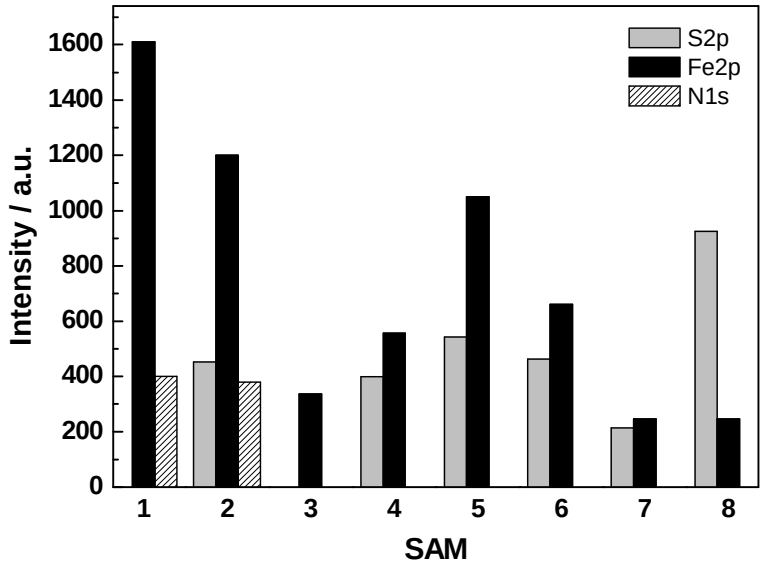

Figure 2-8: Normalised total intensities of the sulfur 2*p*, nitrogen 1*s*, and iron 2*p* XP spectroscopic signals in the films **1** – **8**.

The binding energy (BE) positions of the respective emissions (and of the P $2p_{3/2}$ peak in the case of film **3**) are shown in figure 2-9.

Film	S $2p_{3/2}$	N 1*s*/P $2p_{3/2}$	Fe $2p_{3/2}$	Thickness
1		399.9(2.8)	708.1(1.9)	14.3
2	161.7(2.1)	399.8(3.3)	707.9(2.0)	9.6
3		131.1(1.0)	708.3(1.7)	9.6
4	162.3(2.1) 163.5(2.1)		707.9(1.7)	6.8
5	163.2(1.9)		707.7(1.7) 712.0(1.7)	8.5
6	162.1(2.1) 163.6(2.1)		707.8(1.7) 711.5(1.7)	6.7
7	161.9(1.6) 163.6(1.6)		707.8(1.7)	8.2
8	163.4(2.1)		707.8(1.7)	10.4

Figure 2-9: Binding energy positions [eV] and fwhm [eV] (in parentheses) of the sulfur $2p_{3/2}$, nitrogen 1*s*, phosphorus $2p_{3/2}$ and iron $2p_{3/2}$ photoemission peaks for the films **1** – **8** along with the respective film thickness values [Å].

All films exhibit an iron signal (even though with different intensities) with a characteristic BE of about 708 eV, implying the chemisorption of the respective ferrocene-based adsorbate molecules on the gold substrate. For films **5** and **6**, this signal is accompanied by additional Fe 2*p* emission at a higher BE (~712 eV), which can be related to the partial oxidation and decomposition of the organometallic moieties in the above molecules.

The intensity of the Fe 2*p* signal can be considered as a direct measure of the ferrocene-type content in the films, since the organometallic moieties comprise the film-ambient interface and are almost unaffected by attenuation effects typical for photoemission. Further, all the films, except **3**, exhibit either sulfur or nitrogen signals (film **2** show both signals), in accordance with the molecular composition.

The analysis of the BE positions of the S 2*p*, P $2p_{3/2}$, and N 1*s* emissions gives valuable information about the bonding configuration of the molecular adsorbates in the respective films. This analysis will be performed below as soon as the individual films will be considered.

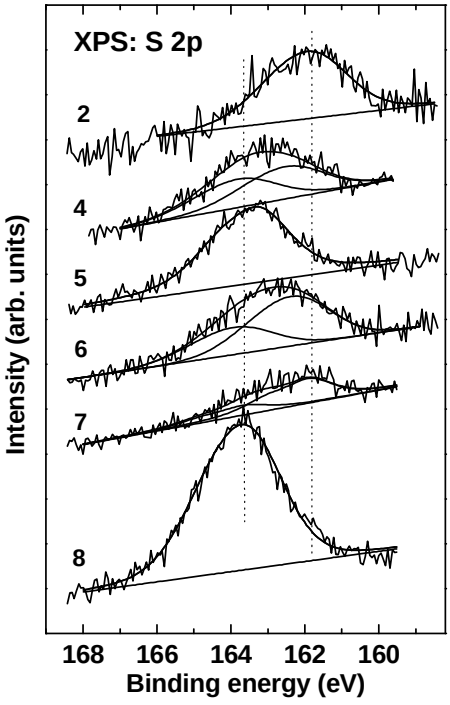

Figure 2-10: Normalised sulfur 2*p* XP spectra of films **2** and **4** – **8**. The decomposition of the spectra into the individual components is shown. A background is drawn.

The S 2*p* XP spectra of the sulfur-containing films (**2**, **4** – **8**) are presented in figure 2-10. The N 1*s* and P 2$p_{3/2}$ XP spectra of films **1**, **2** and **3**, respectively, exhibit only one emission (with parameters given in figure 2-9) and are therefore not presented.

Along with the Fe signal, the amount of the adsorbate molecules in the derived films is represented by the effective film thickness. The respective values were obtained from the C 1*s*/Au 4*f* intensity ratios,[35] using previously reported attenuation lengths.[36] Pertinent data are collected in figure 2-9. Whereas the thicknesses are quite small in each case, implying the formation of monolayer films, they do not fully correlate with the respective Fe 2$p_{3/2}$ intensities (figure 2-8), even if one corrects for the different iron/carbon ratio in the adsorbate molecules. This suggests that part of the carbon signal may originate from hydrocarbon contamination, which was initially present on the gold surface, and, presumably, not completely removed upon the chemisorption of the adsorbate molecules.

Complementary information on the composition and chemical identity of the films investigated is provided by the NEXAFS data. Generally, NEXAFS spectra give an insight into the electronic structure of target films, sampling the electronic structure of the unoccupied molecular orbitals of the film constituents.[37]

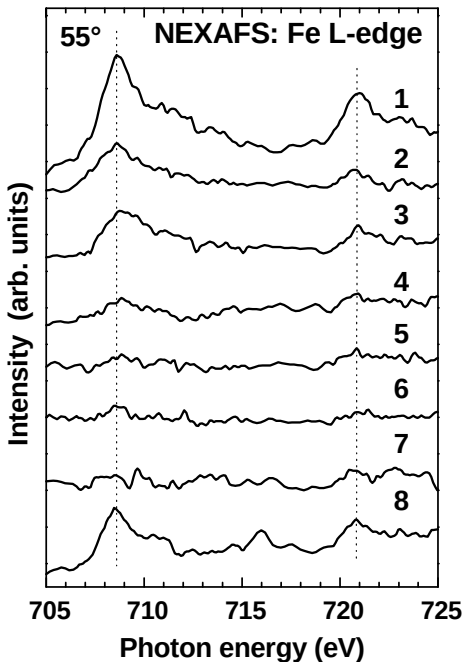

Figure 2-11: Normalised iron *L*-edge NEXAFS spectra of films **1** – **8** acquired at X-ray incidence angles of 55°.

The Fe L-edge spectra of films **1** – **8** recorded at the magic angle of X-ray incidence (55°, at this orientation the spectrum is independent of the molecular orientation) are presented in figure 2-11. These spectra were normalised to the pre-edge intensity and are therefore representative for the amount of iron in the target films. The spectra of all films exhibit the characteristic π* resonances related to the $4e_{1g}$ and $3e_{2u}$ orbitals of ferrocene at both L_2- and L_3-edges,[38,39] suggesting the chemisorption of the adsorbate molecules on the gold substrate and therefore supporting the XPS results. The intensity of these resonances varies significantly from film to film, correlating roughly with the intensity of the XPS Fe 2*p* signal.

The carbon *K*-edge spectra of films **1** – **8** recorded at the magic angle of X-ray incidence are shown in figure 2-12. These spectra exhibit a C 1*s* absorption edge ascribed to the C 1*s* → continuum excitations and a series of absorption resonances characteristic of the adsorbate molecules on the surface.

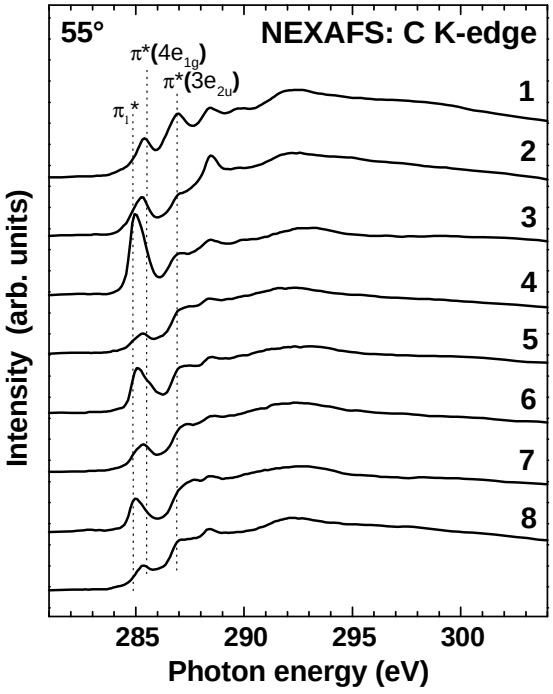

Figure 2-12: Carbon *K*-edge NEXAFS spectra of films **1** – **8** acquired at X-ray incidence angles of 55°. Prominent absorption resonances are indicated.

Most of the spectra exhibit the characteristic π* resonances related to the $4e_{1g}$ and $3e_{2u}$ orbitals of ferrocene at 285.6 eV and 287.2 eV, respectively, and a broad σ* resonance

of this organometallic moiety at ca. 292 eV.[40] For films **3** and **5**, which contain phenyl rings, the corresponding characteristic π_1* resonance at 285.1 eV is unequivocally observed. The characteristic π* resonance of an intact thiophene-type moiety (films **6** and **7**) is expected at 285.6 eV, overlapping, however, with the π*($4e_{1g}$) resonance of the ferrocene nucleus. Furthermore, the σ*(C–S), σ*(C–N), or σ*(C–P) resonances can in principle be observed at ~287 eV,[37] but they are presumably weak and therefore not distinguishable from the π*($3e_{2u}$) resonance of the ferrocene nucleus in most of the spectra. Finally, a π*-like resonance at 288.6 eV observed in some spectra in figure 2-12 can be alternatively assigned to conjugation phenomena (see below) or contamination (CO).

In addition to the insight into the electronic structure of the target systems, NEXAFS data provide valuable information on the orientation of the film constituents, since the cross-section of the resonant photoexcitation process depends on the orientation of the electric field vector of the linearly polarized synchrotron light with respect to the transition dipole moment (TDM) of the probed molecular orbital. This effect is called linear dichroism in X-ray absorption. For ordered molecular films, the intensity of the absorption resonances changes at a variation of the incidence angle of the synchrotron light. A convenient way to monitor these changes is the difference between the spectra acquired at normal (90°) and grazing (20°) incidence. Such carbon *K*-edge difference spectra for films **1** – **8** are displayed in figure 2-13. The transition dipole moment of the π* orbitals is oriented perpendicular to the plane of the C_5 rings and to the NC axis in **1** and **2**. The respective resonances are usually quite sharp, which makes monitoring of the linear dichroism easier as in the case of σ* resonances, which are commonly observed as broad features.

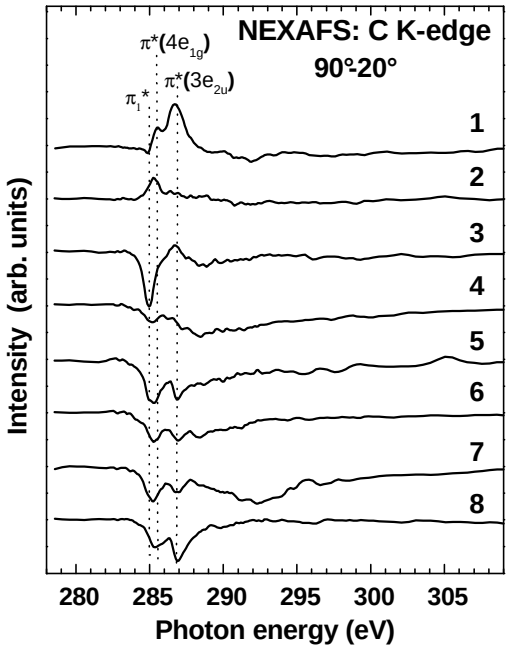

Figure 2-13: Carbon *K*-edge NEXAFS difference spectra of films **1** – **8**. The curves represent the difference between the spectra acquired at X-ray incidence angles of 90° and 20°. The position of the prominent absorption resonances are indicated by dotted lines.

In the following the experimental data for the individual films will be discussed in more detail. These films differ, inter alia, in the headgroups that provide the anchoring to the gold substrate, giving rise to the following categories: isocyanide-based film **1**, isothiocyanate-based film **2**, phosphane-based film **3**, thioether-based films **4**, **5**, and **8**, and thiophene-based films **6** and **7**.

2.3.1 Film 1

This film shows the highest Fe signal both in XP (figure 2-8) and NEXAFS spectra (figure 2-11) and thus exhibits the highest packing density of organometallic moieties among the systems investigated in this study. This agrees well with the highest effective thickness as shown in figure 2-8. Both carbon *K*-edge and iron *L*-edge spectra of film **1** exhibit intense resonance structure, characteristic of intact ferrocene-type units, suggesting non-dissociative chemisorption of the adsorbate molecules.

In XPS only a single nitrogen 1*s* emission related to the isocyanide nitrogen appears at 399.9 eV,[41,42] indicating an exclusive isocyanide-mediated bidentate bonding of **1** to the Au substrate with no contributions from monodentate binding or physisorption.

This interpretation is strongly supported by IRRAS data, which also suggest an essentially vertical orientation of the adsorbate molecules on the gold surface, as shown in figure 2-14.

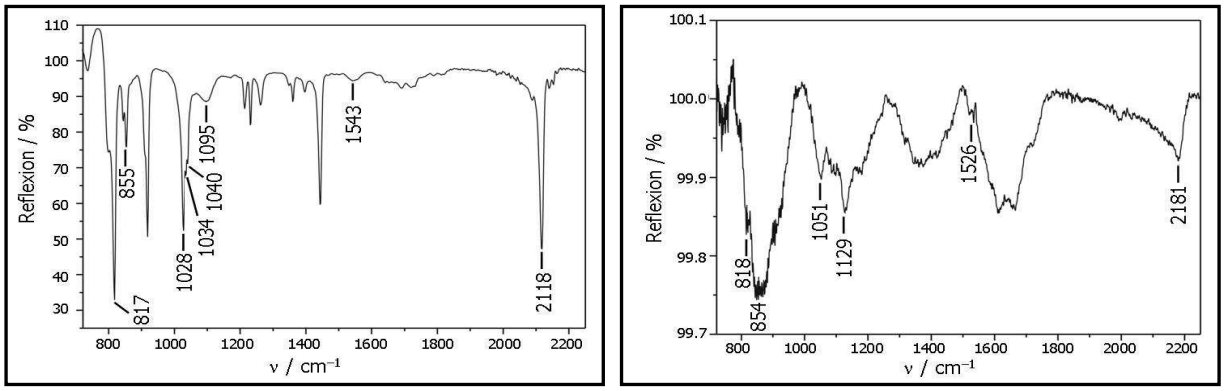

Figure 2-14: IR spectra of **1** as bulk material (left) and after SAM formation on gold (right).

Comparison of the spectra obtained with the modified gold substrate and those obtained from neat **1** reveals characteristic differences. The intensities of the out of plane δ(CH) bands at 1040, 1028 and 817 cm^{-1} are decreased almost below noise level. This confirms essentially parallel orientation of the cyclopentadienyl ring plane with respect to the surface normal,[43,44] as expected for the binding of both isocyano groups. On the other hand, in-plane modes such as ν(NC), ν(CC), δ(CH) and ring distortion modes found in the IR spectrum of neat **1** at 2118, 1543, 1095, 855 cm^{-1}, respectively, are clearly identified in the spectrum of **1** on gold. Interaction with the substrate leads to a strong polarisation of lone pair electron density into the metal and causes a shift of the ν(NC) band from 2118 to 2181 cm^{-1}. This compares well with results obtained with other isocyanides[45,46,47,48,49] and also with the value of 2226 cm^{-1} found for $[(\mu\text{-}\mathbf{1})(AuCl)_2]_n$.[50]

There is no indication for any surface-unbound isocyano groups in the film. These conclusions are further corroborated by the nitrogen *K*-edge NEXAFS spectra of film **1** shown in figure 2-15, which exhibit a single distinct π*(N*C) resonance at 400.4 eV.[41,51,52,53] Features related to the corresponding NC orbital are also visible at the carbon *K*-edge, as a shoulder at 286.6 eV.[41] Furthermore, the relatively strong π*-like

resonance around 288.6 eV can originate from the conjugation of the π* orbitals of the ferrocene nucleus with the π* orbitals of the isocyano unit.[37]

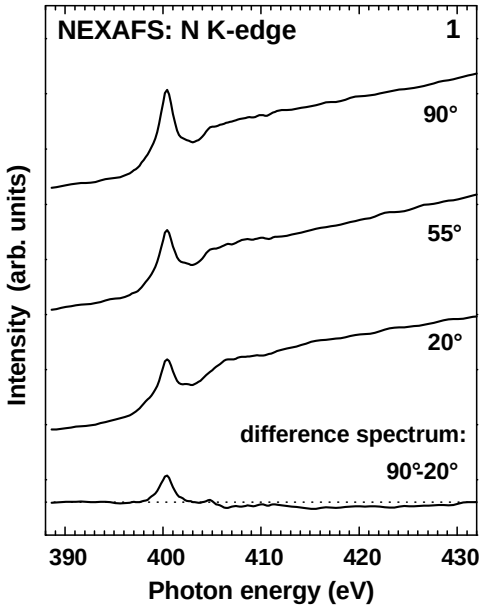

Figure 2-15: Nitrogen *K*-edge NEXAFS spectra of film **1** acquired at X-ray incidence angles of 90°, 55°, and 20°, along with the difference between the spectra acquired at X-ray incidence angles of 90° and 20° (bottom curve).

The NEXAFS difference spectrum of film **1** in figure 2-13 shows the pronounced π*($4e_{1g}$) and π*($3e_{2u}$) peaks characteristic of high orientational order. These peaks have the positive sign (and will be named "positive dichroism" in the following) indicative of a vertical orientation of the cyclopentadienyl decks. Furthermore, a strong positive dichroism is observed for the π*(NC*) resonance at 286.6 eV, indicating a predominantly vertical orientation of the isocyano headgroups. Film **1** exhibits the highest degree of orientational order and comprises vertically oriented molecules.

2.3.2 Film 2

This film differs from film **1** in the attachment of a sulfur atom to each isocyanide moiety, resulting in the formation of isothiocyanato headgroups. According to the XPS (figures 2-8 and 2-9) and NEXAFS (figure 2-11) data, this modification resulted in a noticeable reduction of the packing density, which is, however, still relatively

high as compared to the other films of this study. Both carbon *K*-edge and iron *L*-edge spectra of film **2** exhibit intense resonance structure, characteristic of intact ferrocene-type moieties, suggesting non-dissociative adsorption of the target molecules.

Similar to film **1**, a single N 1*s* XPS emission at 399.8 eV related to the headgroup nitrogen appears in the respective XP spectrum of film **2**.[41,42] Furthermore, only a single doublet at a BE of 161.7 eV (S $2p_{3/2}$) is observed in the sulfur 2*p* XP spectrum (figure 2-10), which is close to the characteristic value for thiolate-type bonding. Since neither additional nitrogen 1*s* emission peaks nor features characteristic of unbound sulfur were found, it can be assumed that **2** adopts a bidentate bonding configuration on the gold substrate similar to **1**.

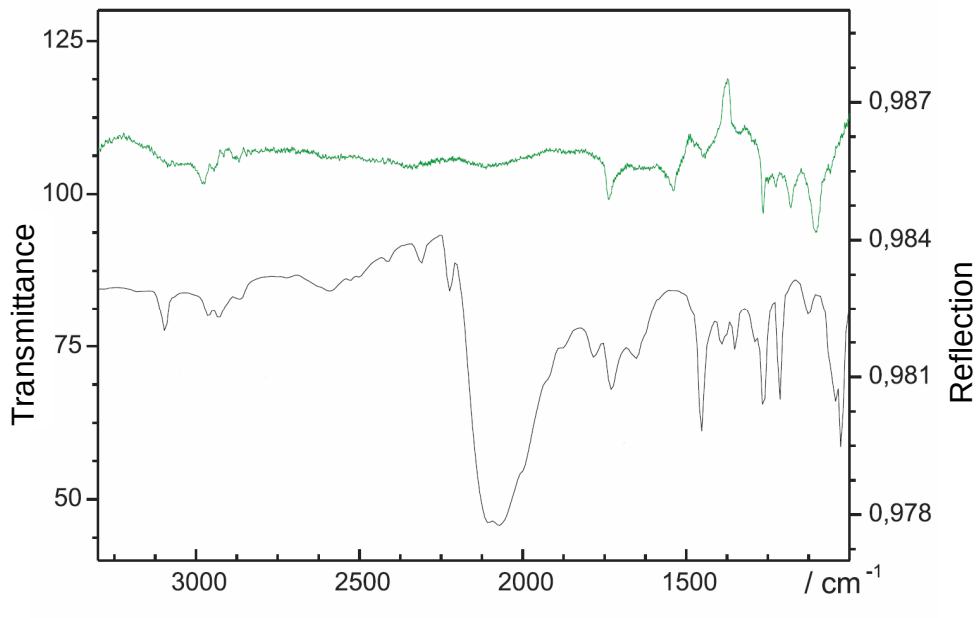

Figure 2-16: IR spectra of neat **2** and after SAM formation on gold (top).

The comparison of the IR spectra obtained from bulk material and those of the modified gold substrate is intriguing in the case of **2**, since the very strong ν(NCS) mode, characteristic for isothiocyanates, completely disappears after SAM formation (figure 2-16). This suggests a dihaptic binding mode of each NCS moiety, where both, the sulfur and the carbon atom attach to the gold substrate. The different binding possibilities of the isothiocyanato group are compared in figure 2-17. For the

sake of simplicity this topic is discussed in general (with R as an abbreviation for any carbon residue) and lone pairs and formal charges are not shown in figure 2-17. The geometry of isothiocyanates is treated as linear (R–N=C=S) in the following, notwithstanding the fact that the C–N–C bond angle of isothiocyanates depends largely on the nature of R and is usually around 140° for aliphatic isothiocyanates, while it may rise to around 160° for aromatic substituents due to mesomeric interaction.[54]

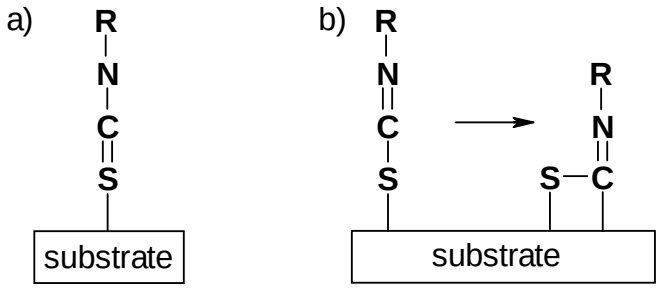

Figure 2-17: Two possible modes for the chemisorption of isothiocyanates on gold.

Isothiocyanates are known to be strong electrophiles, with the carbon as the electrophilic centre. The electron withdrawing strength of the central carbon atom may be explained by the polar resonance structures of the NCS group:

$$R–N^{-}–C^{+}=S \leftrightarrow R–N=C=S \leftrightarrow R–N=C^{+}–S^{-}$$

Considering a chemisorption of the isothiocyanato moiety just by the terminal sulfur atom to the gold substrate, scenario a) in figure 2-17 describes the situation best. In this case the geometry of the NCS group would stay intact and the ν(NCS) stretching mode should be clearly visible in the IR spectrum of the modified gold substrate. Scenario b) shows the other possibility, where the chemisorption is equal to an oxidative addition of the isothiocyanato group to the gold substrate. The binding of the adsorbate is stabilised by a dihaptic linkage, which is thermodynamically beneficial. Loss of the linear NCS geometry is consistent with the IR data obtained.

The NEXAFS difference spectrum of film **2** (in figure 2-13) shows the pronounced $\pi^*(4e_{1g})$ and $\pi^*(3e_{2u})$ peaks characteristic of high orientational order. These peaks have the positive sign indicative of a vertical orientation of the cyclopentadienyl decks.

2.3.3 Film 3

The carbon *K*-edge NEXAFS spectrum of this film (figure 2-12) displays a strong feature at 285.0 eV related to the π_1* orbital of the phenyl moieties[55,56,57,58] of the diphenylphosphanyl headgroups. The comparably high intensity of this resonance is nicely compatible with the molecular composition, since **3** contains four phenyl moieties. A horizontal ("flat") adsorption geometry of the phenyl rings can be deduced from the strongly negative dichroism of the π_1* resonance as seen in the difference spectrum. The orientation of the cyclopentadienyl decks, however, cannot be clearly made out from the difference spectra, since the π*($4e_{1g}$) feature of ferrocene at 285.6 eV overlaps with the strong π_1* difference peak of phenyl.

The phosphorus $2p_{3/2}$ XP spectrum of film **3** exhibits a single emission at a BE of 131.1 eV. This particular BE is commonly related to aromatic diphenylphosphane derivatives which are either unbound[59] or coordinatively bound to zero-valent transition metals in metal complexes.[60,61] In view of the relatively high film density and orientational order, it is very likely in our case that most of the diphenylphosphanyl headgroups are characterised by coordination-type attachment to the gold surface. The low iron intensity observed in the XP Fe 2*p* spectra together with the comparably high film thickness of 9.6 Å is understandable in view of the sterically demanding headgroups. The surface area occupied by **3** in a bidentate binding configuration via its bulky diphenylphosphanyl headgroups is approximately four to five times larger than that of **1**, in agreement with the ~ 5 : 1 Fe 2*p* intensity ratio of **1**/Au and **3**/Au. This is in accord with IR spectroscopic measurements by Westermark et al., who found flat adsorption geometries and intact binding of aromatic phosphanes on a variety of coinage metals.[34]

2.3.4 Films 4, 5 and 8

The carbon *K*-edge NEXAFS spectra of these thioether-based films (figure 2-12) show characteristic spectral features related to the organometallic moiety. In addition, the spectrum of film **5** shows the characteristic π_1* resonance at ~285 eV related to the

terminal phenyl units of the adsorbate molecule. The difference NEXAFS spectra of films **5** and **8** (figure 2-13) exhibit a negative dichroism of the ferrocene $\pi^*(4e_{1g})$ feature at 285.6 eV, accompanied by the negative dichroism of the π_1^* resonance (phenyl rings) for film **5**. Accordingly, the cyclopentadienyl decks (and the phenyl rings in **5**) are strongly inclined. The same is presumably true for film **4** as well, but it seems to be more disordered than films **5** and **8** according to its NEXAFS difference spectrum in figure 2-13.

The sulfur 2*p* XP spectrum of film **4** exhibits two S $2p_{3/2,1/2}$ doublets at BEs of 162.0 eV and 163.8 eV (S $2p_{2/3}$) related to two different sulfur moieties. The former doublet is commonly assigned to a thiolate-type attachment to gold, which suggests the cleavage of covalent C–S bonds for a part of the adsorbate molecules upon their adsorption. Such a binding chemistry has been reported before for thioether headgroups in various molecules.[2,24] The second doublet observed at 163.8 eV is characteristic of unbound or coordination-type bound S in thioethers.[62,63] The coexistence of thiolate, coordination-type and/or unbound sulfur species might be a reason for the low molecular order in film **4**.

In contrast to film **4**, sulfur 2*p* XP spectra of films **5** and **8** are dominated by the doublet at 163.8 eV, suggesting the dominance of weakly bound or unbound adsorbate molecules in the respective films. The intensity of the thiolate-related doublet is very low, indicating that only a small part of the pristine thioether groups was cleaved upon adsorption. In view of the horizontal orientation of the cyclopentadienyl decks in these films, as derived from the corresponding NEXAFS data (figure 2-13), it is very likely that part of the thioether units form coordinative bonds to the surface, whereas the remaining ones are essentially unbound, with the most likely scenario being that the dominant binding configuration on gold is mono- and bidentate for **5** and **8**, respectively.

The overall film quality and packing density differ among films **4**, **5**, and **8**. While films **4** and **8** show only traces of oxygen in the O 1*s* XP spectra and no oxidised iron, film **5** exhibits considerable amounts of oxygen contaminations and oxidised iron (at

~712 eV for Fe $2p_{3/2}$), which indicates that a considerable fraction of the organometallic units got oxidised and presumably decomposed in this film. Films **4** and **8** exhibit relatively low Fe 2*p* XPS signals (figure 2-8) suggesting low packing densities in contrast to film **5**, which has an Fe intensity comparable to the more ordered films **1** and **2**. The sulfur 2*p* signal for film **4** is very high compared to the respective iron intensity (figure 2-10). This might be explained by unbound anchor groups which are oriented towards the film surface so that the respective photoemission signal gets less attenuated. The relatively high S 2*p* signal observed for film **8** is not unexpected since **8** contains four sulfur atoms as opposed to only two present in **4** and **5**.

2.3.5 Films 6 and 7

The thiophene-based compounds **6** and **7** exhibit partial molecular decomposition upon adsorption on the gold surface. The sulfur 2*p* XPS spectra of these films (figure 2-10) show two distinct doublets at ~162 eV (S $2p_{3/2}$) and at 163.6 eV. The former peak can be assigned to thiolate-type sulfur resulting from the cleavage of the C–S bond in the thiophene ring, while the latter species can be ascribed to a weakly-coordinated or unbound thiophene.[29,31,64] This conclusion is supported by the carbon *K*-edge NEXAFS spectra of both films **6** and **7** (figure 2-12), exhibiting an absorption intensity at ~285.0 eV, which has also been found for oligothiophenes and is commonly associated with dissociative adsorption of thiophene,[65] i.e. cleavage of the C–S bond in the thiophene ring to form a thiolate-type attachment to gold. The respective feature is more intense in the spectrum of film **7**, whereas in the spectrum of film **6** this feature represents only a shoulder of a stronger resonance at 285.6 eV, which, in this particular case, is presumably a superposition of the $\pi^*(4e_{1g})$ resonance of ferrocene and the π_1^* resonance of intact thiophene.[37,65] Therefore, the position of the sulfur atom in the thiophene ring with respect to the attached ferrocene nucleus is of importance for the chemical stability of the adsorbate molecules upon their adsorption on the gold surface. This difference in the attachment chemistry is

surprising in view of the minor structural difference of molecules **6** and **7**. However, several authors have pointed out that the binding conformation of thiophene derivatives is strongly influenced by their functional groups.[27,64]

A decomposition of the thiophene headgroup for part of the adsorbate molecules results in a pronounced chemical heterogeneity of the derived film, which is strongly disordered and presumably contains the adsorbate species in both bidentate and monodentate bonding configuration. In fact, the NEXAFS difference spectra of films **6** and **7** (figure 2-13) exhibit a negative dichroism of the $\pi^*(4e_{1g})$ and $\pi^*(3e_{2u})$ resonances (at 285.6 eV and 287.0 eV, respectively) assigned to the cyclopentadienyl decks. Consequently, it can be assumed that these decks show predominantly horizontal orientation.

According to the iron 2*p* XPS data (figure 2-8), film **7** exhibits a much lower Fe content than film **6**. On the other hand, a higher packing density in film **7** as compared to film **6** can be inferred from the film thickness values for these films, being 8.2 and 6.7 Å, respectively. It is possible that the molecular decomposition of **7** upon adsorption affects not only the thiophene moiety but also the ferrocene nucleus. In this hypothesis, iron is lost (by desorption) during the film formation process, allowing a denser packing of the residual, sterically less demanding carbon backbone. Furthermore, the Fe 2*p* XP spectrum of film **6** shows a significant amount of oxidised iron (38% of total Fe intensity), which is a signature of oxidised ferrocene-type iron in this film. In contrast, no noticeable amount of oxidised iron was found in film **7**.

2.3.6 Summary

XPS and NEXAFS data suggest the formation of ferrocene-based, monomolecular films on Au(111) from the adsorbate molecules **1** – **8**. The attachment of these molecules to the Au substrate occurs in a SAM-like manner, through the specific headgroups, which are isocyano (**1**), isothiocyanato (**2**), phosphanyl (**3**), thioether (**4**, **5** and **8**), and thienyl (**6** and **7**). The quality of the resulting films turned out to be

rather different. A high packing density and orientational order was only observed for films **1** and **2**, which exhibit chemisorbed molecules with a predominantly vertical orientation and bidentate binding configuration. These films also show a high degree of chemical homogeneity and can, in view of all above factors, be considered as true SAMs. A relatively high orientational order, chemical homogeneity, and primarily bidentate bonding configuration was also observed in film **3**, but this film is characterised by a lower packing density due to the "flat" adsorption geometry of the bulky PPh_2 headgroups. All other films of this study (**4** – **8**) exhibit chemical inhomogeneity, low orientational order and considerable inclination of the film constituents. There are, presumably, both bidentate and monodentate binding configurations in these films. In the case of the thioether-based films (**4**, **5**, and **8**), C–S bond cleavage was observed upon adsorption for a part of the adsorbate molecules, resulting in the formation of thiolate-anchored moieties, which coexist with more weakly bound molecules anchored to the substrate by coordination-type bonds typical for thioethers. Also for the thiophene-based films (**6** and **7**), a decomposition of the thiophene headgroups took place upon adsorption for a part of the precursor molecules, resulting in the coexistence of strongly bonded thiophene-derived species and more weakly coordinated pristine molecules in the films. The relative portions of these two fractions were found to depend on the exact position of the thiophene sulfur atom with respect to the ferrocene moiety. Partial oxidation and decomposition of the organometallic moiety in some of the films (especially, in films **5** and **6**) cannot be completely excluded.

2.4 Conclusions

1,1'-disubstituted ferrocene derivatives $[Fe(C_5H_4X)_2]$ (**1** – **7**, **9** – **11**) which contain substituents suitable for binding to a gold surface [X = NC, NCS, PPh_2, 2-thienyl, 3-thienyl, and SR (R = Me, Ph, thiazol-2-yl, benzothiazol-2-yl)] were investigated. Compounds **1** – **7** contain two ligating atoms for surface coordination. The atoms are carbon in the case of the isocyanide **1**, phosphorus in case of dppf (**3**), and sulfur in

all other cases. Compounds **9** – **11** contain four potentially ligating sulfur atoms each, similar to the tetrasubstituted ferrocene derivative **8**, which contains four SMe groups. The four sulfur atoms of **8** are chemically equivalent, which is not the case for the structurally more complicated compounds **9** – **11**. Film formation on gold (111) substrates was investigated with the comparatively simple bidentate adsorbate species **1** – **7** and also the simplest of the tetradentate compounds (**8**) in this respect.

The diisocyano derivative **1** afforded well-defined SAMs of good quality. In contrast, with the notable exception of the isothiocyanato derivative **2**, all sulfur-containing adsorbate species investigated in this study failed to give rise to well-defined SAMs. However, the problems encountered with thioether- and thienyl-based anchor groups (especially C–S bond cleavage) are not unprecedented (see above), and the presented findings clearly support the notion that the behaviour of such anchor groups is unreliable in the context of SAM fabrication. In view of these difficulties, an analogous in-depth investigation of the tetradentate S ligands **9** – **11** has been omitted.

The quality of SAMs fabricated from **2** was found to be similar to that of SAMs prepared from **1**. The most likely binding scenario is a dihaptic attachment of the isothiocyanato moieties, involving both, the sulfur and the central carbon atom in the chemisorption.

2.5 References

[1] S. Onclin, B. J. Ravoo, D. N. Reinhoudt, *Angew. Chem. Int. Ed.* **2005**, *44*, 6282.

[2] J. C. Love, L. A. Estroff, J. K. Kriebel, R. G. Nuzzo, G. M. Whitesides, *Chem. Rev.* **2005**, *105*, 1103.

[3] F. Schreiber, *J. Phys.: Condens. Matter* **2004**, *16*, R881.

[4] F. Schreiber, *Prog. Surf. Sci.* **2000**, *65*, 151.

[5] V. Chechik, R. M. Crooks, C. J. M. Stirling, *Adv. Mater.* **2000**, *12*, 1161.

[6] R. G. Nuzzo, D. L. Allara, *J. Am. Chem. Soc.* **1983**, *105*, 4481.

[7] G. Trippé, M. Oçafrain, M. Besbes, V. Monroche, J. Lyskawa, F. Le Derf, M. Sallé, J. Becher, B. Colonna, L. Echegoyen, *New. J. Chem.* **2002**, *26*, 1320.

[8] a) T. Hirsch, M. Zharnikov, A. Shaporenko, J. Stahl, D. Weiss, O. S. Wolfbeis, V. M. Mirsky, *Angew. Chem. Int. Ed.* **2005**, *44*, 6775; b) K. M. Roth, J. S. Lindsey, D. F. Bocian, W. G. Kuhr, *Langmuir* **2002**, *18*, 4030.

[9] For a recent review, see: J. J. Gooding, F. Mearns, W. Yang, J. Liu, *Electroanalysis* **2003**, *15*, 81.

[10] T. Weidner, A. Krämer, C. Bruhn, M. Zharnikov, A. Shaporenko, U. Siemeling, F. Träger, *Dalton Trans.* **2006**, 2767 and references cited therein.

[11] a) C. Metallinos, D. Tremblay, F. B. Barrett, N. J. Taylor, *J. Organomet. Chem.* **2006**, *691*, 2044; b) A. Tárraga, F. Otón, A. Espinosa, M. D. Velasco, P. Molina, D. J. Evans, *Chem. Commun.* **2004**, 458.

[12] Review: a) P. Molina, M. J. Vilaplana, *Synthesis* **1994**, 1197; seminal paper: b) K. Itoh, M. Okamura, Y. Ishii, *J. Organomet. Chem.* **1974**, *65*, 327.

[13] A. Shafir, M. P. Power, G. D. Whitener, J. Arnold, *Organometallics* **2000**, *19*, 3978.

[14] F. Garnier, A. Yassar, Fr. Demande FR 2668154 A1, 1992.

[15] M. D. Rausch, D. J. Ciapenelli, *J. Organometal. Chem.* **1967**, *10*, 127.

[16] B. McCulloch, D. L. Ward, J. D. Woollins, C. H. Brubaker, Jr., *Organometallics* **1985**, *4*, 1425.

[17] Y. Xin, H.-M. Liu, W. Zhang, W.-Q. Zhang, *Acta Crystallogr. Sect. E* **2003**, *59*, o1153.

[18] W. Zhang, H.-M. Liu, C.-B. Li, W.-Q. Zhang, *Acta Crystallogr. Sect. E*, **2003**, *59*, o26.

[19] P. J. Wheatley, *J. Chem. Soc.* **1962**, 3636.

[20] C. J. Matthews, W. Clegg, M. R. J. Elsegood, T. A. Leese, D. Thorp, P. Thornton, J. C. Lockhart, *J. Chem. Soc., Dalton Trans.* **1996**, 1531.

[21] J. Dai, M. Munakata, L.-P. Wu, T. Kuroda-Sowa, Y. Suenaga, *Inorg. Chim. Acta* **1997**, *258*, 65.

[22] D. Käfer, G. Witte, P. Cyganik, A. Terfort, C. Wöll, *J. Am. Chem. Soc.* **2006**, *128*, 1723.

[23] J. J. Hickman, P. E. Laibinis, D. I. Auerbach, C. Zou, T. J. Gardner, G. M. Whitesides, M. S. Wrighton, *Langmuir* **1992**, *8*, 357.

[24] E. B. Troughton, C. D. Bain, G. M. Whitesides, R. G. Nuzzo, D. L. Allara, M. D. Porter, *Langmuir* **1988**, *4*, 365.

[25] M. H. Dishner, J. C. Hemminger, F. J. Feher, *Langmuir* **1996**, *12*, 6176.

[26] H. Sakagushi, H. Matsumura, H. Gong, *Nature Mater.* **2004**, *3*, 551.

[27] M. Haran, J. E. Goose, N. P. Clote, P. Clancy, *Langmuir* **2007**, *23*, 4897 and references cited therein.

[28] J. W. Han, J. Noh, *Mol. Cryst. Liq. Cryst.* **2007**, *464*, 205.

[29] E. O. Sako, H. Kondoh, I. Nakai, A. Nambu, T. Nakamura, T. Ohta, *Chem. Phys. Lett.* **2005**, *413*, 267.

[30] F. Terzi, R. Seeber, L. Pigani, C. Zanardi, L. Pasquali, S. Nannarone, M. Fabrizio, S. Daolio, *J. Phys. Chem. B* **2005**, *109*, 19397.

[31] J. Noh, E. Ito, T. Araki, M. Hara, *Surf. Sci.* **2003**, *532-535*, 1116.

[32] S.-W. Joo, *Surf. Interface Anal.* **2006**, *38*, 173.

[33] A recent publication which claims the anchoring of tripodal isothiocyanates onto gold electrodes in fact deals with the isomeric thiocyanates: J. A. Camerano, M. A. Casado, U. Hahn, J.-F. Nierengarten, E. Maisonhaute, C. Amatore, *New J. Chem.* **2007**, *31*, 1395.

[34] G. Westermark, H. Kariis, I. Persson, B. Liedberg, *Colloids Surf. A* **1999**, *150*, 31.

[35] J. Thome, M. Himmelhaus, M. Zharnikov, Grunze, M. *Langmuir* **1998**, *14*, 7435.

[36] C. L. A. Lamont, J. Wilkes, *Langmuir* **1999**, *15*, 2037.

[37] J. Stöhr, *NEXAFS Spectroscopy*, Springer Series in Surface Science Vol. 25, Springer, Berlin, **1992**.

[38] E. Rühl, C. Heinzel, H. Baumgärtel, A. P. Hitchcock, *Chem Phys.* **1993**, *169*, 243.

[39] A. P. Hitchcock, A. T. Wen, E. Rühl, *Chem Phys.* **1990**, *147*, 51.

[40] The assignment has been performed according to refs. [29] and: a) E. Rühl, A. P. Hitchcock, *J. Am. Chem. Soc*. **1989**, *111*, 5069; b) A. Shaporenko, K. Rössler, H. Lang, M. Zharnikov, *J. Phys. Chem. B* **2006**, *110*, 24621.

[41] S. Frey, A. Shaporenko, M. Zharnikov, P. Harder, D. L. Allara, *J. Phys. Chem. B* **2003**, *107*, 7716.

[42] J. F. Moulder, W. E. Stickle, P. E. Sobol, K. D. Bomben, *Handbook of X-ray Photoelectron Spectroscopy,* ed. J. Chastian, Perkin-Elmer Corp., Eden Prairie, MN, **1992**.

[43] J. T. Young, F. J. Boerio, Z. Zhang, T. L. Beck, *Langmuir* **1996**, *12*, 1219.

[44] M. K. Debe, *J. Appl. Phys.* **1984**, *55*, 3354.

[45] D. L. DuBose, R. E. Robinson, T. C. Holovics, D. R. Moody, E. C. Weintrob, C. L. Berrie, M. V. Barybin, *Langmuir* **2006**, *22*, 4599.

[46] J. J. Stapleton, T. A. Daniel, S. Uppili, U. M. Cabarcos, J. Naciri, R. Shashidhar, D. L. Allara, *Langmuir* **2005**, *21*, 11061;

[47] K. L. Murphy, W. T. Tysoe, D. W. Bennett, *Langmuir* **2004**, *20*, 1732

[48] J. I. Henderson, S. Feng, T. Bein, C. P. Kubiak, *Langmuir* **2000**, *16*, 6183

[49] S. Lin, R. L. McCarley, *Langmuir* **1999**, *15*, 151; A. C. Ontko, R. J. Angelici, *Langmuir* **1998**, *14*, 3071.

[50] U. Siemeling, D. Rother, C. Bruhn, H. Fink, T. Weidner, F. Träger, A. Rothenberger, D. Fenske, A. Priebe, J. Maurer, R. Winter, *J. Am. Chem. Soc.* **2005**, *127*, 1102.

[51] J. M. Ripalda, E. Román, N. Díaz, L. Galán, I. Montero, G. Comelli, A. Baraldi, S. Lizzit, A. Goldoni, G. Paolucci, *Phys. Rev. B*, **1999**, *60*, R3705.

[52] I. Shimoyama, G. Wu, T. Sekiguchi, Y. Baba, *Phys. Rev. B*, **2000**, *62*, R6053.

[53] M. Polcik, M. Kittel, J. T. Hoeft, R. Terborg, R. L. Toomes, D. P. Woodruff, *Surf. Sci.* **2004**, *563*, 159.

[54] Ĺ. Drobnica, P. Kristián, J. Augustin, *The Chemistry of the –NCS Group* In: P. Satai (Ed.), *The Chemistry of Cyanate and their Thio Derivatives*, part 2, Wiley, New York, **1977**, pp. 1091-1221; and references herein.

[55] W. Azzam, B. I. Wehner, R. A. Fischer, A. Terfort, C. Wöll, *Langmuir* **2002**, *18*, 7766.

[56] S. Frey, V. Stadler, K. Heister, W. Eck, M. Zharnikov, M. Grunze, B. Zeysling, A. Terfort, *Langmuir* **2001**, *17*, 2408.

[57] M. Zharnikov, M. Grunze, *J. Phys.: Condes. Matter* **2001**, *13*, 11333.

[58] A. P. Hitchcock, P. Fischer, A. Gedanken, M. B. Robin, *J. Phys. Chem.* **1987**, *91*, 531.

[59] W. E. Morgan, W. Stec, R. G. Albridge, J. R. Van Wazer, *Inorg. Chem.* **1971**, *10*, 926.

[60] B. J. Brisdon, G. F. Griffin, J. Pierce, R. A. Walton, *J. Organometal. Chem.* **1981**, *219*, 53.

[61] W. M. Riggs, *Anal. Chem.* **1972**, *44*, 830.

[62] C.-J. Zhong, R. C. Brush, J. Anderegg, M. D. Porter, *Langmuir* **1999**, *15*, 518.

[63] J. L. Trevor, K. R. Lykke, M. J. Pellin, L. Hanley, *Langmuir* **1998**, *14*, 1664.

[64] J. Noh, E. Ito, K. Nakajima, J. Kim, H. Lee, M. Hara, *J. Phys. Chem. B* **2002**, *106*, 7139.

[65] A. Nambu, H. Kondoh, I Nakai, K. Amemiya, T. Ohta, *Surf. Sci*. **2003**, *530*, 101 and references cited therein.

Chapter 3

Coordination Chemistry of the Ferrocene Ligands

Synthesis as well as failed attempts to obtain complexes between the ferrocene based ligands and especially gold(I) are described. A series of gold(I) acetylides has been successfully coordinated to 1,1'-diisocyanoferrocene, which shows an unprecedented "schizoid" reactivity with the gold(I) acetylide $[Au(C{\equiv}C{-}Fc)]_n$.

3.1 Introduction

Ferrocene-based ligands play a significant role in coordination chemistry[1,2,3] and find applications in any field of recent chemistry, ranging from material science, biomedical chemistry, chemical sensing to catalysis.[4,5] Since SAM formation relies to a large extent on surface coordination chemistry, an investigation of the molecular coordination behaviour of the ferrocene derivatives described appears to be useful. It would be hubris to claim (or to try) an all-embracing exploration of the complex chemistry for all ligands. Since all ligands in this thesis were tailored for a coordination to gold (111) surfaces, a limitation and focusing on the molecular coordination towards gold(I) (and its congener Ag(I)) is rather meaningful on both counts, for the sake of scientific integrity and feasibility.

A feature all of the investigated ligands have in common is that the donor groups are directly bonded to the ferrocene unit. This structural motif is particularly interesting, since the distance between the two cyclopentadienyl decks in ferrocene is 3.32 Å, which is at the lower end of aurophilic interactions.[6] If sterically unhindered, intramolecular Au–Au interactions can lead to formation of a ferrocenophane-like structure by aurophilic aggregation. Such diaura-[6]ferrocenophane structures might serve as a molecular model for surface attachment of the ligands, as we have been able to show previously in the case of 1,1'-diisocyanoferrocene (see below).[7]

Among the broad field of ferrocene-based ligands the chemistry of dppf (**3**) is by far the best investigated and most developed one. It has been argued that the overwhelming success of dppf and related ferrocene-based phosphane ligands in catalysis and coordination chemistry has overshadowed and even delayed the development and use of ferrocene-based ligands with other donor groups.[5] The first gold(I) complex of dppf was [dppf(AuCl)$_2$] published in 1989 by Hill et al.[8] and numerous studies have followed up to now.[9,10] Depending on the ratio of dppf and gold(I) and the respective anion, dppf can act as a bridging or chelating ligand in two-, three-, and four-coordinated fashion. A useful review addressing gold chemistry with dppf as ligand was written by Gimeno and Laguna.[11]

Ferrocene species with sulfur as donor atoms substituted onto the cyclopentadienyl rings have been well known for many years.[12] Symmetrical ligands are usually obtained by reaction of 1,1'-dilithioferrocene with the corresponding disulfide; unsymetrically disubstituted derivatives have been prepared by cleavage of the trisulfur bridge in 1,2,3-trithia[3]ferrocenophane (fcS$_3$).[13,14,15] The coordination chemistry of these ligands has been studied mainly with palladium and platinum, but the coordination chemistry with gold(I) appears underdeveloped. Only one compound has been described so far, where gold(I) is directly bonded to the cyclopentadienyl-substituted sulfur atoms, using the ligand 1,1'-bis(phenylthio)ferrocene, [Fe{C$_5$H$_4$(SPh)}$_2$] (**5**).[16]

1,1'-Diisocyanoferrocene (**1**) was first described in 2001.[17] Surprisingly, the chemistry of **1** has remained completely unexplored. In a preliminary investigation of the coordination behaviour of 1,1'-diisocyanoferrocene (**1**) we realised the complexation of **1** with gold(I) chloride and have been able to obtain an X-ray diffraction analysis of the complex [(AuCl)$_2$(μ-**1**)]$_n$.[7,18] The result is shown in figure 3-1 and may provide, with caution, a model for the arrangement of **1** in SAMs on gold and therefore bridge a gap between aspects of surface and molecular coordination chemistry.

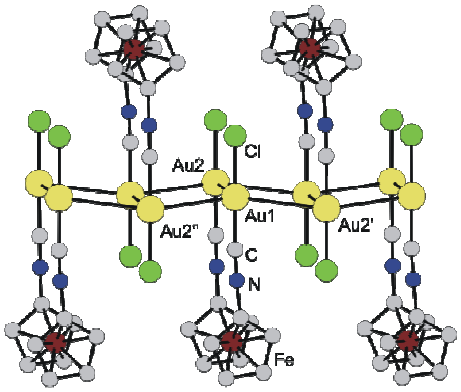

Figure 3-1: View of the association of [(μ-**1**)$(AuCl)_2$] in the crystal. Selected bond lengths [Å]: Au1–Au2 3.336(1), Au1–Au2' 3.484(1), Au1–Au2'' 3.354(1).

Motivated by this result a more in-depth investigation of the coordination behaviour of **1** was envisaged. In view of the isoelectronic nature of isocyanide and acetylide ligands, coordination to gold(I) acteylides is an attractive approach to fathom the gold chemistry of **1**. To get a more complete picture analogous silver(I) species were also addressed for complexation reactions.

Substituted acetylides ($RC{\equiv}C^-$) are particularly interesting as counter ions for gold(I), since it is possible to modify the electronic properties of the acetylide by variation of the substituent R. Alkynyl gold(I) complexes have witnessed increasing attention in versatile applications like non-linear optics, materials science, conjugated linear polymers and liquid crystals.[19,20,21]

The affinity of gold(I) for alkynyl anions is high and their preparation therefore usually easy. Gold(I) acetylides are oligo- or polymeric compounds $(AuC{\equiv}CR)_n$, in which the alkynyl ligand usually bridges by bonding to one gold atom through the σ donor interaction and to a second one by its π electrons.[22] Reactions with isocyanide ligands (R'NC) usually afford monomeric, and therefore mostly soluble, linear complexes of the type [Au(R'NC)(C≡CR)].[23]

3.2 Synthesis and Characterisation of Gold(I) Acetylides $[Au(C{\equiv}CR)]_n$ (12a-e), (a: R = *p*-$C_6H_4CF_3$, b: R = C_6H_5,[23] c: R = *p*-C_6H_4OMe,[24] d: R = *p*-$C_6H_4NMe_2$, e: R = -Fc)

$$R{-}C{\equiv}CH + [AuCl(SMe_2)] \xrightarrow{NEt_3} 1/n\left[R{-}C{\equiv}C{-}Au \right]_n$$

Figure 3-2: Synthesis of Gold(I) Acetylides

The gold(I) acetylides were prepared from $[AuCl(SMe_2)]$[25] and the respective acetylene derivative in the presence of triethylamine in CH_2Cl_2, essentially according to a procedure described by Hogarth,[26] without any precaution against oxygen or moisture if not stated otherwise.

The reactions worked best for acetylides bearing electron-donating substituents, except for ethynylferrocene (HC≡C-Fc),[27] while with HC≡C-*p*-$C_6H_4CF_3$, which contains the strongly electron-withdrawing trifluoromethyl group, the reaction was more sluggish and the yield was only moderate. In the case of HC≡C-Fc a catalytic amount of Cu(I) was found to be crucial for the conversion. Only the preparations of new compounds are presented in more detail in the following.

3.2.1 Synthesis and Characterisation of $[Au(C{\equiv}C\text{-}p\text{-}C_6H_4CF_3)]_n$ (12a)

HC≡C-*p*-$C_6H_4CF_3$ and NEt_3 were added successively under N_2 to a stirred solution of $[AuCl(SMe_2)]$ in deoxygenised CH_2Cl_2 at 0 °C. The solution was stirred for 1h at 0 °C, then deoxygenised MeOH was added. The mixture was stirred for another 2 h at 0 °C and the precipitate was isolated rapidly by centrifugation under ambient conditions. The pale yellow product turned out to be thermally unstable and decomposed slowly at room temperature, affording a violet material. At low temperature (-40 °C) it can be stored for several weeks without detectable change. The yield was moderate (38%) and success of the reaction was confirmed by EA and IR spectroscopy, showing a weak signal at 2003 cm^{-1}, which is assigned to the ν (C≡C) stretching mode of gold(I) acetylides.[26]

3.2.2 Synthesis and Characterisation of $[Au(C{\equiv}C\text{-}\textit{p}\text{-}C_6H_4NMe_2)]_n$ (12d)

The reaction was carried out at room temperature without any special precautions against moisture or oxygen. $HC{\equiv}C\text{-}\textit{p}\text{-}C_6H_4NMe_2$ and NEt_3 were added successively to a stirred solution of $[AuCl(SMe_2)]$ in CH_2Cl_2. Precipitation started after a few minutes and the reaction mixture was stirred overall for ½ h. The product was filtered off, washed with MeOH and Et_2O and dried in the air to give a yellow microcrystalline powder in good yield (92%).

The IR spectrum shows a weak peak at 1999 cm^{-1} characteristic for the ν (C≡C) stretching mode.

3.2.3 Synthesis and Characterisation of $[Au(C{\equiv}C\text{-}\textit{Fc})]_n$ (12e)

A solution of ethynylferrocene in CH_2Cl_2 and NEt_3 were added successively to a stirred solution of $[AuCl(SMe_2)]$ in deoxygenised CH_2Cl_2 under N_2. No precipitation or any detectable reaction took place even over several hours. Addition of a catalytic amount (the tip of a Pasteur pipette) of a copper(I) species (CuCl or CuI) to the reaction mixture led to formation of an orange-red microcrystalline solid. After 14 h reaction time the precipitate was filtered off, washed successively with CH_2Cl_2, MeOH and Et_2O and dried under vacuum, giving **12e** in good yield (71%).

Two ν(C≡C) bands are observed in the IR spectrum at 1976 and 2011 cm^{-1}.

3.3 Synthesis and Characterisation of 1,1'-Diisocyanoferrocene Complexes

Within the scope of the research presented in this thesis a series of complexes between coinage metals in oxidation state I and the 1,1'-diisocyanoferrocene ligand have been realised. The gold(I) complexes will be presented first, followed by the silver(I) analogues.

3.3.1 Synthesis of the Alkynyl Gold(I) Complexes [{Au(C≡C-*p*-C$_6$H$_4$R)}$_2$(μ-1)] (13a–d)

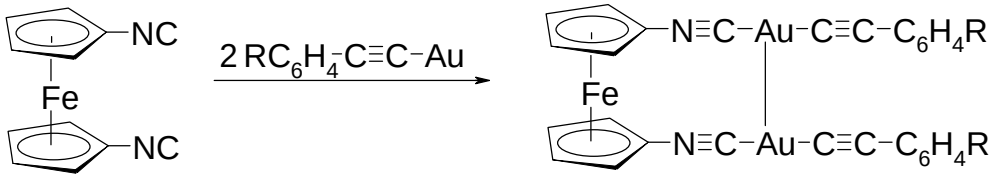

Figure 3-3: Synthesis of Complexes **13a–d**

Reactions of 1,1'-diisocyanoferrocene (**1**) with the corresponding gold(I) acetylide **12a–d** afforded the expected complexes of the type [Fe{(C$_5$H$_4$-N≡C)Au(C≡C-*p*-C$_6$H$_4$R)}$_2$]. The reaction with **12e** turned out to be a special case and will be discussed separately. Complexes **13a–d** were obtained in moderate to good yields by reacting one equivalent of **1** with two equivalents of the respective alkynyl gold(I) complex suspended in CH_2Cl_2. Due to the very poor solubility of the compounds the reaction time was extended and the reactions therefore were performed overnight at room temperature. The products **13a–d** were found to be generally sparingly soluble or insoluble in common organic solvents. Among all tested solvents (THF, acetone, MeOH, $CHCl_3$, CH_2Cl_2, $C_2H_4Cl_2$, CH_3CN) dichloromethane turned out to be the best choice. The solubility in this solvent is highest for the CF_3 bearing compound **13a** and lowest for the NMe_2 bearing analogue **13d**. ^{1}H NMR spectra could be recorded for all four compounds using CD_2Cl_2. However, attempts to recrystallize **13a–d** in order to obtain single crystals suitable for an X-ray diffraction study failed in the case of the least soluble compound **13d**.

3.3.2 Characterisation of [{Au(C≡C-*p*-$C_6H_4CF_3$)}$_2$(μ-1)] (13a)

13a was obtained in moderate yield (56%) as a crystalline solid after reaction of **12a** with **1** overnight. Analytically pure material was obtained after subsequent washing of the precipitate with MeOH and Et_2O and drying under vacuum. The ^1H NMR spectrum of **13a** in CD_2Cl_2 shows two singlets in the region typical for cyclopentadienyl protons at 4.49 and 4.93 ppm and two doublets at 7.28 and 7.32 ppm, typical for aromatic protons. The isocyano stretching mode ν(N≡C) in the IR spectrum is observed as a strong band at 2192 cm^{-1}, while the band due to the ν(C≡C) mode at 2115 cm^{-1} shows medium intensity.

Crystals suitable for an X-ray diffraction analysis were obtained by slow evaporation of a saturated solution of **13a** in thin glass tubes; the result is shown in figure 3-4.

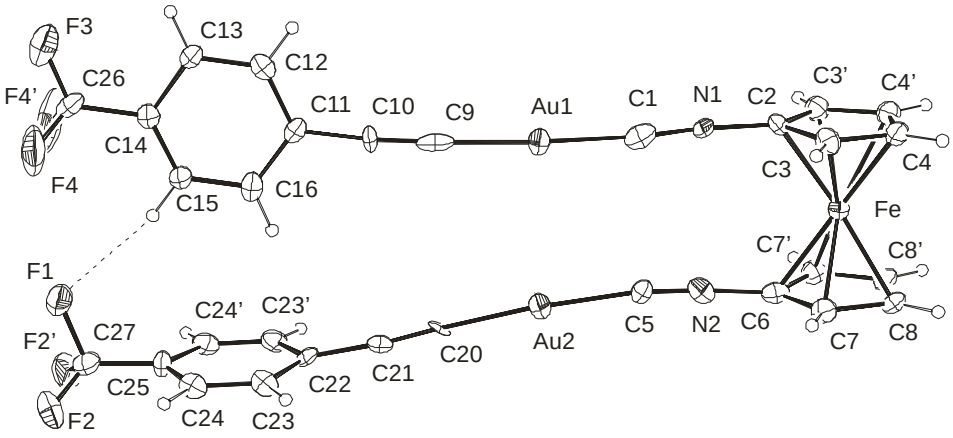

Figure 3-4: Molecular structure of **13a** in the crystal. Selected bond lengths [Å] and angles [°]:C1-N1 1.20(2), C1-Au1 1.92(2), C9-Au1 1.97(2), C9-C10 1.24(2), C5-N2 1.14(2), C5-Au2 1.977(16), C20-C21 1.20(2), C20-Au2 1.989(13), Au1-Au2 3.3011(11), C15-F1 3.47(2), F1-H15 2.54, C1-N1-C2 175.1(17), N1-C1-Au1 175.5(19), C1-Au1-C9 177.0(8), C10-C9-Au1 176.7(15), C9-C10-C11 176.0(19), C5-N2-C6 177.4(18), N2-C5-Au2 172.4(17), C5-Au2-C20 175.3(7), C21-C20-Au2 177.7(13), C20-C21-C22 175.0(16), C15-H15-F1 168.8.

As found for the other structurally characterised complexes **13b** and **13c** the molecular structure of **13a** indicates intramolecular aurophilic bonding, leading to an eclipsed conformation of the cyclopentadienyl decks. A more detailed discussion will follow in comparison of all complexes.

X-ray crystallographic data:

Empirical formula	$C_{30}H_{16}Au_2F_6FeN_2$
Formula weight	968.23
Temperature [K]	143(2)
Crystal system	Monoclinic
Space group	*P* $2_1/m$
a [Å]	11.4667(13)
b [Å]	8.5646(8)
c [Å]	14.1478(16)
α, *β*, *γ* [°]	90, 98.271(9), 90
V [Å^3]	1375.0(3)
Z	2
ρ_{calcd} [g cm^{-3}]	2.339
μ [mm^{-1}]	11.228
F(000)	896
Crystal size [mm]	$0.35 \times 0.21 \times 0.14$
θ range [°]	1.45 – 25.00
Reflections collected	8971
Independent reflections	2601
R_{int}	0.1376
Reflections with $I>2\sigma(I)$	1652
Data/restraints/parameters	2601/0/223
GOF on F^2	0.878
$R1$ ($I>2\sigma(I)$)/w$R2$	0.0455/0.0819
largest diff. peak/hole [e·Å^{-3}]	1.758/–1.639

3.3.3 Characterisation of [{Au(C≡C-*p*-C_6H_5)}$_2$(μ-1)] (13b)

13b was prepared in the same way as **13a** and could be isolated in analytically pure form in moderate yield (40%) as a crystalline solid. The ^{1}H NMR signals of the complex in CD_2Cl_2 were detected at 4.47 and 4.94 ppm, caused by the cyclopentadienyl protons. Two singlets are present at 7.13 and 7.30 ppm with an integral ratio of 8 : 2. The ν(C≡C) and ν(N≡C) stretching modes in the IR spectrum of **13b** are observed at 2121 cm^{-1}, with a medium intensity, and at 2203 cm^{-1}, as a strong band, typical for the pronounced dipole moment of the isocyano moiety.

Figure 3-5 shows the result of an X-ray diffraction analysis of **13b**. Single crystals were obtained by evaporation of a saturated solution of the complex in CH_2Cl_2 in a small beaker.

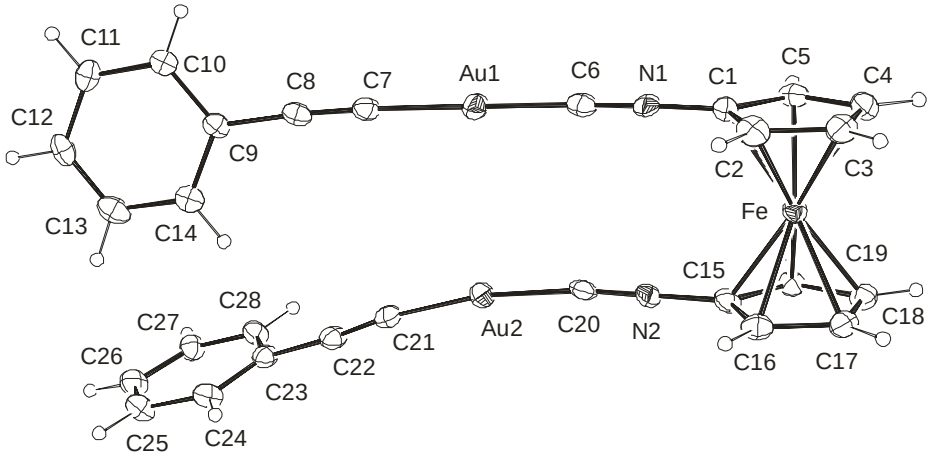

Figure 3-5: Molecular structure of **13b** in the crystal. Selected bond lengths [Å] and angles [°]:C6-N1 1.195(12), C6-Au1 1.940(10), C7-Au1 1.961(9), C7-C8 1.222(12), C20-N2 1.182(11), C20-Au2 1.959(9), C21-Au2 1.962(9), C21-C22 1.230(13), Au1-Au2 3.3617(5), C6-N1-C1 174.3(9), N1-C6-Au1 174.4(7), C6-Au1-C7 173.8(3), C8-C7-Au1 172.2(6), C7-C8-C9 176.4(8), C20-N2-C15 176.3(8), N2-C20-Au2 171.2(7), C20-Au2-C21 171.1(3), C22-C21-Au2 173.2(7), C21-C22-C23 174.5(10).

The arrangement of the phenyl rings and the eclipsed orientation of the cyclopentdienyl decks is mostly the same as in **13a**.

X-ray crystallographic data:

Empirical formula	$C_{28}H_{18}Au_2FeN_2$
Formula weight	832.23
Temperature [K]	173(2)
Crystal system	monoclinic
Space group	$P\,2_1/c$
a [Å]	9.0781(7)
b [Å]	24.9236(18)
c [Å]	13.4933(11)
α, β, γ [°]	90, 128.191(5), 90
V [Å^3]	2399.5(4)
Z	4
ρ_{calcd} [g cm^{-3}]	2.304
μ [mm^{-1}]	12.813
F(000)	1536
Crystal size [mm]	$0.60 \times 0.33 \times 0.02$
θ range [°]	1.63 – 25.00
Reflections collected	14072
Independent reflections	4226
R_{int}	0.1336
Reflections with $I>2\sigma(I)$	3584
Data/restraints/parameters	4226/0/298
GOF on F^2	1.004
$R1$ ($I>2\sigma(I)$)/w$R2$	0.0457/0.1044
largest diff. peak/hole [e·Å^{-3}]	1.853/–2.167

3.3.4 Characterisation of [{Au(C≡C-*p*-C_6H_4OMe)}$_2$(μ-1)] (13c)

Treatment of **1** with **12c** in the same way as described before afforded **13c** in 61% yield. The solubility of **13c** is considerably lower than that of **13a** and **13b** according to the intensities of the ^{1}H NMR signals of saturated samples in CD_2Cl_2 at room temperature. The signal of the methyl group is found as a singlet at 3.72 ppm. The cyclopentadienyl proton shifts are at 4.47 and 4.93 ppm and the aromatic protons lead to two doublets at 6.65 and 7.24 ppm, both showing a coupling constant of ~9 Hz. The relevant IR spectroscopic features are the ν(C≡C) band at 2123 cm^{-1} and a strong band due to the ν(N≡C) stretching mode at 2204 cm^{-1}.

Single crystals were obtained from evaporation of a saturated solution of **13c** in thin glass tubes.

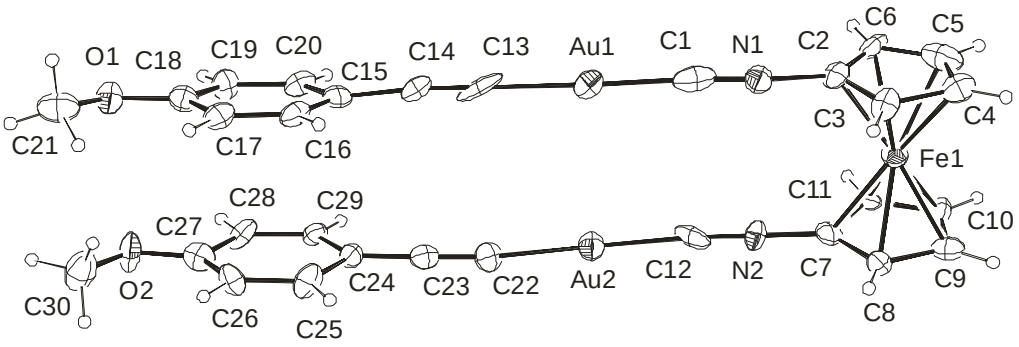

Figure 3-6: Molecular structure of **13c** in the crystal. Selected bond lengths [Å] and angles [°]: C1-N1 1.19(3), C1-Au1 1.95(3), C13-Au1 2.01(3), C13-C14 1.17(3), C12-N2 1.19(2), C12-Au2 1.94(2), C22-Au2 1.99(2), C22-C23 1.22(3), C1-N1-C2 175.9(19), N1-C1-Au1 176.4(18), C1-Au1-C13 178.4(8), C14-C13-Au1 179.0(18), C13-C14-C15 175(2), C12-N2-C7 178.3(19), N2-C12-Au2 174.9(16), C12-Au2-C22 178.7(7), C23-C22-Au2 171.3(17), C22-C23-C24 178(2).

While the eclipsed orientation of the cyclopentadienyl decks is in line with the structures of **13a** and **13b**, the phenyl rings exhibit here a parallel orientation.

X-ray crystallographic data:

Empirical formula	$C_{30.5}H_{23}Au_2ClFeN_2O_2$
Formula weight	934.74
Temperature [K]	173(2)
Crystal system	Triclinic
Space group	*P* –1
a [Å]	8.4412(12)
b [Å]	11.8387(18)
c [Å]	14.197(2)
α, *β*, *γ* [°]	87.290(12), 81.080(11), 84.569(12)
V [Å^3]	1394.6(4)
Z	2
ρ_{calcd} [g cm^{-3}]	2.226
μ [mm^{-1}]	11.134
F(000)	874
Crystal size [mm]	0.53 × 0.10 × 0.03
θ range [°]	1.45 – 25.23
Reflections collected	9181
Independent reflections	4698
R_{int}	0.0995
Reflections with $I>2\sigma(I)$	2523
Data/restraints/parameters	4698/1/349
GOF on F^2	0.820
$R1$ ($I>2\sigma(I)$)/w$R2$	0.0614/0.1363
largest diff. peak/hole [e·Å^{-3}]	1.679/–2.375

3.3.5 Characterisation of [{Au(C≡C-*p*-C$_6$H$_4$NMe$_2$)}$_2$(μ-1)] (13d)

The reaction of **1** with **12d** afforded the complex in a good yield of 66%. The solubility of this compound is extremely poor and attempts to grow single crystals suitable for an X-ray diffraction analysis failed therefore. Nevertheless, full ^{1}H NMR spectroscopic data could be obtained. **13d** shows the expected shifts as a singlet at 2.89 ppm corresponding to the methyl protons, two singlets at 4.47 and 4.92 ppm caused by the cyclopendienyl moieties and two doublets in the aromatic region at 6.47 and 7.19 ppm. The ν(C≡C) band is found at 2115 cm^{-1} with a medium intensity and the ν(N≡C) stretching mode causes a strong adsorption band at 2192 cm^{-1}.

3.3.6 Discussion of the Complexes 13a–d

The ν(C≡C) and ν(N≡C) bands were observed in the IR spectra of **13a–d** at ~2115 cm^{-1} and 2200 cm^{-1}, respectively. This compares well with values reported for closely related compounds such as, for example, [Au(C≡CPh)(C≡NC$_6$H$_3$Me$_2$-2,6)], where the ν(C≡C) band is at 2119 cm^{-1} and the ν(N≡C) stretching mode at 2211 cm^{-1}.[28] The ν(N≡C) band shift is about 100 cm^{-1} with respect to uncoordinated **1** and an even

slightly larger ν(C≡C) band shift occurs with respect to the respective gold(I) acetylide **12**, which is in accord with previous observations.[23] These substantial band shifts to higher energy indicate that the isocyanide acts as a strongly σ-donating ligand, whose coordination to Au(C≡C-*p*-C_6H_4R) reduces the degree of metal−carbon π-bonding in this moiety.[29]

The quality of the crystal structure determinations of **13a–c** was affected by the small size of the crystal in each case. It was further compromised by the presence of disordered solvent of crystallisation in the case of **13c**. Consequently, a meaningful discussion of bond parameters is possible for the heavy atoms only. The C−N≡C−Au−C≡C−C chains are nearly linear for all three compounds with bond angles between ~171° and 178°, as expected for this kind of rigid-rod type molecular units. A prominent feature of all three molecular structures is the fact that the molecules adopt an eclipsed conformation with an intramolecular aurophilic contact. This Au···Au distance apparently depends on the electronic properties of the acetylide ligand C≡C-*p*-C_6H_4R. It is 3.3011(11) Å for **13a** (R = CF_3), 3.3617(5) Å for **13b** (R = H) and 3.6219(12) Å for **13c** (R = OMe). Correlations between Au···Au distances and the `hard´ or `soft´ character of anionic ligands X in linear dicoordinate gold(I) complexes [AuX(L)] have been found in previous theoretical and experimental studies. For example, Pyykkö et al. predicted an increase in the strength of the aurophilic interaction for staggered dimers of the phosphane complexes [AuX(PH_3)] in the series of halogeno ligands with F < Cl < Br < I.[30] This trend was verified by X-ray crystallography for [AuX($PPhMe_2$)] (X = Cl, Br, I) by Balch and coworkers.[31] In the case of isocyanide complexes [AuX(CNR)], an opposite trend was found.[32] A theoretical study performed for dimers of [AuX(CNMe)] (X = Cl, I) revealed that in this case the antiparallel, instead of the staggered, arrangement of monomeric units is preferred.[33] The major attractive contribution between monomeric units was found to originate from the dipole−dipole interaction. Consequently, the Au···Au distance is indicative of the presence, but not commensurate with the strength, of aurophilic

interactions. In view of these results, the eclipsed molecular structures of **13a–c**, which correspond to the parallel arrangement of [AuX(CNR)] units, might appear extraordinary. However, closer inspection of the crystal packing reveals an antiparallel orientation of neighboring molecules as shown in figures 3-7–3-9. This combination of parallel and antiparallel alignments is similar to the structural motif observed for the chloro complex [$(AuCl)_2$(μ-**1**)].[7]

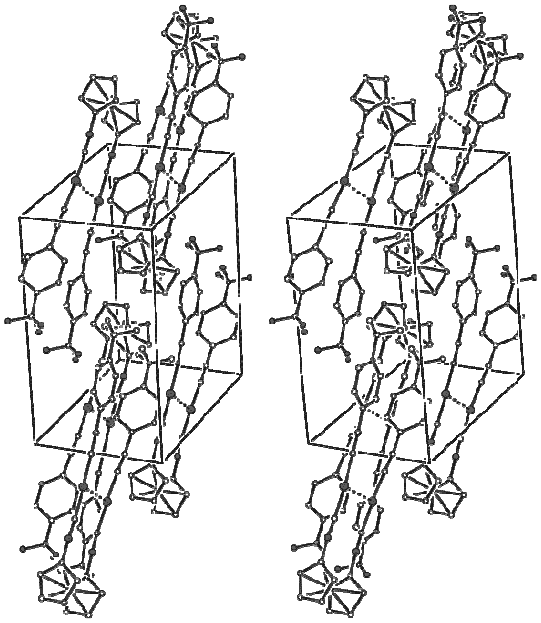

Figure 3-7: Molecular arrangement of **13a** in the crystal.

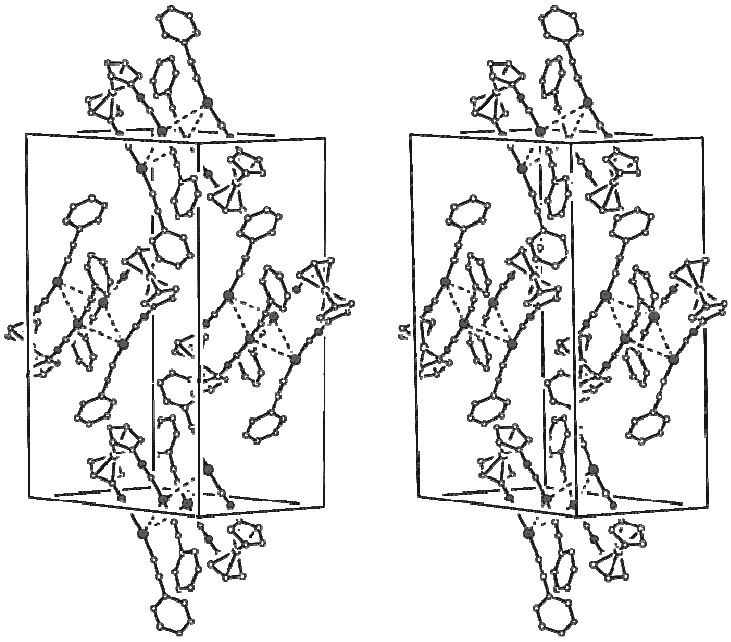

Figure 3-8: Molecular arrangement of **13b** in the crystal.

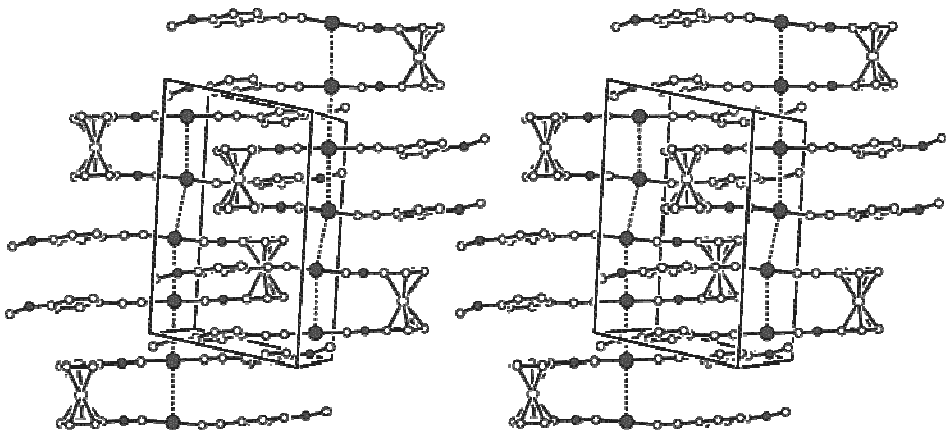

Figure 3-9: Molecular arrangement of **13c** in the crystal.

In the case of **13c**, a one-dimensional chain of antiparallel molecules is formed, whose intermolecular Au···Au distances of 3.5576(15) and 3.5921(16) Å are very similar to the intramolecular distance of 3.6219(12) Å. A similarly nice balance between intra- and intermolecular aurophilicity is present in the case of [(AuCl)$_2$(μ-**1**)], which is aggregated as one-dimensional chains, too.[7] The insoluble nature of [(AuCl)$_2$(μ-**1**)] is reminiscent of the very low solubility of **13c** and the even poorer solubility of the NMe$_2$ substituted analogue **13d**. It is likely therefore that **13d** also forms such one-dimensional chains in the crystal. In the case of **13b**, the molecules are aggregated as antiparallel dimers with intermolecular Au···Au distances of 3.9509(5) Å. In the case of **13a**, which exhibits the shortest intramolecular Au···Au contact in this series, no such intermolecular contacts are present. In addition to the short intramolecular Au···Au contact, an intramolecular C–F···H–C interaction is observed for this compound (indicated by a dotted line in figure 3-4).

The FHC angle of ~168.8° and the F···C and F···H distances of ~3.47 and 2.54 Å, respectively, are compatible with a weak hydrogen bond.[34,35] Although their existence, nature, and supramolecular relevance still is a contentious issue, weak intramolecular C–F···H–C hydrogen bonds have recently been probed and authenticated by NMR spectroscopic methods in solution and by neutron diffraction in the solid state.[36]

3.4 Synthesis and Characterisation of [(Fc-C≡C-Au-C≡N-C_5H_4)Fe{C_5H_4-N=C(Au)-C≡C-Fc}]$_3$ (14)$_3$

Sometimes apparently simple reactions (in terms of foreseeability) may break ranks in a prodigious way. The reaction of [Au(C≡C-Fc)]$_n$ (**12e**) with **1** is such an extraordinary case within the scope of this thesis. In view of the results just described, a coordination of **1** with 2/*n* equivalents [Au(C≡C-Fc)]$_n$ should lead to the formation of an 'orthodox' complex [Fe{C_5H_4(NC-Au-C≡C-Fc)}$_2$] (**13e**) in analogy to **13a-d**. Furthermore, it is expectable that the product would exhibit an eclipsed molecular conformation similar to that found for **13a–c**, so that an efficient communication between the two redox-active terminal ferrocenyl units could give rise to some interesting redox-chemical behaviour.

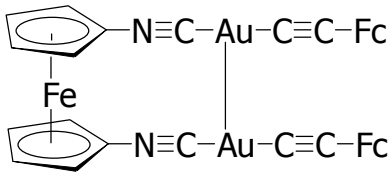

Figure 3-10: Anticipated molecular structure of **13e**.

The reaction was carried out as described for **13a–d** by addition of **1** to a stirred suspension of **12e** in CH_2Cl_2. The solubility of the product again was poor in common organic solvents and CH_2Cl_2 proved to be the best solvent here as well. Nevertheless, the solubility of the complex was significantly better than that of **13a-d** and the workup differed. Shortly after addition of a solution of **1** in CH_2Cl_2 to the suspended gold(I) acetylide the reaction mixture became dark red and nearly cleared up after several hours. After 14 h the reaction mixture was filtered and concentrated. Addition of MeOH caused almost complete precipitation of the product, which was subsequently washed with MeOH and Et_2O. After drying under vacuum the complex was obtained in 71% yield. It was purified by recrystallisation from CH_2Cl_2. Microanalytical data of the product agree well with the composition of **13e**. However, its ^{1}H NMR spectrum is not compatible with **13e**, since it exhibits too many signals for a species of such symmetry.

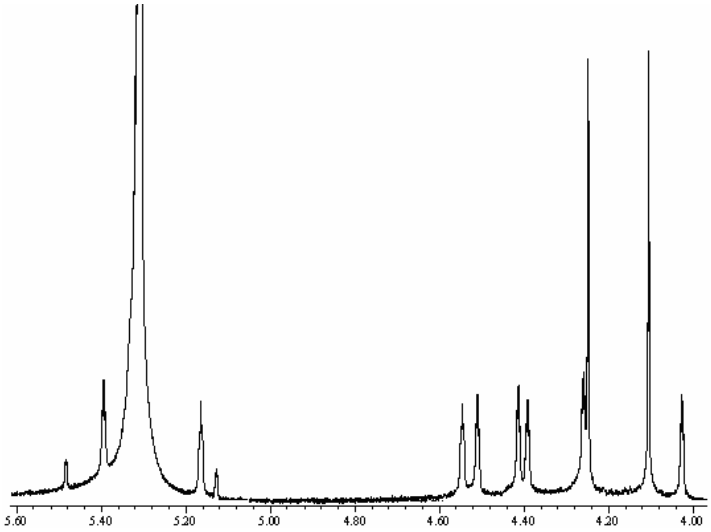

Figure 3-11: ^{1}H NMR spectrum of **14** in CD_2Cl_2 (causing the main peak).

Single crystals suitable for an X-ray structure analysis were obtained by repeated recrystallisation from CH_2Cl_2. The result of the diffraction analysis proved that the product is not **13e**, but rather the hexanuclear gold cluster [(Fc-C≡C-Au-C≡N-C_5H_4)Fe{C_5H_4-N=C(Au)-C≡C-Fc}]$_3$, which is composed of three subunits **14**.

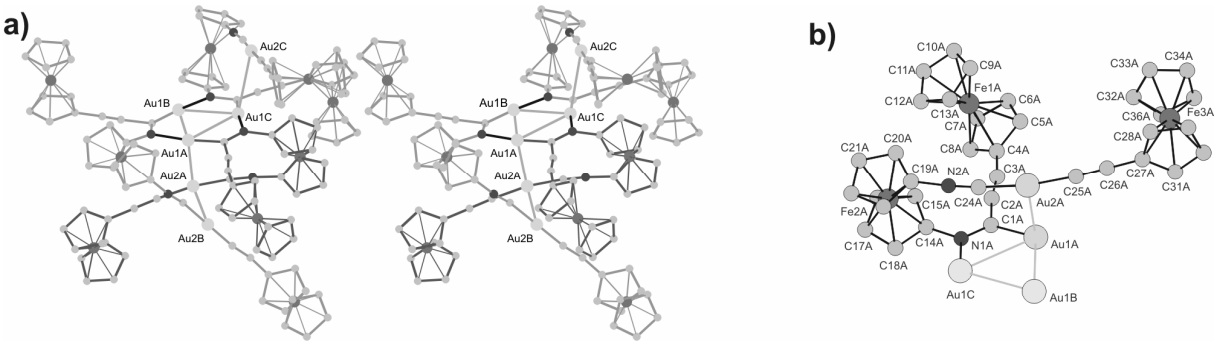

Figure 3-12:(a)Molecular structure of (**14**)$_3$ in the crystal (stereographic representation with subunits marked in different grey scales). Interatomic distances <4.0 Å in the Au_6 cluster: Au1A-Au1B 3.356(2), Au1A-Au1C 3.278(2), Au1A-Au2A 3.352(2), Au2A-Au2B 3.165(2), Au1B-Au1C 3.284(2), Au1C-Au2C 3.391(2) Å. (b) Molecular structure of one subunit (darkest grey) in (a). Selected bond lengths (Å): C1A-N1A 1.31(3), C1A-C2A 1.40(4), C1A-Au1A 1.98(3), C2A-C3A 1.22(4), C24A-N2A 1.15(3), C24A-Au2A 1.90(3), C25A-C26A 1.25(5), C25A-Au2A 1.95(3), N1A-Au1C 1.99(2).

The reaction that took place instead of the expected formation of **13e** is therefore a combination of an 'orthodox' coordination to one of the isocyano moieties and an unprecedented 1,1-insertion of the other isocyano group into the gold(I) acetylide. (Figure 3-13).

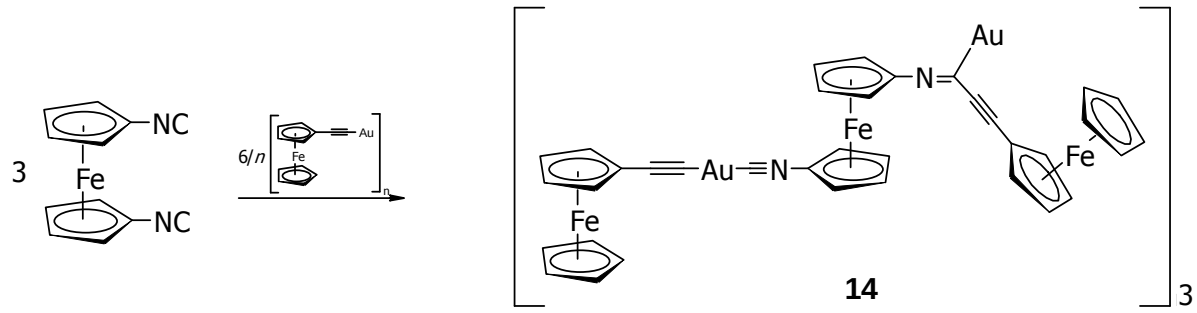

Figure 3-13: Reaction of **1** with $[Au(C{\equiv}C–Fc)]_n$.

The spectroscopic data are fully in accord with this result. As shown in figure 3-11 there are ten peaks present in the ^{1}H NMR spectrum in the region typical for cyclopentadienyl protons, eight pseudo-triplets at 4.04, 4.37, 4.40, 4.42, 4.52, 4.56, 5.18 and 5.41 ppm and two singlets at 4.12 and 4.26 ppm, displaying an integral of the 2.5-fold size of the triplets, indicative for the unsubstituted cyclopentadienyl decks. The characterisation of the complex was hampered by its poor solubility. It was only possible to obtain limited ^{13}C NMR data for the compound, despite an extended recording time of 3 days. Ten peaks were found in a region between 67.9 and 72.3 ppm, typical for ferrocene-type carbon signals. However, the signals of the quaternary C atoms could not be detected.

The IR spectrum is also in line with $(\mathbf{14})_3$. In particular, due to the presence of the σ,μ_2-iminoacyl group a ν(N=C) vibrational band is observed at 1491 cm^{-1} in addition to the expected ν(N≡C) and ν(C≡C) bands at 2201 and 2155 cm^{-1}, respectively. For comparison, the ν(C=N) band of Ph-C≡C-C(=NPh)Ph is located at 1560 cm^{-1},[37] while it occurs at 1530 cm^{-1} in the case of the mononuclear iminoacyl complex [Pd{C(C≡C-Ph)(=NPh)}Cl$(PEt_3)_2$].[38] It is well documented for binuclear complexes that a σ,μ_2-iminoacyl coordination leads to a notable energy decrease of this band of ~ 60 cm^{-1} with respect to the parent imine.[39]

X-ray crystallographic data:

Empirical formula	$C_{110}H_{82}Au_6Cl_4Fe_9N_6$
Formula weight	3314.07
Temperature [K]	133(2)
Crystal system	Triclinic
Space group	*P* –1
a [Å]	13.6125(18)
b [Å]	19.243(3)
c [Å]	23.262(3)
α, *β*, *γ* [°]	110.426(10), 104.403(10), 108.902(10)
V [Å^3]	4932.0(15)
Z	2
ρ_{calcd} [g cm^{-3}]	2.232
μ [mm^{-1}]	10.323
F(000)	3120
Crystal size [mm]	0.25 × 0.10 × 0.04
θ range [°]	1.27 – 24.80
Reflections collected	24014
Independent reflections	12254
R_{int}	0.1122
Reflections with $I>2\sigma(I)$	5764
Data/restraints/parameters	12254/0/927
GOF on F^2	0.859
$R1$ ($I>2\sigma(I)$)/w$R2$	0.0715/0.1567
largest diff. peak/hole [e·Å^{-3}]	2.569/–2.859

3.4.1 Discussion for $(14)_3$

Due to the poor quality of the crystal, the data/parameter ratio of the X-ray structure analysis is rather low. Consequently, a detailed discussion of bond parameters is meaningful only for the heavy atoms. The gold cluster exhibits Au–Au distances which are typical for aurophilic interactions, ranging from 3.165(2) to 3.391(2) Å. The cluster core is a triangle of gold atoms whose three sides are each bridged by the N=C unit of a single iminoacyl ligand. Such σ,μ$_2$-bridging iminoacyl ligands RN=CR′ are quite common. In fact, even several clusters are known with a side of an M_3 triangle bridged by a σ,μ$_2$-iminoacyl ligand, especially in the chemistry of osmium.[40] In contrast, clusters with two bridged triangular sides of this type are rare.[41,42] (**14**)$_3$ is unique since bridging of all three sides of an M_3 triangle with σ,μ$_2$-RN=CR′ ligands has not been described to date. However, the general structural motif is not unfamiliar in the chemistry of gold. Several triply bridged triangular clusters of the type [Au$_3${σ,μ$_2$-RN=C(OR′)}$_3$] have been reported which contain carbeniate ligands RN=C(OR′), which are akin to iminoacyl ligands RN=CR′. These gold clusters were obtained from the reaction of [AuCl(L)] (L = SMe_2, PPh_3) with isocyanides RNC in a suitable alcohol R′OH in the presence of KOH.[43,44,45,46,47] They usually aggregate in the

solid state due to aurophilic interactions.[48] For example, [Au_3{σ,μ_2-*p*-TolN=C(OEt)}$_3$] forms dimeric units in the crystal through two intermolecular Au–Au contacts.[49] A similar motif is observed for (**14**)$_3$, where two atoms of the Au_3 triangle are each connected with a further gold atom – in this case, however, *intra*molecularly. This is caused by the Au–Au contact present within two of the three subunits of (**14**)$_3$. These Au–Au interactions altogether result in an unprecedented chain of five gold atoms with two neighboring atoms being bridged by a sixth one.

Finally let us focus on the component of **14** which is based on 1,1'-diisocyanoferrocene. This unit was formed in a peculiar way. One of the two isocyano groups shows the usual, and expected, coordination of the gold acetylide unit Au(C≡C-Fc). In contrast, the other one has undergone a 1,1-insertion reaction with the Au–C bond of the gold acetylide, thus forming an iminoacyl group. 1,1-insertion or α-addition reactions are common in the chemistry of isocyanides and can occur with a wide range of metal–carbon bonds. For example, metalated aldimines are formed in their reaction with organolithium compounds and Grignard reagents, respectively.[50] Analogous reactions are observed with M–C bonds of transition metal complexes, which often lead to the formation of η^2-iminoacyl complexes, especially in the case of early transition metals.[51,52] Insertion reactions of isocyanides with transition metal acetylide complexes are currently attracting particular attention. This is primarily due to two reasons. Firstly, multiple and successive insertions have been observed with heterodinuclear complexes of the type [Cl(PR_3)$_2$Pd-C≡C-Pt(PR_3)$_2$Cl], and even the living polymerization of aryl isocyanides has been described with this system.[53,54] Secondly, examples have been reported for the catalytic coupling of isocyanides with terminal alkynes.[55,56,57] These reactions afford 1-aza-1,3-enines, which are useful synthons in Organic Chemistry.[58] Surprisingly, despite the recent dynamic progress in the chemistry of gold,[59,60,61] insertion reactions of isocyanides with Au–C bonds are practically unknown. Only two examples have been described to date,[62,63] and only one of these involves a gold(I) species, viz. the 1,1-insertion of

2,6-dimethylphenylisocyanide into the Au–C bond of the gold(I) enolate [Au{$CH_2C(O)Ph$}(PPh_3)].[63]

The 1,1-insertion of an isocyanide into an Au–C bond is very unusual as such. It is even more unusual that in the present case this reaction occurs in conjunction with a second, different, reaction. This observation requires some reflection. It is common knowledge that two equivalent groups in a molecule often do not react independently from one another. The fact that the reaction of the first group influences that of an equivalent second group is known as induced reactivity asymmetry.[64] This effect can be thermodynamic (different equilibrium constants) and/or kinetic (different reaction rates) in origin. Simple examples reflecting a thermodynamic influence are polyprotic acids such as, for example H_3PO_4, where the consecutive decrease in acidity (pK_{a1} = 2.16, pK_{a2} = 7.21, pK_{a3} = 12.32) is mainly due to electrostatic reasons. Essentially the same holds true for the different redox potentials observed for the two formally identical subunits of 1,1′-biferrocene (Fc–Fc) ($E^{0\prime}_1$ = +0.31 V, $E^{0\prime}_2$ = +0.64 V vs. SCE).[65,66] With respect to kinetic effects, a common observation is that the reaction rate slows down in consecutive reactions of equivalent groups. Due to their relevance to polymer chemistry, the kinetics of consecutive reactions of difunctional substrates has been treated theoretically, both for interacting and non-interacting functional groups already half a century ago.[67] A simple and particularly well studied example in this context is the reaction of aromatic diisocyanates with alcohols.[68]

Although the induced reactivity asymmetry is a commonly known and widely studied phenomenon in chemistry, the discussed variant is extraordinary, since the consecutive reactions are not the same. To the best of my knowledge, it has never been observed before that two chemically equivalent groups in a molecule undergo a different specific reaction with the same reagent. This `schizoid´ reactivity observed for **1** in its reaction with **12e** constitutes a novel phenomenon in chemistry. Unfortunately, attempts to study the course of the reaction by ^{1}H NMR spectroscopy

have not been successful so far because of the essentially insoluble nature of both the gold acetylide starting material and the gold cluster product.

3.5 Synthesis and Characterisation of Complexes of 1 with Ag(I) (15a–b)

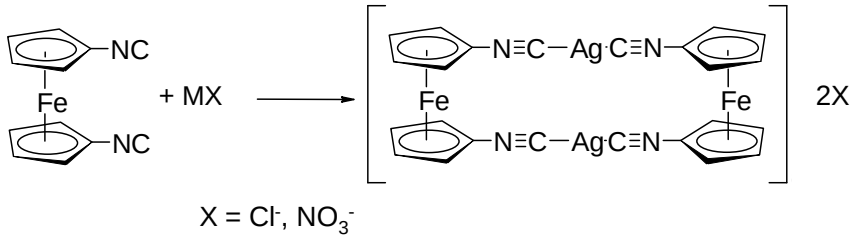

Figure 3-14: Synthesis of the Complexes **15a**–**b**

The intriguing results obtained in the chemistry of gold(I) drew the attention to silver(I), whose isocyanide coordination chemistry has been somewhat overshadowed by that of its heavier congener. While gold(I) strongly prefers a two-coordinated, linear arrangement of the ligands, the structures of silver(I) species are more flexible, often being tri- or tetra-coordinate. The reactions were therefore carried out in an 1 : 1 ratio of **1** with the respective Ag(I) salt.

3.5.1 Synthesis and Characterisation of $[Ag_2(\mu\text{-}1)_2](NO_3)_2 \cdot H_2O$ (15a)

The reaction of **1** with silver(I) nitrate (ratio 1 : 1) was carried out in CH_3CN at room temperature overnight. The product was obtained as golden shining platelets. Workup was done by filtration and subsequent washing with MeOH, CH_3CN and Et_2O. After drying under vacuum **15a** was obtained in analytically pure form. The complex is sparingly soluble in CH_2Cl_2 and $CHCl_3$, it is insoluble in all other common organic solvents tested. Its characterisation was therefore hampered and only ^1H NMR data were recorded. The signals are shifted considerably from 4.26 and 4.69 ppm (uncoordinated **1** in $CDCl_3$) to 4.47 and 5.30 ppm.

The IR spectrum of $[Ag_2(\mu\text{-}\mathbf{1})_2](NO_3)_2$ exhibits a single ν(NC) band, which is located at 2193 cm^{-1}, a shift of 75 cm^{-1} compared to the ν(NC) mode of the free ligand at 2118 cm^{-1}.

Single crystals suitable for an X-ray diffraction study were obtained by recrystallisation form CH_2Cl_2.

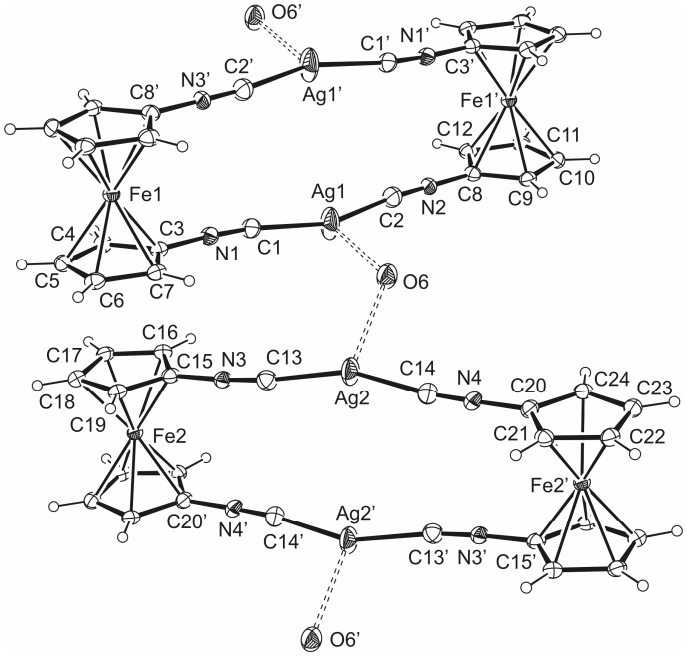

Figure 3-15. View of the association of $[Ag_2(\mu\text{-}\mathbf{1})_2](NO_3)_2 \bullet H_2O$ in the crystal. The nitrate anions are not shown. Selected bond lengths [Å] and angles [°]: C3-N1 1.407(7), C1-N1 1.15, C1-Ag1 2.086(6), C2-Ag1 2.088(6), C2-N2 1.153(7), C8-N2 1.387(7), C15-N3 1.390(7), C13-N3 1.157(7), C13-Ag2 2.080(6), C14-Ag2 2.097(6), C14-N4 1.144(8), C20-N4 1.378(7), Ag1-O6A 2.497(9), Ag1-O6 2.506(10), Ag2-O6A 2.426(9), Ag2-O6 2.516(10), C1-N1-C3 175.9(6), N1-C1-Ag1 171.6(5), C1-Ag1-C2 159.8(3), N2-C2-Ag1 173.5(6), C2-N2-C8 178.7(6), C13-N3-C15 176.5(6), N3-C13-Ag2 172.3(5), C13-Ag2-C14 157.8(2), C14-N4-C20 177.8(6), O6A-O6-Ag1 77.5(8), O6A-O6-Ag2 73.0(8), Ag1-O6-Ag2 119.9(4), Ag2-O6A-Ag1 124.1(3).

X-ray crystallographic data:

Empirical formula	$C_{48}H_{36}Ag_4Fe_4N_{12}O_{14}$
Formula weight	1659.77
Temperature [K]	153(2)
Crystal system	monoclinic
Space group	*C* 2/*c*
a [Å]	30.442(3)
b [Å]	15.0416(7)
c [Å]	11.6227(10)
α, *β*, *γ* [°]	90, 103.262(7), 90
V [Å^3]	5180.1(7)
Z	4
ρ_{calcd} [g cm^{-3}]	2.128
μ [mm^{-1}]	2.646
F(000)	3248
Crystal size [mm]	$0.60 \times 0.17 \times 0.04$
θ range [°]	1.37 – 24.63
Reflections collected	15748
Independent reflections	4354
R_{int}	0.0723
Reflections with $I>2\sigma(I)$	3264
Data/restraints/parameters	4354/0/389
GOF on F^2	1.014
$R1$ ($I>2\sigma(I)$)/w$R2$	0.0427/0.1073
largest diff. peak/hole [e·Å^{-3}]	1.038/–1.178

3.5.2 Synthesis and Characterisation of $[Ag_2(\mu\text{-}1)_2]Cl_2$ (15b)

The preparation was performed in analogy to **15a**, except that silver(I) chloride is insoluble in CH_3CN and therefore gave a suspension. The yellow solution gradually turned to a suspension of shining platelets and after 3 days the complex was obtained after washing (MeOH and Et_2O) and drying under vacuum in analytically pure form. **15b** proved to be insoluble in all tested common organic solvents, so its characterisation was limited to IR spectroscopy and elemental analysis, whose results are in accord with the formulation of **15b**.

In the IR spectrum of $[Ag_2(\mu\text{-}\mathbf{1})_2]Cl_2$ a single ν(NC) band is found, which is located at 2165 cm^{-1}. The shift caused by the coordination is less pronounced than in the case of the nitrate analogue therefore.

3.5.3 Discussion of 15a

The first report concerning this class of compounds comes from the year 1952 and describes the preparation of $[Ag(p\text{-Tol-NC})_4](NO_3)\cdot H_2O$ from $AgNO_3$ and *p*-tolyl isocyanide, together with the formation of $[Ag(p\text{-Tol-NC})_2](NO_3)$ from this product during its recrystallisation from $CHCl_3/Et_2O$.[69] This earliest example already nicely reflects a fundamental feature of silver(I) isocyanide complexes in comparison to related gold(I) compounds. The structures of the silver(I) species are more flexible, with the Ag atoms often being tri- or tetra-coordinate. (Quasi-)linear two-coordination of the metal by isocyanide ligands, which is the rule for gold(I), is the exception for silver(I), where usually strong interactions with the anion are observed.[70,71] The coordination-induced ν(NC) band shift is 34 cm^{-1} less than that observed in the case of the gold complex $[(\mu\text{-}\mathbf{1})(AuCl)_2]_n$ (see above), which is fully in accord with results of a recent study which compares such band shifts for a variety of gold and silver complexes.[72]

The obtained crystal structure analysis shows that one additional water molecule per formula unit is incorporated in **15a**. Two independent $[Ag_2(\mu\text{-}\mathbf{1})_2]^{2+}$ species (A and B) are present in the crystal, whose bond parameters are very similar. The water

molecule is disordered over two sites. It acts as a bridging ligand and connects neighbouring A and B species which alternate in the resulting polymeric chain [A(μ-H_2O)B(μ-H_2O)]$_n$. This μ_2 coordination mode of water is unusual, but not unprecedented, in the chemistry of silver(I).[73] The silver-coordinated water forms hydrogen bridges with one of the two nitrate anions. This anion is disordered over two sites with split positions for the O atoms in each case. Figure 3-15 shows the molecular structure of an A(μ-H_2O)B unit, indicating a section of the polymeric chain.

Each silver atom strongly interacts with two isocyanide C atoms and one water O atom. The Ag–O distances are ~ 2.50 Å, which compares well to the value of 2.468(3) Å reported for the isocyanide complex [Ag(OTf)(μ-4-NC-3,5-*i*Pr$_2$-C_6H_2-NC)]$_n$ [71] as well as to the Ag–OH_2 distances of 2.482(5), 2.50(1) and 2.51(1) Å found for the three-coordinate Ag atoms in the μ-aqua complex [Ag_8(μ_3-hmt)$_2$(μ_4-hmt)$_2$(μ-btc)$_2$(μ-H_2O)$_3$]·18H_2O (hmt = hexamethylenetetramine, btc = 1,2,4,5-benzenetetracarboxy-late).[73] It is also in the same range as the short Ag–O contacts typically found in salts with oxyanions.[74,75,76,77] The closest Ag···O contact which involves a nitrate anion is ~ 2.8 Å and therefore represents a rather weak, but non-negligible, interaction by commonly accepted criteria.[78] The Ag atom is therefore embedded in a 3 + 1 coordination environment. The Ag–C and N–C bond lengths are ~ 2.09 Å and 1.15 Å, respectively, which is similar to the corresponding values reported for closely related complexes such as, for example, [Ag(κ^2-NO_3)(TosCH_2NC)$_2$] (2.106(4) Å; 1.133(4) Å),[70] [Ag_2(μ,κ^1-NO_3)$_2$(μ-dmb)$_2$] (2.084(7) Å; 1.132(11) and 1.089(17) Å),[79] [Ag(4-NC-3,5-*i*Pr$_2$-C_6H_2-NC)$_2$][BF_4] (2.092(5) and 2.098(5) Å; 1.125(6) and 1.128(6) Å),[71] and [Ag(2,4,6-*t*Bu-C_6H_2-NC)$_2$][PF_6] (2.075(14) Å; 1.148(17) Å).[80] The C–N–C–Ag units deviate slightly from linearity, the nitrogen bond angles and N–C–Ag angles ranging from 172.3° to 173.6° and from 171.6° to 173.5°, respectively. In contrast, the C–Ag–C angles of 158° and 160° are considerably smaller than 180°, which is due to the additional interaction of the Ag atom with the water O atom. The Ag–O–Ag bond angle is 120° and 124°, respectively, for the two disordered sites.

3.6 Synthesis and Characterisation of [(Au-C≡C-Fc)$_2$(μ-3)] (16)

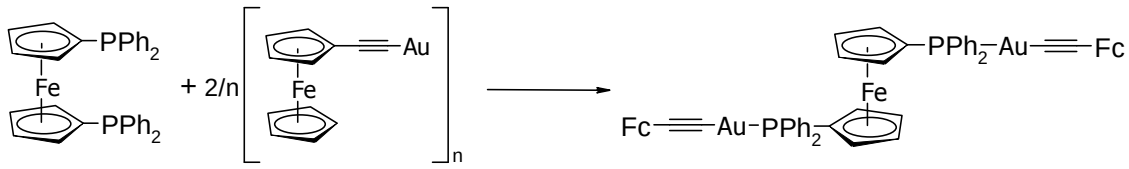

Figure 3-16: Synthesis of **16**

While the reaction of **12e** with 1,1'-diisocyanoferrocene (**1**) proved to be somewhat unusual (see above), its reaction with 1,1'-bis(diphenylphosphino)ferrocene (**3**, dppf) gave the expected result, namely the complex [(Au-C≡C-Fc)$_2$(μ-**3**)] (**16**), which was isolated in high yield (89%) as a yellow, microcrystalline solid. The reaction was carried out in CH_2Cl_2 at room temperature without any precautions against oxygen or moisture.

The ν(C≡C) vibrational band is observed at 2110 cm^{-1} in the IR spectrum, which is very similar to the values of 2105 cm^{-1} and 2115 cm^{-1} reported for the closely related [{Au-C≡C-C(CH$_2$)Me}$_2$(μ-**3**)][81] and [(Au-C≡C-Ph)$_2$(μ-**3**)],[82] respectively. It is also in line with the value of ~ 2115 cm^{-1} found in the case of **13a–d**.

The complex is nicely soluble in CH_2Cl_2 and $CHCl_3$ and the characterisation by NMR was easily possible. In the ^{1}H NMR spectrum of **16** in $CDCl_3$ five peaks are found in the region typical for cyclopentadienyl protons, as expected. Four singlets display an integral size corresponding to four protons at 4.05, 4.11, 4.36 and 4.44 ppm and one singlet is found at 4.21 with an integral size corresponding to ten protons. The signals of the aromatic protons are found as a complex multiplet in a range of 7.28 – 7.36 ppm with a respective intensity (20 H). The ^{13}C{^{1}H} NMR spectrum exhibits cycplopentadienyl carbon signals at 65.8, 67.5, 67.8, 69.9 and 71.8 ppm, followed by two doublets at 73.4 (J = 12.3 Hz) and 74.5 ppm (J = 12.7 Hz) due to coupling between the ^{31}P hetero nuclei with the respective carbon atoms. Two signals at 98.7 and 102.1 ppm are indicative for the alkynyl function. Signals in the typical region for aromatic carbon atoms are found at 128.2 (J = 12.1 Hz) and 128.6 ppm (J = 9.5 Hz) as doublets, a singlet at 130.4 ppm, a doublet at 131.2 ppm (J = 10.0 Hz), a singlet at 131.6 ppm and

a doublet at 133.6 ppm and can be assigned to the phenyl rings. The $^{31}P\{^{1}H\}$ NMR signal is observed as a singlet at 24.8 ppm, which is very similar to the value of 27.4 ppm reported for the chloro analogue $[(AuCl)_2(\mu\text{-}\mathbf{5})]$.[8]

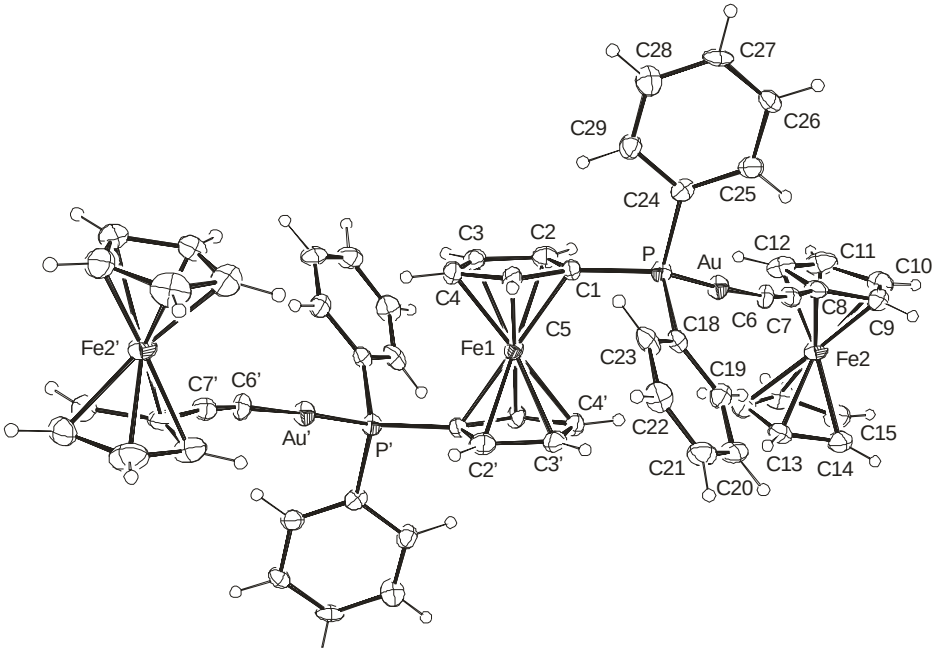

Figure 3-17: Molecular structure of **16** in the crystal. Selected bond lengths [Å] and angles [°]:C1-P 1.790(9), C6-C7 1.221(14), C6-Au 1.998(10), C7-C8 1.415(15), P-Au 2.293(2), C1-P-Au 110.9(3), C6-Au-P 178.0(3), C7-C6-Au 173.6(9), C6-C7-C8 173.4(11).

X-ray crystallographic data:

Empirical formula	$C_{58}H_{46}Au_2Fe_3P_2$
Formula weight	1366.37
Temperature [K]	143(2)
Crystal system	orthorhombic
Space group	*P b c a*
a [Å]	14.6431(8)
b [Å]	11.7790(5)
c [Å]	27.4725(15)
α, *β*, *γ* [°]	90, 90, 90
V [Å^3]	4738.5(4)
Z	4
ρ_{calcd} [g cm^{-3}]	1.915
μ [mm^{-1}]	7.174
F(000)	2640
Crystal size [mm]	0.25 × 0.09 × 0.02
θ range [°]	1.48 – 25.00
Reflections collected	15824
Independent reflections	3995
R_{int}	0.1162
Reflections with $I>2\sigma(I)$	2466
Data/restraints/parameters	4354/0/389
GOF on F^2	0.879
$R1$ ($I>2\sigma(I)$)/w$R2$	0.0430/0.0808
largest diff. peak/hole [e·Å^{-3}]	1.579/–0.702

3.6.1 Discussion of 16

A single-crystal X-ray structure determination was performed for [(Au-C≡C-Fc)$_2$(μ-**5**)] (Figure 8). The molecule exhibits crystallographically imposed inversion symmetry. The P−Au−C≡C−C chain is essentially linear, with bond angles between ~ 173° and 178°. The Au−P bond length of 2.293(2) Å is similar to the values found for closely related compounds such as, for example, [{Au-C≡C-C(CH$_2$)Me}$_2$(μ-**5**)] (2.279(2) Å),[81] [{(AuC≡CCH$_2$O)$_2$-*p*-C$_6$H$_4$}{μ-Ph$_2$P(CH$_2$)$_3$PPh$_2$}] (2.261(7) and 2.278(7) Å),[83] and [{(Ph$_3$P)$_2$Au}$_2${μ-1,12-(C≡C)$_2$-1,12-C$_2$B$_{10}$H$_{10}$}] (2.2743(14) Å).[84] These Au−P bond length are marginally longer than those of the chloro complex [(AuCl)$_2$(μ-**5**)] (2.239(3) Å),[8] which reflects the comparatively higher *trans* influence of an alkynyl ligand as opposed to a chloro ligand. The Au−C bond length of 1.998(10) Å found for [(Au-C≡C-Fc)$_2$(μ-**5**)] compares well with values observed for similar compounds such as the three dinuclear gold(I) acetylide complexes just mentioned; the corresponding values are 2.005(10) Å for [{Au-C≡C-C(CH$_2$)Me}$_2$(μ-**5**)], 2.03(2) and 2.05(3) Å for [{(AuC≡CCH$_2$O)$_2$-*p*-C$_6$H$_4$}{μ-Ph$_2$P(CH$_2$)$_3$PPh$_2$}] and 2.007(5) Å for [{(Ph$_3$P)$_2$Au}$_2${μ-1,12-(C≡C)$_2$-1,12-C$_2$B$_{10}$H$_{10}$}]. The structure of [{Au-C≡C-C(CH$_2$)Me}$_2$(μ-**5**)], which seems to be closest structurally characterized relative of [(Au-C≡C-Fc)$_2$(μ-**5**)], also exhibits centrosymmetric molecules. Aurophilic interactions are absent in both cases, which is probably due to the steric bulk of the acetylide ligands. In the structure of [(AuCl)$_2$(μ-**5**)], which contains the much less bulky chloro ligand, two crystallographically independent molecules are present. One of them exhibits crystallographically imposed inversion symmetry with exactly staggered cyclopentadienyl rings, too. In contrast to the two acetylide complexes [(Au-C≡C-Fc)$_2$(μ-**5**)] and [{Au-C≡C-C(CH$_2$)Me}$_2$(μ-**5**)], particularly short intermolecular Au···Au distances of 3.083(1) Å are observed in this case.[8] With the di(acetylide) ligand (C≡C-CH$_2$O-*p*-C$_6$H$_4$)$_2$SO$_2$, which is unbranched at the α-carbon atom and therefore "leaner" than C≡C-C(CH$_2$)Me and C≡C-Fc, aurophilic aggregation to dimeric units has been observed.[85] However, the Au···Au distance of 3.1488(7) Å is still longer than that of the chloro complex [(AuCl)$_2$(μ-**5**)].

3.7 Complexation Reactions between Gold(I) and the Ferrocene based S-Donor Ligands (4-11, fcS_3)

As far as I am aware the only gold(I) complex of a di(thioether)-substituted ferrocene with a direct attachment of gold(I) to the cyclopentadienyl-bonded sulfur atoms is a result of the reaction between 1,1′-di(phenylthio)ferrocene, [Fe{C_5H_4(SPh)}$_2$] (**5**) and [Au(PPh_3)]OTf, giving rise to [Au(PPh_3){Fe{C_5H_4(SPh)}$_2$}]OTf.[16]

A very similar complex (**17**) was prepared within the scope of this research with 1,1′-di(thien-2-ylthio)ferrocene (**9**) as ligand.

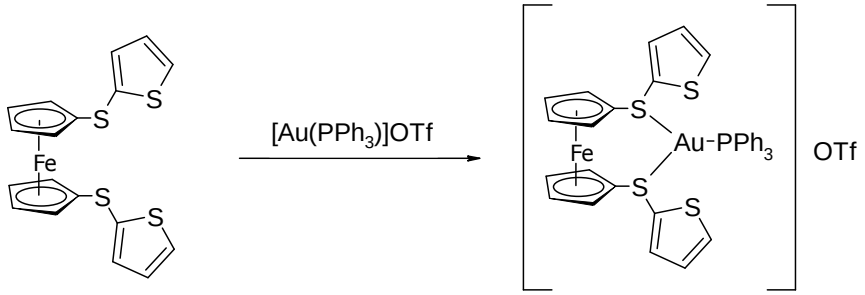

Figure 3-18: Synthesis of **17**.

All other attempts to obtain a complex of a di(thioether)-substituted ferrocene derivative with gold(I) lacking a coordinated phosphane ligand to the gold(I) failed.

3.7.1 Attempts to Synthesise Two-coordinate Gold(I) Complexes of the S-Donor Ligands

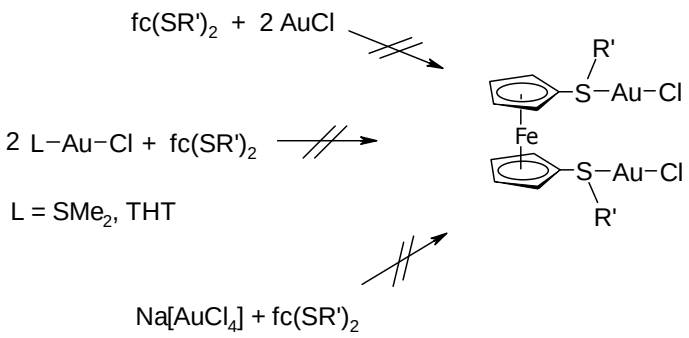

Figure 3-19: Attempted synthetic strategies to obtain gold(I) complexes with the S-based ligands **4**–**11**.

Three synthetic strategies were tested, two of them more thoroughly, in several variations. The first approach was the metathesis of the ferrocene derivatives $fc(SR)_2$ and another sulfur ligand L (L = DMS or THT) from a respective complex [AuCl(L)] in CH_2Cl_2 solution. A second route involved the redox reaction of the ferrocene-based ligand with $Na[AuCl_4]$ in solution, in analogy to the formation of the gold(I) complexes $[AuCl(SMe_2)]$[25] and $[AuCl(SC_4H_8)]$.[86] Finally, several attempts were carried out to obtain complexes by direct coordination reactions between the ligands and AuCl suspended in CH_2Cl_2.

Route I: Metathesis reactions were tried with all of the ferrocene derivatives (**4**–**11**) as well as with 1,2,3-trithia[3]ferrocenophane on an NMR tube-scale. The reactions were carried out in $CDCl_3$ with [AuCl(tht)] at room temperature and monitored by ^1H NMR spectroscopy over the course of several hours. In each case the spectra indicated oxidation of the ferrocene units after a prolonged reaction time. (The samples became paramagnetic). On the other hand, no additional signals or shifts occurred in any case. Elemental gold was formed apparently, since all samples became dark and in some cases a golden mirror on the glass was observed.

Especially the ligands $[Fe\{C_5H_4(SMe)\}_2]$ (**4**), $[Fe\{C_5H_4(SC_7H_4NS)\}_2]$ (**11**) and fcS_3 were tested intensively on larger scales (~ 150 mg). The modifications of the reaction conditions were a systematic variation of the temperature (–10°, 0°, ambient temperature and ~ 40°C), impact of the concentration, the solvent (CH_2Cl_2, acetone) and the ratio of ligand to gold(I). The manipulations were carried out in an inert gas atmosphere and purified solvents. In any case reduction of the gold species took place (elemental gold deposited on the glass-ware) and no evidence for successful complexation could be made out by ^1H NMR spectroscopy. However, decomposition was much slower in the cold, as expected.

Route II: Ligand **4**, $fc(SMe)_2$, and 1,2,3-trithia[3]ferrocenophane, fcS_3, were tested in an analogous reaction to that of the preparation of chloro(tetrahydrothiophene) gold(I) from tetrachloroaurate(III),[86] namely:

$$2\ Na[AuCl_4] + SC_4H_8 + H_2O \rightarrow [AuCl(SC_4H_8)] + OSC_4H_8 + 3\ HCl$$

Due to the redox sensitivity of the ferrocene moieties this approach seems not very promising. Two control reactions were tried and indeed immediate formation of elemental gold took place without any evidence for a successful coordination of gold(I) to the S-donor ligands by ^{1}H NMR.

Route III: The possibility to obtain the respective chloro gold(I) complexes by reacting appropriate ligands (SR_2, SeR_2, RNC, PR_3) directly with solid AuCl is long known.[87] Several thioether gold(I) complexes were successfully realised this way and since no oxidation process is involved and no other ligands have to be displaced, this approach appears as the most promising. Several reactions were performed with the ligands **4**, **11** and also with fcS_3 in CH_2Cl_2, mostly under inert gas atmosphere. The reactions were carried out at room temperature and in the cold at 0° and –10°C. At –10°C no reaction was detectable, while at 0°C the result was the same as for the reactions at ambient temperature, just considerably slower. In all cases formation of a gold mirror on the glass was observed and a darkening of the previously bright suspensions. It was not possible to isolate any complexes or to find any spectroscopic evidence for their existence by ^{1}H NMR of the tested samples. However, the deposition of elemental gold as a thin layer from solution shows, that a complexation must have occurred, but the complexes formed are chemically unstable and undergo an oxidation of the ferrocene moieties with concomitant reduction of gold(I) to the bulk metal.

3.7.2 Synthesis and Characterisation of $[Au(PPh_3)\{fc(SC_4H_3S)_2\}]OTf$ (17)

The three-coordinate gold(I) complex was prepared by addition of one equivalent of **9** to $[Au(PPh_3)(OTf)]$ in CH_2Cl_2 at room temperature, as shown in figure 3-18. The reaction mixture was stirred for 1 h and concentrated under vacuum. Addition of Et_2O caused the precipitation of **17** as an intensively yellow-brownish material. The complex is unstable in solution and decomposes slowly at ambient conditions. Purification was achieved by recrystallisation form CH_2Cl_2 at –40°C and yielded **17** in

moderate yield (28%). Attempts to obtain single crystals failed because of the decomposition of the complex.

The NMR data obtained in $CDCl_3$ are in line with the results of the corresponding 1,1'-di(phenylthio)ferrocene complex,[16] but were affected by the slow decomposition of **17** during the experiment. The aromatic protons give rise to a multiplet in the ^1H NMR spectrum in the region between 7.45 and 7.64 ppm. Another thiophene proton NMR signal is found at 6.81 ppm. These typical aromatic proton resonances are more or less well-resolved signals, while the cyclopentadienyl protons cause a single, very broad multiplet at 4.48 ppm, indicative of a strong interaction between the gold(I) atom and the ferrocene nucleus. The ^{13}C NMR spectrum shows the typical aromatic resonances at 123.8, 126.9, 129.6, 130.0, 132.8 and 134.0 ppm.

3.8 Summary and Conclusions

The ferrocene-based ligands of this study have been investigated in their ability for complexation towards gold(I). While the sulfur-based ferrocene ligands [$fc(SR)_2$] failed to give stable gold(I) complexes, their reaction with AuCl provides clear evidence that complexation with these thioethers takes place, followed by a redox-chemical decomposition to elemental gold.

In contrast, 1,1'-diisocyanoferrocene (**1**) proved to be an excellent ligand for the complexation of gold(I). Several complexes were prepared and characterised utilising a series of gold(I) acetylides. These complexes show interesting structural motifs, since intramolecular aurophilic interactions lead to a parallel orientation of the isocyano moieties, combined with an antiparallel alignment of neighbouring units. The reaction of **1** with the gold(I) acetylide $[Au(C{\equiv}C{-}Fc)]_n$ turned out to be very unusual, not to say 'impertinent' in terms of an 'orthodox' coordination chemistry, since the two chemically equivalent isocyano groups undergo a different reaction. One group shows an ordinary coordination and the other undergoes an extraordinary 1,1-insertion into the Au-C bond. This type of 'schizoid' reactivity is unprecedented and gives scope for further research in the future. Reaction of

$[Au(C{\equiv}C–Fc)]_n$ with the dppf ligand yielded the expected complex $[(Au\text{-}C{\equiv}C\text{-}Fc)_2(\mu\text{-}dppf)]$ and structural data confirm an ordinary coordination mode. The coordination behaviour with silver(I) was also investigated to fathom the coordination chemistry of **1** and the structure of the complex $[Ag_2(\mu\text{-}\mathbf{1})_2](NO_3)_2{\cdot}H_2O$ was determined by X-ray diffraction analysis.

3.9 References

[1] N. J. Long, *Metallocenes: An Introduction to Sandwich Complexes*, Blackwell Science, Oxford, UK, **1998**.

[2] P. Stepnicka (Ed.), *Ferrocenes: Ligands, Materials and Biomolecules*, Wiley, Chichester, **2008**.

[3] A. Togni, T. Hayashi, (Ed.), *Ferrocenes*, VCH, Weinheim, **1995**.

[4] R. C. J. Atkinson, V. C. Gibson, N. J. Long, *Chem. Soc. Rev.* **2004**, *33*, 313.

[5] U. Siemeling, T.-C. Auch, *Chem. Soc. Rev.* **2005**, *34*, 584.

[6] H. Schmidbaur. S. Cronje, B. Djordjevic, O. Schuster, *Chem. Phys.* **2005**, *311*, 151.

[7] U. Siemeling, D. Rother, C. Bruhn, H. Fink, T. Weidner, F. Träger, A. Rothenberger, D. Fenske, A. Priebe, J. Maurer, R. Winter, *J. Am. Chem. Soc.* **2005**, *127*, 1102.

[8] D. T. Hill, G. R. Girard, F. L. McCabe, R. K. Johnson, P. D. Stupik, J. H. Zhang, W. M. Reiff, D. S. Eggleston, *Inorg. Chem.* **1989**, *28*, 3529.

[9] J. Arias, M. Bardají, P. Espinet, *Inorg. Chem.* **2008**, *47*, 1597.

[10] T. V. Segapelo, I. A. Guzei, J. Darkwa, *J. Organomet. Chem.* **2008**, *693*, 701.

[11] M. C. Gimeno, A. Laguna, *Gold Bull.* **1999**, *32*, 90.

[12] B. McCulloch, D. L. Ward, J. D. Woolins, C. H. Brubaker, *Organometallics* **1985**, *4*, 1425.

[13] V. C. Gibson, N. J. Long, A. J. P. White, C. K. Williams, D. J. Williams, *Chem. Commun.* **2000**, 2359.

[14] V. C. Gibson, N. J. Long, A. J. P. White, C. K. Williams, M. Fontani, P. Zanello, *J. Chem. Soc., Dalton Trans.* **2003**, *23*, 3599.

[15] V. C. Gibson, N. J. Long, R. J. Long, A. J. P. White, C. K. Williams, D. J. Williams, E. Grigiotti, P. Zanello, *Organometallics* **2004**, *23*, 957.

[16] S. Canales, O. Crespo, A. Fortea, M. C. Gimeno, P. G. Jones, A. Laguna, *J. Chem. Soc., Dalton Trans.* **2002**, 2250.

[17] D. van Leusen, B. Hessen, *Organometallics* **2001**, *20*, 224.

[18] D. Rother, Wissenschaftliche Hausarbeit für die Erste Staatsprüfung für das Lehramt an Gymnasien, Kassel, **2004**.

[19] R. V. Parish, *Gold Bull.* **1997**, *30*, 3.

[20] R. J. Puddephatt, *Chem. Commun.* **1998**, 1055.

[21] G. Hogarth, M. M. Álvarez-Falcón, *Inorg. Chim. Acta* **2005**, *358*, 1386.

[22] D. M. P. Mingos, J. Yau, S. Menzer, D. J. Williams, *Angew. Chem. Int. Ed. Engl.* **1995**, *34*, 1894.

[23] G. E. Coates, C. Parkin, *Chem. Soc.* **1962**, 3220.

[24] S. K. Yip, W. H. Lam, N. Zhu, V. W.-W. Yam, *Inorg. Chim. Acta* **2006**, *359*, 3639.

[25] S. Ahmad, A. A. Isab, H. P. Perzanowski, M. S. Hussain, M. N. Akhtar *Transition Met. Chem.* **2002**, *27*, 177.

[26] G. Hogarth, M. M. Álvarez-Falcón, *Inorg. Chim. Acta* **2005**, *358*, 1386.

[27] J. Polin, H. Schottenberger, *Org. Synt.*, **1996**, *73*, 262.

[28] H. Xiao, K.-K. Cheung, C.-M. J. Che, *J. Chem. Soc., Dalton Trans*. **1996**, 3699.

[29] F. A. Cotton, F. Zingales, *J. Am. Chem. Soc.* **1961**, *83*, 351.

[30] P. Pyykkö, J. Li, N. Runeberg, *Chem. Phys. Lett.* **1994**, *218*, 133.

[31] D. V. Toronto, B. Weissbart, D. S. Tinti, A. L. Balch, *Inorg. Chem.* **1996**, *35*, 2484.

[32] W. Schneider, K. Angermaier, A. Sladek, H. Schmidbaur, *Z. Naturforsch. B: Chem. Sci.* **1996**, *51*, 790.

[33] R.-Y. Liau, T. Mathieson, A. Schier, R. J. F. Berger, N. Runeberg, H. Schmidbaur, *Z. Naturforsch. B: Chem. Sci.* **2002**, *57*, 881.

[34] K. Reichenbächer, H. I. Süss, J. Hulliger, *Chem. Soc. Rev.* **2005**, *34*, 22.

[35] G. R. Desiraju, *Acc. Chem. Res.* **2002**, *35*, 565.

[36] M. W. C. Chan, S. C. F. Kui, J. M. Cole, G. J. McIntyre, S. Matsui, N. Zhu, K.-H. Tam, *Chem. Eur. J.* **2006**, *12*, 2607.

[37] E.-U. Würthwein, R. Weigmann, *Angew. Chem. Int. Ed. Engl.*, **1987**, *26*, 923.

[38] K. Onitsuka, H. Ogawa, T. Joh, S. Takahashi, Y. Yamamoto, H. Yamazaki, *J. Chem. Soc. Dalton Trans.* **1991**, 1531.

[39] D. Seyferth, J. B. Hoke, *Organometallics* **1988**, *7*, 524.

[40] A. J. Deeming, *Adv. Organomet. Chem.* **1986**, *26*, 1.

[41] K. I. Hardcastle, H. Minassian, A. J. Arce, Y. De Sanctis, A. J. Deeming, *J. Organomet. Chem.* **1989**, *368*, 119.

[42] C. Choo Yin, A. J. Deeming, *J. Organomet. Chem.* **1977**, *133*, 123.

[43] A. L. Balch, M. M. Olmstead, J. C. Vickery, *Inorg. Chem.* **1999**, *38*, 3494.

[44] G. Minghetti, F. Bonati, *Inorg. Chem.* **1974**, *13*, 1600.

[45] J. E. Parks, A. L. Balch, *J. Organomet. Chem.* **1974**, *71*, 453.

[46] G. Minghetti, F. Bonati, *Gazz. Chim. Ital.* **1972**, *102*, 205.

[47] G. Minghetti, F. Bonati, *Angew. Chem. Int. Ed. Engl.* **1972**, *11*, 429.

[48] A. Burini, A.A. Mohamed, J.P. Fackler, Jr., *Comments Inorg. Chem.* **2003**, *24*, 253.

[49] A. Tiripicchio, M. Tiripicchio Camellini, G. Minghetti, *J. Organomet. Chem.* **1979**, *171*, 399.

[50] M. B. Smith, J. March, *March's Advanced Organic Chemistry*; 6th Ed., Wiley, New York, **2007**, pp. 1466.

[51] Y. Kayaki, A. Yamamoto in: *Current Methods in Inorganic Chemistry*; H. Kurosawa, A. Yamamoto, A. (Eds.), Elsevier, Amsterdam, **2003**, Vol. 3, pp. 373.

[52] L. D. Durfee, I. P. Rothwell, *Chem. Rev.* **1988**, *88*, 1059.

[53] K. Onitsuka, K. Yanai, F. Takei, T. Joh, S. Takahashi, *Organometallics* **1994**, *13*, 3862.

[54] K. Onitsuka, T. Joh, S. Takahashi, *Angew. Chem. Int. Ed. Engl.* **1992**, *31*, 851.

[55] K. Komeyama, D. Sasayama, T. Kawabata, K. Takehira, K. Takaki, *J. Org. Chem.* **2005**, *70*, 10679.

[56] K. Komeyama, D. Sasayama, T. Kawabata, K. Takehira, K. Takaki, *Chem. Commun.* **2005**, 634.

[57] E. Barnea, T. Andrea, M. Kapon, J.-C. Berthet, M. Ephritikhine, M. S. Eisen, *J. Am. Chem. Soc.* **2004**, *126*, 10860.

[58] M. D.Stadnichuk, A. V. Khramchikhin, Y. L. Piterskaya, I. V. Suvorova, *Russ. J. Gen. Chem.* **1999**, *69*, 593.

[59] A. S. K. Hashmi,G. J. Hutchings, *Angew. Chem. Int. Ed.* **2006**, *45*, 7896.

[60] H. Schmidbaur, A. Schier in: *Science of Synthesis*, I. A. O'Neil (Ed.), Thieme, Stuttgart, **2003**, Vol. 3, pp. 691.

[61] H. Schmidbaur (Ed.), *Gold. Progress in Chemistry, Biochemistry and Technology*, Wiley, Chichester, UK, **1999**.

[62] W. Henderson, B. K. Nicholson, A. L. Wilkins, *J. Organomet. Chem.* **2005**, *690*, 4971.

[63] M. Murakami, M. Inouye, M. Suginome, Y. Ito, *Bull. Chem. Soc. Jpn.* **1988**, *61*, 3649.

[64] M. Levi, R. Biondi, F. Danusso, *Eur. Polym. J.* **1998**, *34*, 1689.

[65] W. H. Morrison, Jr., S. Krogsrud, D. N. Hendrickson, *Inorg. Chem.* **1973**, *12*, 1998.

[66] S. Barlow, D. O'Hare, *Chem. Rev.* **1997**, *97*, 637.

[67] L. C. Case, *J. Polym. Sci.* **1960**, *48*, 27.

[68] F. H. Brock, *J. Org. Chem.* **1959**, *24*, 1802.

[69] F. Klages, M. Monkemeyer, R. Heinle, *Chem. Ber.* **1952**, *85*, 109.

[70] B. Djordjevic, O. Schuster, H. Schmidbaur, *Z. Naturforsch. B* **2006**, *61*, 6.

[71] M.-X. Li, K.-K. Cheung, A. Mayr, *J. Solid State Chem.* **2000**, *152*, 247.

[72] M. Benouazzane, S. Coco, P. Espinet, J. M. Martín-Alvarez, J. Barberá, *J. Mater. Chem.* **2002**, *12*, 691.

[73] S.-L. Zheng, J.-P. Zhang, X.-M. Chen, S.-W. Ng, *J. Solid State Chem.* **2003**, *172*, 45 and references cited therein.

[74] R. A. Stein, C. Knobler, *Inorg. Chem.* **1977**, *16*, 242.

[75] J. H. Meiners, J. C. Clardy, J. G. Verkade, *Inorg. Chem.* **1975**, *14*, 632.

[76] C. S. Gibbons, J. Trotter, *J. Chem. Soc. A* **1971**, 2058.

[77] J. Cooper, R. E. Marsh, *Acta Crystallogr.* **1961**, *14*, 202.

[78] See, for example: A. Guitard, A. Mari, A. L. Beauchamp, Y. Dartiguenave, M. Dartiguenave, *Inorg. Chem.* **1983**, *22*, 1603.

[79] D. Fortin, M. Drouin, P. D. Harvey, F. G. Herring, D. A. Summers, R. C. Thompson, *Inorg. Chem.* **1999**, *38*, 1253.

[80] Y. Yamamoto, K. Aoki, H. Yamazaki, *Inorg. Chim. Acta* **1982**, *68*, 75.

[81] V. W.-W.Yam, K.-L. Cheung, E. C.-C. Cheng, N. Zhu, K.-K. Cheung, *Dalton Trans.* **2003**, 1830.

[82] V. W.-W.Yam, S. W.-K. Choi, K.-K. Cheung, *J. Chem. Soc., Dalton Trans.* **1996**, 3411.

[83] W. J. Hunks, M.-A. MacDonald, M. C. Jennings, R. J. Puddephatt, *Organometallics* **2000**, *19*, 5063.

[84] J. Vicente, M.-T. Chicote, M. M. Alvarez-Falcón, M. A. Fox, D. Bautista, *Organometallics* **2003**, *22*, 4792.

[85] F. Mohr, M. C. Jennings, R. J. Puddephatt, *Eur. J. Inorg. Chem.* **2003**, 217.

[86] R. Usón, A. Laguna, M. Laguna, *Inorg. Synth.* **1989**, *26*, 86.

[87] K. C. Dash, H. Schmidbaur, *Chem. Ber.* **1973**, *106*, 1221.

Chapter 4
Studies of Ferrocene Derivatives for Surface Reactions

Several ferrocene derivatives were examined in view of their suitability for reactions on monolayers. Azidoferrocene and 1,1'-diazidoferrocene were found to be improper precursors for 'click' reactions, while 1,1'-diisothiocyanatoferrocene proved to be an excellent candidate for subsequent functionalisation of SAMs bearing terminal amino groups. Reactions of azido- and 1,1'-diazidoferrocene with dppf were examined as well.

4.1 Introduction

Highly functionialised SAMs are needed for applications e.g. in medicine, biology or microarray technology. Synthesis of functionalised ligands (like thiols or isocyanides) is usually difficult even for 'simple' species. SAMs addressed for applications in biology and medicine or micraoarray technology on the other hand mostly require large and complex ligands and functional units in terminal position. This leads to a conflict between the demand of a highly dense coverage of the surface in a SAM and the steric demand of the functional molecules. Chemical transformations on SAMs provide a versatile route to tailor surface properties and to build up complex nanostructures, also with large and complex terminal functional moieties, in a wide range. [1,2,3,4]

Several classes of organic reactions have been explored for modifying SAMs, including nucleophilic substitutions, nucleophilic additions, esterification and acylation. These reactions ideally should be highly selective and efficient, in the best case quantitative, to ensure a highly ordered SAM functionalisation. 1,3-dipolar cycloadditions of azides with acetylides have attracted considerable attention in this context, since they are both, efficient and selective.[5] The so called 'click' chemistry[6,7] is a very viable route for the selective modification of surfaces, for example by micro-contact printing[8] or by surface reactions on demand (controlled reactions by external

stimuli).[3,9] Functionalisation of SAMs with ferrocene moieties has been carried out very successfully by this approach with ethynylferrocene and other ferrocene acetylenes on SAMs bearing terminal azides.[8,10,11] Huisgen cycloadditions have been described also with azidoferrocene[12] but not with 1,1'-diazidoferrocene so far, which might be an interesting candidate for 'click' reactions, since it could undergo subsequent 'click' reactions on the surface in bridging fashion.

Isothiocyanates are highly reactive and undergo diverse nucleophilic addition reactions. The electrophilic centre at the carbon atom of the –N=C=S group reacts rapidly and under mild conditions with oxygen-, sulfur- or nitrogen-centred nuclesophiles to give rise to carbamates, thiocarbamates or thiourea derivatives respectively.[13,14,15] 1,1'-Diaminoferrocene has been successfully applied for the preparation of respective 1,1'-bissubstituted thiourea and amide derivatives in very good yields by reacting $fc(NH_2)_2$ with hexylisothiocyanate or lipoic acid. SAMs on gold surfaces of these ferrocene derivatives have been prepared and investigated in their ability for electrochemical sensing in this context.[16] Functionalisation of SAMs bearing terminal amino groups with isothiocyanates has also been found to be an excellent pathway for tailored surfaces.[17,18] Testing 1,1'-diisothiocyanatoferrocene (**2**) for its applicability to form disubstituted thioureas is a meaningful extension of the research therefore.

SAMs with terminal azido groups have found widespread use for subsequent modification by 'click' reactions. The related approach to react azides on surfaces with phosphanes in terms of Staudinger reactions[19] has not been described yet, although several chiral iminophosphoranylferrocenes have been obtained by the Staudinger reaction of dppf and arylazides. These compounds proved to be excellent ligands for catalysis, exhibiting enantioselectivities up to 99%.[20,21,22,23] Within the scope of this thesis azido- and 1,1'-diazidoferrocene have been investigated for the Staudinger reaction with dppf.

4.2 Synthesis of 'Click' Compounds (18a–c)

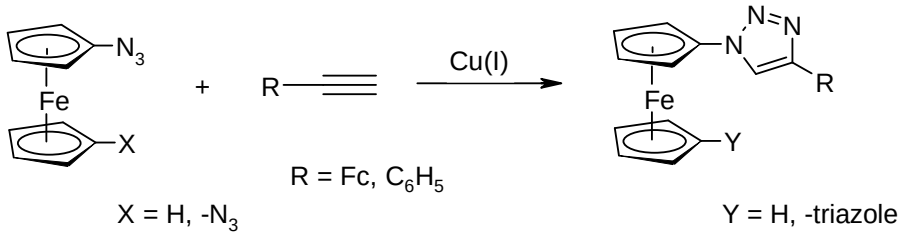

Figure 4-1: 'Click' reactions with azido ferrocenes.

The 'click'-products were obtained in moderate yields by the reactions of azido- or 1,1'-diazidoferrocene with ethynylferrocene or phenylacetylene in the respective stoichiometry. The preparations were carried out in dry THF under an atmosphere of nitrogen using Schlenk technique and with exclusion of light at room temperature overnight. CuCl was used as catalyst. Purification was achieved by column chromatography on Al_2O_3 (grade II) with CH_2Cl_2 as eluent. Attempts to obtain single crystals failed.

4.2.1 Characterisation of [Fc–N_3C_2H–Fc] (18a)

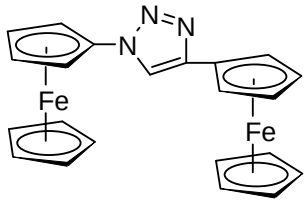

Figure 4-2: Structure of **18a**.

Reaction of azidoferrocene with ethynylferrocene afforded the corresponding 1,2,3-triazole in 41% yield. The product is sparingly soluble in acetone, THF, CH_2Cl_2 and chloroform, and is insoluble in Et_2O and hexane. The ^1H NMR spectrum ($CDCl_3$) exhibits six signals in the region typical for cyclopentadienyl resonances between 4.08 and 4.21 ppm, both with a 2.5-fold integral size compared to the signals found at 4.26, 4.31, 4.75 and 4.86 ppm. A singlet at 7.64 ppm can be assigned to the single triazole proton. Only one signal is present in the ^{13}C NMR spectrum in the region typical for triazole carbon atoms and is found at 118.3 ppm, the quaternary carbon

could not be detected even after a prolonged recording time of two days. In the region of the cyclopentadienyl carbon atoms there are six signals at 62.2, 66.8, 66.9, 69.0, 69.8 and 70.4 ppm. The quaternary cyclopentadienyl carbon atoms could not be detected.

4.2.2 Characterisation of [fc(N_3C_2H–Fc)$_2$] (18b)

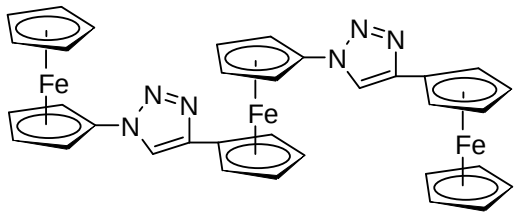

Figure 4-3: Structure of the bis(1,2,3-triazole) **18b**.

The bis(1,2,3-triazole) from the reaction of 1,1'-diazidoferrocene and ethynylferrocene was isolated in 38% yield. The NMR spectra are very similar to those of its monosubstituted analogue **18a**. The two triazole protons give rise to a singlet in the ^{1}H NMR spectrum in $CDCl_3$ at 7.61 ppm. Four signals representing 4 H atoms each, are present at 4.27, 4.36, 4.70 and 4.85 ppm, which correspond to the substituted cyclopentadienyl rings, and the prominent singlet at 4.05 ppm belongs to the unsubstituted cyclopentadienyl decks. Again, only the tertiary triazole carbon atom signal could be detected in the ^{13}C NMR spectrum at 118.3 ppm, while five signals are present in the ferrocene region at 64.0, 66.8, 68.4, 68.7 and 69.5 ppm, the latter one with the highest intensity. No signals could be detected in a region typical for quaternary cyclopentadienyl carbon atoms.

4.2.3 Characterisation of [fc–(N_3C_2H–C_6H_5)$_2$] (18c)

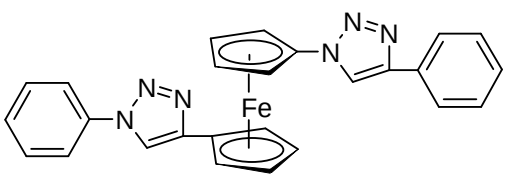

Figure 4-4: Structure of **18c**.

18c was isolated in 29% yield, since the purification was extraordinarily cumbrous in this case. However, the NMR data obtained are nicely in accord with the formulation of the target compound: two sharp singlets at 4.39 and 4.96 ppm can be assigned to the cyclopentadienyl protons. The phenyl protons are found in the typical region as a singlet at 7.25 ppm, very close to the solvent peak ($CDCl_3$), a quartet of double integral size at 7.28 and a doublet at 7.65 ppm. The triazole proton signal shows the most pronounced high-field shift and is found at 7.76 ppm. In the ^{13}C NMR spectrum two cyclopentadienyl signals are present at 63.6 and 68.3 ppm. The triazole ring again displays only one carbon signal at 118.5 ppm and in the region of the phenyl carbon signals four peaks are present at 125.6, 128.1, 128,7 and 129.7 ppm.

4.2.4 Discussion

'Click' reactions were described by Sharpless and co-workers as proper procedures for undergraduates,[24] since they are inter alia highly selective, mostly efficient, and their products are easy to purify and insensitive to air and water. The general procedures for the copper(I) catalysed reaction of azides with alkynes described in ref. [24] are all carried out under ambient conditions and in aqueous media and yields of >80% are reported. The first approach to 'click' 1,1'-diazidoferrocene therefore essentially adopted the general procedures published by Sharpless,[24] modified in regard to the starting materials of course. Several attempts failed to isolate the envisaged 1,2,3-triazoles, also with variations in temperature (0°C and ~50°C) and prolonged reaction time. Instead, considerable yields of the respective Glaser coupling products of the terminal alkynes were obtained, bisacetylenes from ethynylferrocene [Fc–C≡C–C≡C–Fc] or phenylacetylene [C_6H_5–C≡C–C≡C–C_6H_5]. Formation of such byproducts is known in this context,[25,26] and exclusion of oxygen and use of a nitrogen-containing base are recommended to minimise the side reactions. Disappointingly, first attempts with 1,1'-diazidoferrocene and ethynylferrocene, which were carried out in the presence of ammonia under nitrogen

with deoxygenation of all components led only to the 'byproduct', bisacetyleneferrocene.

However, the 1,3-dipolar cycloaddition succeeded in dry THF as solvent and strict exclusion of oxygen. CuCl was used as catalyst in the absence of any nitrogen-containing base. The reactions were carried out at room temperature overnight and yields were moderate. The necessity to work under an inert gas atmosphere is a significant limitation of the synthetic advantages described for the copper-mediated 1,3-cycloadditions: the high selectivity of both azide and alkyne groups in their reactivity, their inertness to most chemical functionalities and their stability in a wide range of solvents, temperatures and pH values.[5] 1,3-Dipolar cycloadditions should be strongly favoured thermodynamically, and with respect to this demands both, the mono- and the disubstituted ferrocene azide, failed in terms of 'click' chemistry.

4.3 Synthesis of Ferrocene-based Thiourea Derivatives (19a–b)

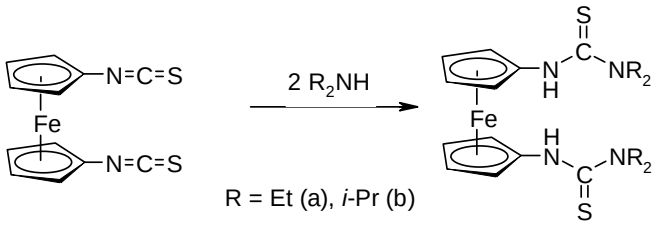

Figure 4-5: Synthesis of the ferrocene thioureas **19a–b**.

The preparation of the thiourea derivatives was carried out under an atmosphere of nitrogen in dry Et_2O. Two equivalents of the respective secondary amine were added to a stirred solution of 1,1'-diisothiocyanatoferrocene (**2**) in one portion at room temperature. In the case of diethylamine a yellow precipitate formed within seconds and after a few minutes the intensively coloured solution turned to a colourless suspension. In the case of the sterically more demanding diisopropylamine the reaction took more time (several hours) until the solution lost colour. The supernatant solutions were filtered by cannula and the crude products dried under vacuum. In both cases the yield of the crude product was quantitative, and the

product proved to be analytically pure by ^{1}H NMR and elemental analyses. The thiourea derivatives are not stable towards oxygen and decomposition slowly takes place over the course of several hours in solution.

4.3.1 Characterisation of {fc(NHCSNEt$_2$)$_2$} (19a)

19a is well soluble in acetone and chlorinated solvents like $CHCl_3$ and CH_2Cl_2, but is insoluble in *n*-hexane and Et_2O. The ^{1}H NMR spectrum of **19a** in $CDCl_3$ shows signals at 1.27 and 3.37 ppm caused by the ethyl substituents. The cyclopentadienyl protons give rise to two singlets at 4.07 and 4.60 ppm and the NH signal of the thiourea function is found at 7.27 ppm. All expected signals are also found in the ^{13}C NMR spectrum. The ethyl carbon signals are located at 12.8 and 45.6 ppm, followed by two peaks at 65.0 and 65.8 ppm, which can be assigned to the cyclopentadienyl rings. The quaternary carbon atom resonance is located at 98.4 ppm and the thiourea signal (C=S) is found at 179.4 ppm.

4.3.2 Characterisation of {fc(NHCSN-*i*-Pr$_2$)$_2$} (19b)

The solubility of **19b** is similar to that of **19a**. The ^{1}H NMR spectrum displays a pronounced doublet at 1.35 ppm, caused by the CH_3 protons of the isopropyl groups and a broad multiplet at 4.82 ppm that corresponds to the respective CH protons, which is an extraordinary low-filed shift. The cyclopentadienyl signals are found at 4.14 and 4.53 ppm and the NH signal is located at 6.88 ppm. In the ^{13}C NMR spectrum of **19b** two signals are present at 20.9 and 49.3 ppm, belonging to the isopropyl carbon atoms. The cyclopentadienyl signals are found at 66.3, 67.7 and 96.7 ppm and the thiourea carbon signal is located at 182.1 ppm.

4.3.3 Discussion

Reaction of amines with isothiocyanates are well known to give rise to the corresponding thiourea derivatives in high yields. The fact that 1,1'-diisothiocyanatoferrocene reacted quantitatively in both cases and that the products

were obtained in analytically pure form is a nice result from a preparative point of view. **2** is therefore a most promising candidate for surface reactions on monolayers. In addition, it is also an interesting precursor for other highly functionalised disubstituted ferrocenes.[16] The fact that the thiourea derivatives are sensitive to oxygen is of course disadvantageous in this context. It is well known that N-substituted ferrocenes with hydrogen at the nitrogen are generally not stable towards oxidation.[27] Subsequent substitution to a tertiary amine should enhance the stability significantly, but would mean a loss of the preparative ease.

4.4 Synthesis and Characterisation of Bis(iminophosphoranyl)ferrocene Derivatives from Dppf with Azido- and 1,1'-Diazidoferrocene

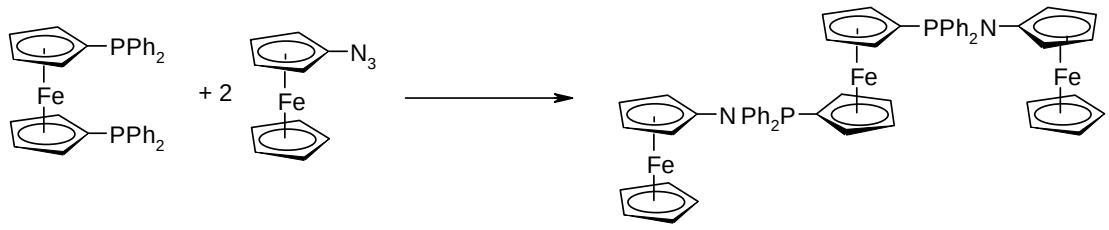

Figure 4-6: Synthesis of {fc-(PPh_2=N-Fc)$_2$} (**20**).

The reaction of azidoferrocene (2 equivalents) with dppf was carried out in dry CH_2Cl_2 at room temperature under nitrogen, according to the procedure published by Metallinos and co-workers for 1,1'-bis(triphenylphosphoranylidenamino)-ferrocene.[28] After reaction overnight volatile compounds were removed under vacuum. ^{1}H NMR spectroscopy confirmed that the crude product largely consisted of the bis(iminophosphoranyl)ferrocene **20**. Unfortunately, purification was hampered since the product is sensitive to moisture and oxygen. However, the identification of the product by NMR is easily possible as shown in figure 4-7.

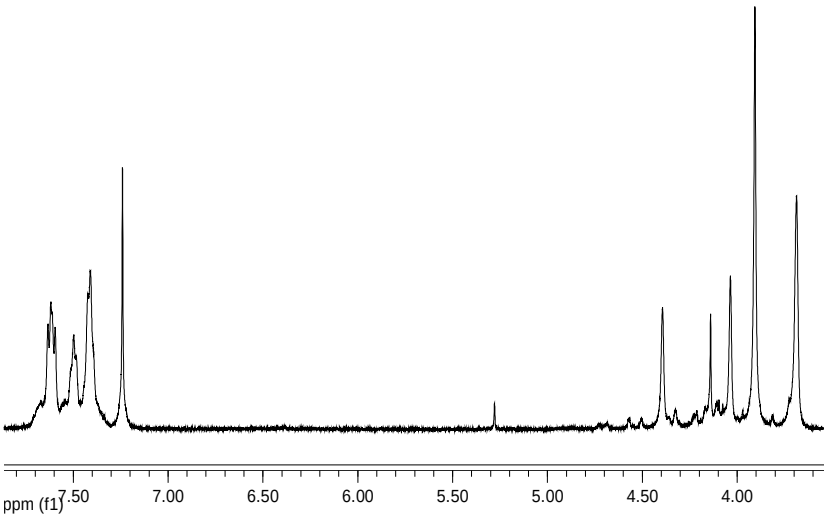

Figure 4-7: ^{1}H NMR spectrum of **20**.

The ferrocene moieties display five singlets at 3.69, 3.91, 4.04, 4.14 and 4.39 ppm. The second one can be clearly attributed to the unsubstituted cyclopentadienyl decks owing to its characteristic integral. The protons belonging to the phenyl groups show resonances at 7.41, 7.50 and 7.62 ppm. In the ^{13}C NMR spectrum six signals can be assigned to the cyclopentadienyl carbon atoms at 62.3, 67.9, 68.6, 73.7, 74.4 and 98.4 ppm, one of the quaternary cyclopentadienyl carbon atoms was not detectable, however. Three peaks at 128.3, 131.5 and 132.4 ppm can be assigned to the resonances of the phenyl carbon atoms. The ^{31}P NMR spectrum displays a single singlet at 5.9 ppm, in line with shifts reported for similar compounds.[23,29]

The analogous reaction of 1,1'-diazidoferrocene with dppf was tested in some variations, but only the formation of a sticky solid mass was observed. The most probable explanation for this result is that both, dppf and $fc(N_3)_2$, act as bridging units and therefore formation of a polymer takes place, as shown in figure 4-8.

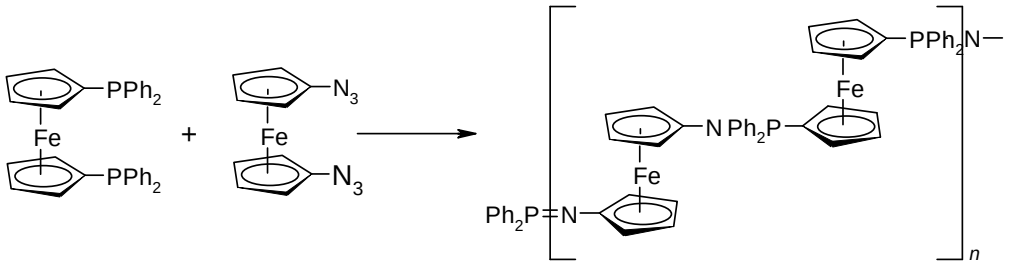

Figure 4-8: Formation of a ferrocenediyl iminophosphorane polymer.

4.4.1 Discussion

The Staudinger reaction between dppf and azidoferrocene works well but the formed product is not very robust to ambient conditions, which of course limits the range of potential applications. For the purpose of a subsequent monolayer functionalisation Staudinger reactions appear therefore a priori not as the best choice, since imino-phosphoranes usually oxidise readily. On the other hand the dppf ligand is an interesting candidate for further SAM modification, since it should act as a bridging unit in perpendicular orientation to the surface due to the steric demand of the PPh_2 groups.

Ferrocene-containing polymers have attracted considerable attention in the recent past in material science and have been intensively investigated as prototypes of molecular electronic devices and molecular conductors.[30] Oligonuclear ferrocene systems with unsaturated hydrocarbon or heteroatom bridges usually show strong interaction between neighbouring ferrocene units.[31] The formation of a (imino-phosphoranyl)ferrocene-based polymers is intriguing in this context, since both prerequisites are present.

4.5 Summary and Conclusion

As a sideline of the research of this thesis several ferrocene derivatives have been tested for their suitability for potential surface reactions. The copper(I) mediated 1,3-dipolar cycloadditions of azidoferrocene derivatives seemed very promising in this context, but failed to a certain extent in terms of 'click' chemistry, since the formation of the triazoles depended on the strict exclusion of oxygen and moisture and yields were only moderate.

In the case of Staudinger reactions between dppf and azidoferrocene derivatives only the monosubstituted species, FcN_3, gave rise to a well defined product. 1,1'-Diazidoferrocene probably leads to the formation of polymeric material. Ferrocene-based polymers are interesting for material science, and such compounds would be worth for a more detailed investigation.

The nucleophilic additions of secondary amines to 1,1'-diisothiocyanatoferrocene (**2**) were very satisfying from a preparative point of view, since the yields were quantitative. **2** is therefore best suited for reactions on monolayers with terminal amino groups. The ferrocene-based thiourea derivatives are an interesting class of compounds on their own and their use as chemical sensors has already been probed.[16] The potential of **2** as precursor for other nucleophilic addition reactions, with alcohols or thiols for example, is also very promising and investigations could be extended to the whole arsenal of isothiocyanato chemistry.[14,32] **2** can also act as a bridging ligand and can therefore give rise to ferrocene-containing polymers. It should be also suitable for subsequent surface modifications this way.

4.6 References

[1] J. C. Love, L. A. Estroff, J. K. Kriebel, R. G. Nuzzo, G. M. Whitesides, *Chem. Rev.* **2005**, *105*, 1103.

[2] T. P. Sullivan, W. T. S. Huck, *Eur. J. Org. Chem*. **2003**, 17.

[3] I. S. Choi, Y. S. Chi, *Angew. Chem. Int. Ed.* **2006**, *45*, 4894.

[4] M. C. Pirrung, *Angew. Chem. Int. Ed.* **2002**, *41*, 1276.

[5] V. O. Rodionov, V. V. Fokin, M. G. Finn, *Angew. Chem. Int. Ed.* **2005**, *44*, 2210.

[6] H. C. Kolb, M. G. Finn, K. B. Sharples, *Angew. Chem. Int. Ed.* **2001**, *40*, 2004.

[7] J.-F. Lutz, *Angew. Chem.* **2007**, *119*, 1036.

[8] D. I. Rozkiewicz, D. Jańczewski, W. Verboom, B. J. Ravoo, D. N. Reinhoudt, *Angew. Chem. Int. Ed.* **2006**, *45*, 5292.

[9] N. K. Devaraj, P. H. Dinolfo, C. E. D. Chidsey, J. P. Collman, *J. Am. Chem. Soc.* **2006**, *128*, 1794.

[10] J. P. Collman, N. K. Devaraj, C. E. D. Chidsey, *Langmuir* **2004**, *20*, 1051.

[11] N. K. Devaraj, R. A. Decreau, W. Ebina, J. P. Collman, C. E. D. Chidsey, *J. Phys. Chem. B* **2006**, *110*, 15955.

[12] M. E. N. P. R. A. Silva, A. J. L. Pombeiro, J. J. R.Fraústo da Silva, R. Herrmann, N. Deus, R. E. Bozak, *J. Organomet. Chem.* **1994**, *480*, 81.

[13] Ĺ. Drobnica, P. Kristián, J. Augustin, *The Chemistry of the –NCS Group* In: P. Satai (Ed.), *The Chemistry of Cyanate and their Thio Derivatives*, part 2, Wiley, New York, **1977**, pp. 1091-1221.

[14] A. K. Mukerjee, R. Ashare, *Chem. Rev.* **1991**, *91*, 1.

[15] R. P. Verma, *Eur. J. Org. Chem.* **2003**, 415.

[16] P. D. Beer, J. J. Davis, D. A. Drillsma-Milgrom, F. Szemes, *Chem. Commun.* **2002**, 1716.

[17] E. Delamarche, G. Sundarababu, H. Biebuyck, B. Michel, Ch. Gerber, H. Sigrist, H. Wolf, H. Ringsdorf, N. Xanthopoulos, H. J. Mathieu, *Langmuir* **1996**, *12*, 1997.

[18] I. Haller, *J. Am. Chem. Soc.* **1978**, *100*, 8050.

[19] Y. G. Gololobov, L. F. Kasukhin, *Tetrahedron* **1992**, *48*, 1353.

[20] V. D. M. Hoang, P. A. N. Reddy, T.-J. Kim, *Organometallics* **2008**, *27*, 1026.

[21] T. T. Co, T.-J. Kim, *Chem Commun.* **2006**, 3537.

[22] V. D. M. Hoang, P. A. N. Reddy, T.-J. Kim, *Tetrahedron Lett.* **2007**, *48*, 8014.

[23] P. Molina, A. Tárraga, J. L. López, J. C. Martínez, *J. Organomet. Chem.* **1999**, *584*, 147.

[24] W. D. Sharpless, P. Wu, T. V. Hansen, J. G. Lindberg, *J. Chem. Edu.* **2005**, *82*, 1833.

[25] C. W. Tornøe, C. Christensen, M. Meldal, *J. Org. Chem.* **2002**, *67*, 3057.

[26] A. Sakar, T. Mukherjee, S. Kapoor, *J. Phys. Chem. C* **2008**, *112*, 3334.

[27] M. Herberhold, M. Ellinger, W. Kremnitz, *J. Organomet. Chem.* **1983**, *241*, 227.

[28] C. Metallinos, D. Tremblay, F. B. Barrett, N. J. Taylor, *J. Organomet. Chem.* **2006**, *691*, 2044.

[29] P. Molina, A. Arques, A. García, M. C. Ramírez de Arellano, *Eur. J. Inorg. Chem.* **1998**, 1359.

[30] Y. Matsuura, K. Matsukawa, *Chem. Phys. Let.* **2007**, *436*, 224.

[31] Y. Matsuura, K. Matsukawa, *Chem. Phys. Let.* **2007**, *447*, 101.

[32] S. Braverman, M. Cherkinsky, M. L. Birsa, *Isothiocyanates* in: J. G. Knight (Ed.), *Science of Synthesis* **2005**, Houben-Weyl, *Vol. 18*, pp. 188.

Chapter 5
Experimental

5.1 General Techniques and Methods

All preparations involving air-sensitive compounds were carried out under an atmosphere of dry nitrogen using standard Schlenk techniques or a conventional glove box. Solvents and reagents were appropriately dried and purified by conventional methods.

NMR spectra were recorded on a Varian Unity INOVA 500 (500.13 MHz for ^{1}H) spectrometer.

Microanalyses were carried out at the microanalytical laboratories of the University of Kassel by Jörg Ho and at the London Metropolitan University by Stephen Boyer.

FT-IR spectra were recorded with a BIO-RAD FTS-40a spectrometer in attenuated total reflection (ATR) geometry. The spectral resolution was 2 cm^{-1}. Fourier transform infrared reflection absorption spectroscopic investigations of the monolayer films on gold were performed using an evacuated Bruker IFS 66v/S spectrometer equipped with a liquid nitrogen cooled mercury cadmium telluride detector. P-polarized light was incident on the sample at an angle of 80°. A total of 2000 scans were measured at a spectral resolution of 2 cm^{-1}.

Electrochemistry was performed in a home-built cylindrical one compartment cell with Ag/AgCl reference electrode and Pt working and auxiliary electrodes. The electroactive species was investigated in 0.0001 M solution in CH_2Cl_2 with 0.1 M $[N^nBu_4][PF_6]$ as supporting electrolyte at a scan rate of 50 mV/s at room temperature. Ferrocene was used as internal standard, where an appropriate amount of ferrocene was added after the scans had been recorded. Electrochemical data were acquired with a computer controlled Princeton Applied potentiostat model Versa Stat II utilising the Princeton PowerSuite (vers. 2.58) software package.

X-ray crystallographic data collection was performed using a Stoe IPDS-II diffractometer with an area detector. Graphite-monochromatised MoK_α radiation (λ

= 0.71073 Å) was used in each case. The data sets are corrected for Lorentz and polarisation effects. A numerical absorption correction was applied and the structures were solved by direct methods. The program SHELXS-97[1] was used for structure solution and refinement was carried out using SHELXL-97 by full-matrix least-squares refinement on F^2. All non H atoms were refined anisotropically except atom C7 in **9** which is affected by disorder of the thiophene ring around the C1–S1 axis, and was refined isotropically. H atoms were included at calculated positions using a riding model. In $[Ag_2(\mu\text{-}\mathbf{1})_2](NO_3)_2{\cdot}H_2O$ the H atoms of the solvent molecule could not be located and are not included in the model.

The gold substrates for film fabrication were prepared by thermal evaporation of 100 nm gold (99.99% purity) onto polished single-crystal silicon (111) wafers (Silicon Sense) primed with a 5 nm Ti layer for adhesion promotion. The resulting films were polycrystalline with a grain size of 20 – 50 nm and predominantly possessed (111) orientation.[2,3] Films were formed by immersion of freshly prepared gold substrates in ~10 μM solutions of **1** – **8** in DMF, ethanol and acetonitrile (**1**, **2**, **4** – **8**) or toluene (**3**) at room temperature for 18 h. After immersion the samples were carefully rinsed with the respective solvent, blown dry with argon and kept in plastic containers backfilled with argon until characterisation.

The XPS measurements were carried out under UHV conditions at a base pressure better than $1.5{\cdot}10^{-9}$ mbar. The experiments were performed using an Al Kα X-ray source and an LHS11 analyser. The energy resolution was ~0.9 eV. The X-ray source was operated at a power of 260 W and positioned about 1.5 cm away from the samples. The energy scale was referenced to the Au $4f_{7/2}$ peak of alkanethiol-coated gold at a binding energy of 84.0 eV.

NEXAFS spectroscopic measurements were performed at the HE-SGM beamline of the synchrotron storage ring BESSY II in Berlin, Germany. The spectra were collected at the carbon *K*-edge, nitrogen *K*-edge, and iron *L*-edge with a retardation voltage of –150 V for the C *K*-edge and –300 V for the N *K*-edge and the Fe *L*-edge. Linearly polarised light was used. The energy resolution was approximately 0.4 eV and the

incidence angle of the light was varied from 90° to 20°. Raw NEXAFS spectra were normalised to the incident photon flux by division through a spectrum of a clean, freshly sputtered gold sample. The photon energy scale was referenced to the prominent π_1^* resonance of highly oriented pyrolytic graphite at 285.38 eV. Further, the spectra were reduced to the standard form by subtracting linear pre-edge background and normalizing to the unity edge jump determined by a horizontal plateau 40 – 50 eV above the absorption edge.

5.2 Starting Material

Following compounds were synthesised by literature procedures:

1,1′-dilithioferrocene[4]

1,1′-bis(diphenylphosphino)ferrocene[5]

1,1′-dibromoferrocene[6]

1,1′-diazidoferrocene[6]

1,1′-diisocyanoferrocene (**1**)[7]

1,1′-di(methylthio)ferrocene (**4**)[8]

1,1′-di(phenylthio)ferrocene (**5**)[3]

1,1′-di(2-thienyl)ferrocene (**6**)[9]

1,1′,2,2′-tetra(methylthio)ferrocene (**8**)[10]

2,2′-di(thien-2-yl)disulfide[11]

2,2′-di(thiazol-2-yl)disulfide[12]

1,1′-bis(triphenylphosphoranylidenamino)ferrocene[13]

Ethynylferrocene[14]

[AuCl(PPh_3)][15]

[AuCl(SMe_2)][16]

[AuCl(tht)][17]

[Au(OTf)(PPh_3)][18]

Azidoferrocene was prepared from Bromoferrocene in analogy to 1,1′-diazidoferrocene.[6]

Bromoferrocene was prepared by monolithiation of 1,1′-dibromoferrocene and subsequent hydrolysis with water according to a procedure by Butler and Quayle.[19] All other reagents were commercially available and used as received.

5.3 Experimental Procedures

Unless stated otherwise all preparations were carried out under an atmosphere of dry nitrogen using standard Schlenk techniques.

5.3.1 1,1'-Diisothiocyanatoferrocene (2)

CS_2 (40 ml) was added to 1,1′- bis(triphenylphosphoranylidenamino)ferrocene (1.50 g, 2.00 mmol) in a thick-walled `Rotaflo´ ampoule. The suspension was stirred for 3 h at 90 °C. The resulting clear solution was allowed to cool to room temperature. Volatile components were removed in vacuo. The crude product was dissolved in a minimal amount of dichloromethane and purified by column chromatography (silica gel, *n*-hexane), which afforded an orange, microcrystalline powder (490 mg, 82 %). ^{1}H NMR ($CDCl_3$): δ 4.20 (s, 4 H), 4.51 (s, 4 H) ppm; $^{13}C\{^1H\}$ NMR ($CDCl_3$): δ 67.1, 68.0, 87.0, 133.8 ppm. IR (cm^{-1}): ν(NCS) 2088(b, vs). Elemental analysis (%) calcd for $C_{12}H_8FeN_2S_2$ (300.19): C 48.01, H, 2.69, N, 9.33; found: C, 48.13; H, 2.69; N, 9.39.

5.3.2 1,1'-Di(3-thienyl)ferrocene (7)

A 1.60 M solution of *n*-BuLi in hexane (15.0 ml, 24.0 mmol) was added in one portion to finely ground ferrocene (2.00 g, 10.8 mmol). The mixture was stirred and TMEDA (1.37 g, 11.8 mmol) was added drop wise. Stirring was continued for 14 h. The precipitate (TMEDA adduct of 1,1′-dilithioferrocene, ~3.3 g) was filtered off, washed with *n*-hexane (2 × 15 ml) and was subsequently suspended *n*-hexane (15 ml). A solution of $ZnCl_2$ (2.73 g, 20.0 mmol) in THF (15 ml) was added dropwise and the mixture was stirred for 3 h. 3-Bromothiophene (3.26 g, 20.0 mmol) and $[Pd(PPh_3)_4]$ (0.23 g, 0.2 mmol) were added sequentially. After 4 d the mixture was hydrolysed

with 1 N hydrochloric acid (15 ml) and subsequently extracted with diethyl ether (3 × 20 ml) and dichloromethane (1 × 30 ml). The combined organic layers were dried with Na_2SO_4, which was subsequently removed by filtration. Volatile components were removed in vacuo. The crude product was purified by column chromatography (silica gel, *n*-hexane/dichloromethane 20:1). The first two bands contained ferrocene and (3-thienyl)ferrocene (460 mg). The third band afforded the product as an orange, microcrystalline solid. Yield 2.39 g (68 %).

^{1}H NMR ($CDCl_3$): δ 4.21 (s, 4 H, C_5H_4), 4.39 (s, 4 H, C_5H_4), 6.90 (s, 2 H, thienyl), 6.95 ("d", apparent J = 5.0 Hz, 2 H, thienyl), 7.18 (m, 2 H, thienyl) ppm; ^{13}C{^{1}H} NMR ($CDCl_3$): δ 68.1, 69.9, 118.0, 125.2, 126.3, 138.6 ppm. Elemental analysis (%) calcd for $C_{18}H_{14}FeS_2$ (350.29): C 61.72, H 4.03; found: C 62.64, H 4.53.

5.3.3 1,1'-Di(thien-2-ylthio)ferrocene (9)

A solution of di(2-thienyl)disulfide (2.60 g, 11.3 mmol) in toluene (40 ml) was added dropwise with stirring to a suspension of the TMEDA adduct of 1,1'-dilithioferrocene (~1.7 g) in *n*-hexane (15 ml), which had been prepared as described above from ferrocene (1.00 g, 5.4 mmol), *n*-BuLi (7.5 ml of a 1.60 M solution in hexane, 12.0 mmol) and TMEDA (0.70 g, 6.0 mmol). After 14 h water (15 ml) was added and stirring was continued for 10 min. The organic layer was separated, washed with water (2 × 10 ml) and dried with $MgSO_4$, which was subsequently removed by filtration. Volatile components were removed in vacuo. The yellow sticky crude product was dissolved in a minimal amount of CH_2Cl_2 and purified by column chromatography (silica gel, *n*-hexane/dichloromethane 10:1), affording the product as a yellow, microcrystalline solid. Yield 1.40 g (68 %).

^{1}H NMR ($CDCl_3$): δ 4.27 (s, 4 H, C_5H_4), 4.42 (s, 4 H, C_5H_4), 6.89 (m, 2 H, thienyl), 7.04 (d, J = 2.4 Hz, 2 H, thienyl), 7.23 (d, J = 5.4 Hz, 2 H, thienyl) ppm; ^{13}C{^{1}H} NMR ($CDCl_3$): δ 66.9, 74.2, 127.2 128.4 ppm. Elemental analysis (%) calcd for $C_{18}H_{14}FeS_4$ (414.42): C 52.17, H 3.41; found: C 52.23, H 3.35.

5.3.4 1,1'-Di(thiazol-2-ylthio)ferrocene (10)

A solution of di(2-thiazolyl)disulfide (0.93 g, 4.0 mmol) in toluene (20 ml) was added dropwise with stirring to a suspension of the TMEDA adduct of 1,1'-dilithioferrocene (~0.6 g) in *n*-hexane (10 ml), which had been prepared as described above from ferrocene (0.37 g, 2.0 mmol), *n*-BuLi (2.5 ml of a 1.60 M solution in hexane, 4.0 mmol) and TMEDA (0.34 g, 2.1 mmol). After 14 h water (10 ml) was added and stirring was continued for 10 min. The organic layer was separated, washed with water (2 × 10 ml) and dried with $MgSO_4$, which was subsequently removed by filtration. Volatile components were removed in vacuo. The brownish-yellow sticky crude product was dissolved in a minimal amount of dichloromethane and purified by chromatography (neutral alumina, activity grade II, *n*-hexane/dichloromethane 3:1), affording the product as a dark yellow, microcrystalline solid. Yield 0.32 g (38 %).

^{1}H NMR ($CDCl_3$): δ 4.45 (s, 4 H, C_5H_4), 4.61 (s, 4 H, C_5H_4), 7.10 (d, J = 2.9 Hz, 2 H, thiazolyl), 7.58 (d, J = 2.8 Hz, 2 H, thiazolyl) ppm; $^{13}C\{^1H\}$ NMR($CDCl_3$): δ 69.8, 72.6, 76.3, 119.0, 143.1, 169.2 ppm. Elemental analysis (%) calcd for $C_{16}H_{12}FeN_2S_4$ (416.39): C 46.15, H 2.90, N 6.73; found: C 45.37, H 2.87, N 7.40.

5.3.5 1,1'-Di(benzothiazol-2-ylthio)ferrocene (11)

A solution of di(2-benzothiazolyl)disulfide (6.80 g, 20.5 mmol) in toluene (70 ml) was added dropwise with stirring to a suspension of the TMEDA adduct of 1,1'-dilithioferrocene (~3.3 g) in *n*-hexane (50 ml), which had been prepared as described above from ferrocene (2.00 g, 10.8 mmol), *n*-BuLi (15.0 ml of a 1.60 M solution in hexane, 24.0 mmol) and TMEDA (1.37 g, 11.8 mmol). After 14 h water (50 ml) was added and stirring was continued for 10 min. The dark yellow precipitate was isolated by filtration and dried in vacuo. Its purity turned out to be already > 95 % by NMR spectroscopic analysis. Yield 4.74 g (92 %). An analytical sample was obtained by column chromatography (silica gel, *n*-hexane/dichloromethane 3:1).

^{1}H NMR ($CDCl_3$): δ 4.59 (s, 4 H, C_5H_4), 4.70 (s, 4 H, C_5H_4), 7.23 ("t", 2 H, benzothiazolyl), 7.37 ("t", 2 H, benzothiazolyl), 7.63 (d, J = 8.0 Hz, 2 H,

benzothiazolyl) , 7.82 (d, *J* = 7.7 Hz, 2 H, benzothiazolyl) ppm; $^{13}C\{^{1}H\}$ NMR($CDCl_3$): δ 73.0, 78.0, 82.8, 120.8, 121.8, 124.1, 126.1 ppm. Elemental analysis (%) calcd for $C_{24}H_{16}FeN_2S_4$ (516.51): C 55.81, H 3.12, N 5.42; found: C 55.71, H 3.22, N 5.49.

5.3.6 Synthesis of Gold(I) Acetylides (12a–e)

These compounds were prepared according to a route described by Hogarth and co-workers[20] from [AuCl(SMe_2)] and the respective acetylene derivative in the presence of triethylamine. The reactions were carried out at room temperature in CH_2Cl_2 without exclusion of oxygen and any precautions against moisture if not stated otherwise.

5.3.6.1 Synthesis of [AuC≡C-*p*-$CC_6H_4CF_3$]$_n$, (12a)

HC≡C-*p*-$C_6H_4CF_3$-4 (255 mg, 1.5 mmol) and NEt_3 (1 ml, ~730 mg, 7.3 mmol) were added sequentially to a stirred solution of [AuCl(SMe_2)] (442 mg; 1.5 mmol) in deoxygenised CH_2Cl_2 (20 ml) at 0 °C under N_2. The solution was stirred for 1h. Cold MeOH (20 ml) was added and the reaction mixture was stirred at 0°C for a further 2 h. The pale yellow precipitate was isolated by centrifugation and dried under vacuum. Yield: 210 mg (38%). The complex is thermally unstable and decomposes slowly at room temperature to a violet powder. At low temperature (-40 °C) it can be stored for several weeks without any detectable change.

IR (cm^{-1}): ν(C≡C) 2003(w). Elemental analysis (%) calcd for $C_9H_4AuF_3$ (366.09): C 29.53, H 1.10; found: C 29.31, H 1.06.

5.3.6.2 Synthesis of [AuC≡C-*p*-$C_6H_4NMe_2$]$_n$ (12d)

HC≡C-*p*-$C_6H_4NMe_2$ (218 mg, 1.5 mmol) and NEt_3 (300 mg, 3.0 mmol) were added sequentially to a stirred solution of [AuCl(SMe_2)] (442 mg, 1.5 mmol) in dichloromethane (20 mL). After 30 min the yellow precipitate was filtered off,

washed with methanol (5 mL) and diethyl ether (5 mL) and dried in vacuo. Yield: 470 mg (92%).

IR (cm^{-1}): ν(C≡C) 1999(w). Elemental analysis (%) calcd for $C_{10}H_{10}AuN$ (341.16): C 35.21, H 2.95, N 4.11; found: C 35.28, H 2.98, N 3.92.

5.3.6.3 Synthesis of $[AuC{\equiv}C\text{-}Fc]_n$ (12e)

A solution of ethynylferrocene (315 mg, 1.5 mmol) in 10 ml dry CH_2Cl_2 and NEt_3 (0.4 ml, ~300 mg, 3 mmol) were added successively to a stirred solution of $[AuCl(SMe_2)]$ (442 mg; 1.5 mmol) in deoxygenised CH_2Cl_2 under N_2. After 10 min. a catalytic amount of CuCl (tip of a pipette) was added and the reaction mixture was stirred overnight. MeOH (10 ml) was added and the suspension was stirred for another 20 min. The resulting dark red complex was filtered, washed with MeOH and Et_2O and dried under vacuum to give 1**2e** in 71% yield (430 mg).

IR (cm^{-1}): ν(C≡C) 1976(w), 2011(w). Elemental analysis (%) calcd for $C_{12}H_9AuFe$ (406.02): C 35.50, H 2.23; found: C 35.78, H 2.31.

5.3.7 Synthesis of Alkynyl Gold(I) Complexes $[\{Au(C{\equiv}C\text{-}p\text{-}C_6H_4R)\}_2(\mu\text{-}1)]$ (13a–d)

General procedure: A solution of **1** (50 mg, 0.21 mmol) in CH_2Cl_2 (10 mL) was added to a stirred suspension of the respective gold(I) acetylide (**2**) (0.42 mmol; **a** 155 mg, **b** 126 mg, **c** 140 mg, **d** 145 mg) in CH_2Cl_2 (50 mL). The mixture was stirred for 14 h. The product was isolated by cannula filtration, washed with methanol (10 mL) and diethyl ether (10 mL) and dried in vacuo.

5.3.7.1 $[\{Au(C{\equiv}C\text{-}p\text{-}C_6H_4CF_3)\}_2(\mu\text{-}1)]$ (13a)

Yield: 115 mg (56%). ^1H NMR (CD_2Cl_2): δ 7.33 (d, J = 7.9 Hz, 4 H, C_6H_4), 7.28 (d, J = 8.8 Hz, 4 H, C_6H_4), 4.93 (s, 4 H, C_5H_4), 4. 49 (s, 4 H, C_5H_4) ppm. IR (cm^{-1}): ν(C≡C) 2115(m), ν(N≡C) 2192(s). Elemental analysis (%) calcd for $C_{30}H_{16}Au_2F_6FeN_2 \cdot ½\ CH_2Cl_2$ (1010.71): C 36.25, H 1.70, N 2.77; found: C 35.77, H 1.54, N 2.48.

5.3.7.2 [{Au(C≡C-*p*-C_6H_5)}$_2$(μ-1)] (13b)

Yield: 70 mg (40%). ^{1}H NMR (CD_2Cl_2): δ 7.30 (s, 2 H, Ph), 7.13 (s, 8 H, Ph), 4.94 (s, 4 H, C_5H_4), 4. 47 (s, 4 H, C_5H_4) ppm. IR (cm^{-1}): ν(C≡C) 2121(m), ν(N≡C) 2203(s). Elemental analysis (%) calcd for $C_{28}H_{18}Au_2FeN_2 \cdot ½\ CH_2Cl_2$ (832.25·½84.93): C 39.13, H 2.19, N 3.20; found: C 39.58, H 2.80, N 3.03.

5.3.7.3 [{Au(C≡C-*p*-C_6H_4OMe)}$_2$(μ-1)] (13c)

Yield 115 mg (61%). ^{1}H NMR (CD_2Cl_2): δ 7.24 (d, *J* = 8.6 Hz, 4 H, C_6H_4), 6.66 (d, *J* = 8.8 Hz, 4 H, C_6H_4), 4.93 (s, 4 H, C_5H_4), 4. 47 (s, 4 H, C_5H_4), 3.72 (s, 6 H, Me) ppm. IR (cm^{-1}): ν(C≡C) 2123(w); ν(N≡C) 2204(s). Elemental analysis (%) calcd for $C_{30}H_{22}Au_2FeN_2O_2 \cdot ½\ CH_2Cl_2$ (934.78): C 39.19, H 2.48, N 3.00; found: C 39.27, H 2.37, N 2.92.

5.3.7.4 Synthesis of [{Au(C≡C-*p*-$C_6H_4OMe_2$)}$_2$(μ-1)] (13d)

Yield 130 mg (66%). ^{1}H NMR (CD_2Cl_2): δ 7.18 (d, *J* = 8.9 Hz, 4H, C_6H_4), 6.48 (d, *J* = 9.1 Hz, 4H, C_6H_4), 4.92 (s, 4H, C_5H_4), 4. 47 (s, 4H, C_5H_4), 2.89 (s, 12H, NMe_2) ppm. IR (cm^{-1}): ν(C≡C) 2115(m), ν(N≡C) 2192(s). Elemental analysis (%) calcd for $C_{32}H_{28}Au_2FeN_4 \cdot ½\ CH_2Cl_2$ (960.87): C 40.63, H 3.04, N 5.83; found: C 40.57, H 3.03, N 5.92.

5.3.7.5 Synthesis of [(Fc-C≡C-Au-C≡N-C_5H_4)Fe{C_5H_4-N=C(Au)-C≡C-Fc}]$_3$ (14)

A solution of **1** (67 mg, 0.28 mmol) in CH_2Cl_2 (15 ml) was added to a suspension of **12e** in dichloromethane (15 ml). The reaction mixture was stirred overnight and filtered. The residue was washed with CH_2Cl_2 (2 x 10 ml) and the combined filtrates reduced to dryness in vacuo, yielding 216 mg (72%) crude product. Purification was achieved by subsequent recrystallisation from dichloromethane.

^{1}H NMR (CD_2Cl_2): δ 5.41 (“t”, apparent *J* = 1.9 Hz, 6 H), 5.18 (“t”, apparent *J* = 1.9 Hz, 6 H), 4.56 (“t”, apparent *J* = 1.8 Hz, 6 H), 4.52 (“t”, apparent *J* = 1.7 Hz, 6 H), 4.42 (“t”, apparent *J* = 1.7 Hz, 6 H), 4.40 (“t”, apparent *J* = 2.0 Hz, 6 H), 4.27 (“t”, apparent *J* = 1.8 Hz, 6 H), 4.26 (s, 15 H), 4.04 (“t”, apparent *J* = 1.8 Hz, 6 H) ppm. IR (cm^{-1}): ν(N=C)

1491(m), ν(C≡C) 2115(m), ν(N≡C) 2192(s). Elemental analysis (%) calcd for $C_{108}H_{78}Au_6Fe_9N_6$ (3144.30): C 41.26, H 2.50, N 2.67; found: C 40.96, H 2.57, N 2.80.

5.3.8 Synthesis of Silver Complexes with 1 (15a–b)

Silver complexes of 1,1′-diisocyanoferrocene were obtained by reaction with the respective silver salt in 1 : 1 ratio in acetonitile at room temperature.

5.3.8.1 Synthesis of $[Ag_2(\mu\text{-}1)_2](NO_3)_2$ (15a)

A solution of silver nitrate (170 mg, 1.00 mmol) in acetonitrile (15 ml) was added to a stirred solution of 1,1′-diisocyanoferrocene (**1**) (236 mg, 1.00 mmol) in acetonitrile (50 ml). The mixture was stirred in the dark for 14 h. The product precipitated as shiny golden platelets, which were filtered off, washed with acetonitrile (5 ml) and diethyl ether (2 × 5 ml) and dried in vacuo. Yield 465 mg (57%). An analytical sample of the monohydrate was obtained by recrystallisation from dichlormethane.

^{1}H NMR ($CDCl_3$): δ 5.30 (“t”, 4 H), 4.47 (“t”, 4 H) ppm. IR (cm^{-1}): ν(NC) 2193(vs). Elemental analysis (%) calcd for the hydrate $C_{24}H_{22}Ag_2Fe_2N_6O_7$ (833.91): C 33.57, H 2.66, N 10.08; found: C 33.06, H 2.43, N 9.55.

5.3.8.2 Synthesis of $[Ag_2(\mu\text{-}1)_2]Cl_2$ (15b)

To a solution of **1** (120 mg, 0.50 mmol) in acetonitrile (30 ml) was added solid AgCl (72 mg, 0.50 mmol) and the suspension was stirred in the dark overnight. The product formed as golden microcrystalline powder. After filtration the sold material was washed with acetonitrile (10 ml) and ether (10 ml) and dried in vacuo. Yield: 120 mg (63%).

IR (cm^{-1}): ν(NC) 2165(s). Elemental analysis (%) calcd for $C_{24}H_{16}Ag_2Cl_2Fe_2N_4$ (758.76): C 37.99, H 2.13, N 7.38; found: C 37.72, H 2.62, N 6.98.

5.3.9 Synthesis of [(Au-C≡C-Fc)$_2$(μ-5)] (16)

Dppf (110 mg, 0.2 mmol) was added to a stirred suspension of **12e** (160 mg, 0.4 mmol) in CH_2Cl_2 (50 ml). The mixture was stirred for 3 h. The slightly turbid solution was filtered to remove traces of insoluble material. The volume of the filtrate was reduced in vacuo to ~10 ml. The product was precipitated by slow addition of diethyl ether (10 ml). Yield 242 mg (89%).

^{1}H NMR ($CDCl_3$): δ 7.36–7.28 (m, 20 H, Ph), 4.44 (s, 4 H, C_5H_4), 4. 36 (s, 4 H, C_5H_4), 4.21 (s, 10 H, Cp), 4.11 (s, 4 H, C_5H_4), 4.05 (s, 4 H, C_5H_4) ppm; ^{13}C{^{1}H} NMR ($CDCl_3$): δ 133.6, (d, *J* = 15.5 Hz), 131.6, 131.2 (d, *J* = 10.0 Hz), 130.4, 128.6, (d, *J* = 9.5 Hz), 128.2 (d, *J* = 12.1 Hz), 102.2, 98.7, 82.0, 81.6, 74.5 (d, *J* = 12.7 Hz), 73.4 (d, *J* = 12.3 Hz), 71.8, 69.9, 67.8 ppm; ^{31}P{^{1}H} NMR ($CDCl_3$): δ 24.8 ppm. IR (cm^{-1}): ν(C≡C) 2110(w). Elemental analysis (%) calcd for $C_{58}H_{46}Au_2Fe_3P_2$ (1366.44): C 50.98, H 3.39; found: C 51.56, H 3.92.

5.3.10 Synthesis of [Au(PPh$_3$){fc(SC$_4$H$_3$S)$_2$}]OTf (17)

A solution of fc(STh)$_2$ (50 mg, 0.12 mmol) in CH_2Cl_2 (20 ml) was added to a stirred solution of [Au(OTf)(PPh_3)] (73 mg, 0.12 mmol) in CH_2Cl_2 (30 ml). The reaction mixture was stirred for 1 h at room temperature and than reduced in vacuo to ~5 ml. Addition of Et_2O (10 ml) caused precipitation of **17** in form of a yellow-brown material. The product is sensitive to oxygen in solution and decomposes slowly under ambient conditions. Purification was achieved by recrystallisation form CH_2Cl_2 at -40 °C. Yield: 35 mg (28%).

^{1}H NMR ($CDCl_3$): δ 7.64–7.45 (m, 19H, Ph+C_4H_3S), 6.81 (s, 2H, C_4H_3S), 4.48 (m, broad, 8H, C_5H_4) ppm; ^{13}C{^{1}H} NMR ($CDCl_3$): δ 134.0 (Ph), 132.8 (Ph), 130.0 (Ph), 129.6 (Ph), 126.9 (C_4H_3S), 123.8 (C_4H_3S) ppm. Elemental analysis (%) calcd for $C_{37}H_{29}AuF_3FeO_3PS_5$ (1022.75): C 43.45, H 2.86; found: C 41.60, H 3.11.

5.3.11 Synthesis of Ferrocenyl-1,2,3-Triazoles (18a–c)

The reactions were carried out in dry THF at room temperature under inert gas.

5.3.11.1 Synthesis of [Fc–N_3C_2H–Fc] (18a)

Ethynylferrocene (105 mg, 0.50 mmol) and a small spatula of CuI (~10 mg) were added to a solution of azidoferrocene (115 mg, 0.51 mmol) in dry THF (15 ml). The reaction mixture was stirred in the dark for 3 d. The yellow precipitate was filtered off and dried in vacuo. Purification was achieved by column chromatography on Al_2O_3 (grade II, 3% H_2O) with CH_2Cl_2 as eluent. Yield: 90 mg (41%).

^1H ($CDCl_3$): δ 7.64 (s,1H, N_3C_2H), 4.86 (s, 2 H, C_5H_4), 4.75 (s, 2H, C_5H_4), 4.31 (s, 2H, C_5H_4), 4.26 (s, 2H, C_5H_4), 4.21 (s, 5H, C_5H_5), 4.08 (s, 5H, C_5H_5) ppm; $^{13}C\{^1H\}$ NMR: δ 118.3 (N_3C_2H), 70.4 (C_5H_4), 69.8 (C_5H_4), 69.0 (C_5H_4), 66.9 (C_5H_4), 66.9 (C_5H_4), 62.2 (C_5H_4) ppm. Elemental analysis (%) calcd for $C_{22}H_{19}Fe_2N_3$ (437.11): C 60.45, H 4.38, N 9.61; found: C 60.13, H 4.40, N 9.58.

5.3.11.2 Synthesis of [fc–$(N_3C_2H$–Fc$)_2$] (18b)

Ethynylferrocene (420 mg, 2.00 mmol) and CuCl (30 mg, 15 mol%) were added to a solution of 1,1'-diazidoferrocene (270 mg, 1.00 mmol) in dry THF (20 ml). The reaction mixture was stirred in the dark for 14 h. The formed crude product was filtered off and purified by column chromatography (Al_2O_3 grade II, CH_2Cl_2). Yield: 260 mg (38%).

^1H ($CDCl_3$): δ 7.61 (s, 2H, N_3C_2H), 4.85 (s, 4 H, C_5H_4), 4.70 (s, 4H, C_5H_4), 4.36 (s, 4H, C_5H_4), 4.27 (s, 4H, C_5H_4), 4.27 (s, 4H, C_5H_4), 4.05 (s, 10H, C_5H_5) ppm; $^{13}C\{^1H\}$ NMR: δ 118.3 (N_3C_2H) , 69.5 (C_5H_4), 68.7 (C_5H_4), 68.4 (C_5H_4), 66.8 (C_5H_4), 64.0 (C_5H_4) ppm. Elemental analysis (%) calcd for $C_{34}H_{28}Fe_3N_6$ (688.18): C 59.34, H 4.10, N 12.21; found: C 58.71, H 4.07, N 12.00.

5.3.11.3 Synthesis of [fc–(N_3C_2H–C_6H_5)$_2$] (18c)

Phenyacetylene (205 mg, 2.00 mmol) and CuI (38 mg, 10 mol%) were added to a solution of 1,1′-diazidoferrocene (270 mg, 1.00 mmol) in dry THF (30 ml). The reaction mixture was stirred in the dark for 14 h. The precipitate was filtered off and purified by column chromatography on Al_2O_3 (grade II) with CH_2Cl_2 as eluent. Yield: 140 mg (29%).

^{1}H ($CDCl_3$): δ 7.76 (s, 2H, N_3C_2H), 7.65 (d, *J* = 6.8 Hz, 4H, C_6H_5), 7.28 (m, 4H, C_6H_5), 7.25 (s, 2H, C_6H_5), 4.96 (s, 4H, C_5H_4), 4.39 (s, 4H, C_5H_4) ppm; ^{13}C{^{1}H} NMR: δ = 129.7 (C_6H_5), 128.7 (C_6H_5), 128.1 (C_6H_5), 125.6 (C_6H_5), 118.5 (N_3C_2H) , 68.3 (C_5H_4), 63.6 (C_5H_4) ppm. Elemental analysis (%) calcd for $C_{26}H_{20}FeN_6$ (472.34): C 66.12, H 4.27, N 17.79; found: C 64.40, H 4.60, N 14.42.

5.3.12 Synthesis of Ferrocene-based Thiourea Derivatives (19a–b)

The preparations were carried out at room temperature under inert gas atmosphere.

5.3.12.1 Synthesis of {fc(NHCSNEt$_2$)$_2$} (19a)

Diethylamine (74 mg, 1.00 mmol) was added to a solution of 1,1′-diisothiocyanatoferrocene (**2**) (150 mg, 0.50 mmol) in dry ether (50 ml). After stirring for ½ h the solution turned colourless and a yellow precipitate was formed. All residues were removed in vacuo and gave rise to analytically pure product in quantitative yield (225 mg).

^{1}H ($CDCl_3$): δ 7.27 (s, 2H, NH), 4.60 (s, 4H, C_5H_4), 4.07 (s, 4H, C_5H_4), 3.73 (s, 8H, CH_2), 1.27 (s, 12H, CH_3) ppm; ^{13}C{^{1}H} NMR: δ 179.4 (C=S), 98.4 (C_5H_4), 65.8 (C_5H_4), 65.0 (C_5H_4), 45.6 (CH_2), 12.8 (CH_3) ppm. Elemental analysis (%) calcd for $C_{20}H_{30}FeN_4S_2$ (446.46): C 53.81, H 6.77, N 12.55; found: C 53.52, H 6.76, N 12.48.

5.3.12.3 Synthesis of {fc(NHCSN*i*-Pr$_2$)$_2$} (19b)

DiPa (110 mg, 1.00 mmol) was added to a solution of **2** (150 mg, 0.50 mmol) in dry ether (50 ml). After stirring for 4 h the reaction mixture turned colourless and all residues were removed in vacuo. **19b** was obtained in analytically pure form in almost quantitative yield (256 mg, 98%).

^{1}H ($CDCl_3$): δ 6.88 (s, 2H, NH), 4.82 (m, broad, CH), 4.53 (s, 4H, C_5H_4), 4.14 (s, 4H, C_5H_4), 1.35 (d, *J* = 6.7 Hz, 24H, CH_3) ppm; ^{13}C{^{1}H} NMR: δ 182.1 (C=S), 96.7(C_5H_4), 67.7 (C_5H_4), 66.2 (C_5H_4), 49.3 (CH), 20.9 (CH_3) ppm. Elemental analysis (%) calcd for $C_{24}H_{38}FeN_4S_2$ (502.57): C 57.36, H 7.62, N 11.15; found: C 57.31, H 7.79, N 11.55.

5.3.13 Synthesis of Bis(iminophosphorane)ferrocene-derivative {fc(PPh$_2$=N-Fc)$_2$} (20)

Dppf (138 mg, 0.25 mmol) was added to a solution of azidoferrocene (113 mg, 0.50 mmol) in dry dichloromethane (20 ml). The reaction mixture was stirred in the dark for 14h. All volatile compounds were removed in vacuo and the crude product washed with petrol ether (3 x 10 ml) under inert gas. Yield: 208 mg (83%). Further purification was hampered since the product is sensitive to air.

^{1}H ($CDCl_3$): δ 7.61 (q, *J* = 11.5, 8 H, Ph), 7.50 (m, 4 H, Ph), 7.41 (d, *J* = 6.3 Hz, 8 H, Ph), 4.39 (s, 4 H, C_5H_4), 4.14 (s, 4 H, C_5H_4), 4.04 (s, 4 H, C_5H_4), 3.91 (s, 10 H, C_5H_5), 3.69 (s, 4 H, C_5H_4) ppm; ^{13}C{^{1}H} NMR: δ 132.4 (d, |*J*| = 9.0 Hz, PPh_2), 131.5 (s, PPh_2), 128.3 (d, |*J*| = 11.3 Hz, PPh_2), 98.4 (C_5H_4), 74.4 (C_5H_4), 73.7 (C_5H_4), 68.6 (C_5H_4), 67.9 (C_5H_4), 62.3 (C_5H_4) ppm; ^{31}P NMR: δ 5.9 ppm. Elemental analysis (%) calcd for $C_{54}H_{46}Fe_3N_2P_2$ (952.47): C 68.10, H 4.87, N 2.94; found: C 66.27, H 4.95, N 2.58.

5.4 References

[1] G. M. Sheldrick, *Programs for crystal structure analysis,* University of Göttingen (D), **1997**.

[2] C. J. Satterley, K. R. J. Lovelock, I. Thom, V. R. Dhanak, M. Buck, R. G. Jones, *Surf. Sci.* **2006**, *600*, 4825. b)

[3] K. Heister, M. Zharnikov, M. Grunze, L. S. O. Johansson, *J. Phys. Chem. B* **2001**, *105*, 4085.

[4] M. D. Rausch, D. J. Ciapenelli, *J. Organometal. Chem.* **1967**, *10*, 127.

[5] J. J. Bishop, A. Davison, M. L. Katcher, D. W. Lichtenberg, R. E. Merrill, J. C. Smart, *J. Organomet. Chem.* **1971**, *27*, 241.

[6] A. Shafir, M. P. Power, G. D. Whitener, J. Arnold, *Organometallics* **2000**, *19*, 3978.

[7] D. van Leusen, B. Hessen, *Organometallics* **2001**, *20*, 224.

[8] B. McCulloch, D. L. Ward, J. D. Woollins, C. H. Brubaker, Jr., *Organometallics* **1985**, *4*, 1425.

[9] F. Garnier, A. Yassar, Fr. Demande FR 2668154 A1, 1992.

[10] K. Bushell, C. Gialou, C. H. Goh, N. J. Long, J. Martin, A. J. P. White, C. K. Williams, D. J. Williams, M. Fontaine, P. Zanello, *J. Organomet. Chem.* **2001**, *637–639*, 418.

[11] B. P. Fedorov, F. M. Stoyanovich, *Zh. Obsh. Khim.* **1963**, *33*, 2251.

[12] U. Schmidt, G. Pfleiderer, F. Bartkowiak, *Anal. Biochem.* **1984**, *138*, 217.

[13] C. Metallinos, D. Tremblay, F. B. Barrett, N. J. Taylor, *J. Organomet. Chem.* **2006**, *691*, 2044.

[14] J. Polin, H. Schottenberger, *Org. Synt.* **1996**, *73*, 262.

[15] R. Usón, A. Laguna, *Inorg. Synth.* **1982**, *21*, 71.

[16] S. Ahmad, A. A. Isab, H. P. Perzanowski, M. S. Hussain, M. N. Akhtar *Transition Met. Chem.* **2002**, *27*, 177.

[17] R. Usón, A. Laguna, *Inorg. Synth.* **1989**, *26*, 85.

[18] S. Canales, O. Crespo, A. Fortea, M. C. Gimeno, P. G. Jones, A. Laguna, *J. Chem. Soc., Dalton Trans.*, **2002**, 2250.

[19] I.R. Butler, S. C. Quayle. *J. Organomet. Chem*. **1998**, *552*, 63.

[20] G. Hogarth, M. M. Álvarez-Falcón, *Inorg. Chim. Acta* **2005**, *358*, 1386.